

DISS. ETH NO.: 17213

Cadmium in the Oceans - Studies of Cd Isotope Variations
in Seawater and Cd/Ca in in-situ Sampled
Planktonic Foraminifera

A dissertation submitted to

ETH ZÜRICH

For the degree of

DOCTOR OF SCIENCES (DR. SC. ETH ZÜRICH)

Presented by

SONJA RIPPERGER

Diplom-Geologin (Univ.)

Ludwig-Maximilians-Universität München

Born 29.11.1970

Citizen of Germany

Accepted on recommendation of

Prof. Dr. J. A. McKenzie (referee)

Prof. Dr. A. N. Halliday (co-referee)

Dr. M. Rehkämper (co-referee)

Dr. R. Schiebel (co-referee)

Prof. Dr. G. Henderson (external co-referee)

Zürich 2007

Front cover: Picture of a living planktonic foraminifer of the species *Globigerinoides ruber*. The central calcite shell is surrounded by dinoflagellate symbiotic algae (gold-colour) and a rhizopodial web (bluish-colour). The calcite spines that extend from the shell are used to carry symbionts and capture prey.

Credit: Howard Spero, UC Davis (spero@geology.ucdavis.edu).

Contents

Abstract	1
Kurzfassung.....	5
1. Introduction	9
1.1 Cadmium in Seawater.....	10
1.2 Cadmium in Planktonic Foraminifers.....	11
1.3 Cadmium Stable Isotope Geochemistry	12
1.4 Motivation of this Study	14
1.4.1 Cd/Ca Ratios of in-situ Collected Planktonic Foraminifers	14
1.4.2 Cadmium Isotope Variations in Seawater	15
1.5 Outline of the Thesis.....	16
2. A Highly Sensitive MC-ICPMS Method for Cd/Ca Analyses of Foraminiferal Tests	19
2.1 Introduction	21
2.2 Laboratory Methods and Reagents	22
2.2.1 Laboratory Methods	22
2.2.2 Standard Solutions.....	22
2.2.3 Spike Solutions	23
2.3 Samples and Sample Handling	24
2.3.1 Samples.....	24
2.3.2 Cleaning of Foraminiferal Tests	25
2.3.3 Spiking of Samples	28
2.3.4 Column Chemistry	28
2.3.5 Mass Spectrometry	29
2.3.6 Data Processing	31
2.4 Results	33
2.4.1 Procedural Blanks and Detection Limit.....	33
2.4.2 Analyses of Standard Solutions.....	34
2.4.3 Accuracy of Isotopic Data - Analyses of Unspiked Foraminiferal Tests	35
2.4.4 Evaluation of Molecular Interferences	37
2.4.5 Reproducibility of Cd/Ca Ratios	38
2.5 Discussion.....	39
2.6 Summary and Conclusions	41

3. The Cd/Ca Ratios of in-situ Collected Planktonic Foraminiferal Tests	43
3.1 Introduction	45
3.2 Samples.....	46
3.2.1 In-situ Samples	46
3.2.2 Surface Sediment Samples	48
3.3 Oceanographic Setting of the Sampling Areas.....	50
3.3.1 Seawater Parameters for in-situ Collected Planktonic Foraminifers.....	50
3.3.2 Seawater Parameters for Surface Sediment Samples	52
3.4 Analytical Methods.....	52
3.4.1 General.....	52
3.4.2 Examination of Foraminiferal Cleaning Procedure.....	55
3.4.3 Data Presentation.....	55
3.5 Results	56
3.5.1 Evaluation of Leaching Procedure	56
3.5.2 Analytical Reproducibility and Natural Variability of Cd/Ca Ratios.....	59
3.5.3 Cd/Ca Ratios of in-situ Collected Planktonic Foraminifers	60
3.5.4 Cd/Ca Ratios of Planktonic Foraminiferal Shells of Surface Sediments	64
3.6 Discussion.....	65
3.6.1 Incorporation of Cd into the Shell Calcite of Live Foraminifers	65
3.6.2 Cd/Ca Ratios of Settling Shells	67
3.6.3 Cd/Ca Ratios of in-situ Collected and Sedimentary Foraminiferal Tests ...	67
3.7 Summary and Conclusions	73
4. Precise Determination of Cadmium Isotope Fractionation in Seawater	
by Double Spike MC-ICPMS	77
4.1 Introduction	79
4.2 Methods	80
4.2.1 General.....	80
4.2.2 Standard Solutions and Cd Isotope Notation.....	80
4.2.3 Cadmium Double Spike.....	82
4.2.4 Samples and Sample Handling	85
4.2.5 Mass Spectrometry	87
4.2.6 Data Reduction	88
4.3 Results and Discussion	89

4.3.1 Analyses of Standard Solutions.....	89
4.3.2 Analyses of Seawater Samples.....	93
4.4 Conclusions	99
5. Cadmium Isotope Fractionation in Seawater – A Signature of Biological	
Activity.....	101
5.1 Introduction	103
5.2 Samples.....	104
5.3 Methods	107
5.3.1 Chemical Separation.....	107
5.3.2 Mass Spectrometry	107
5.3.3 Data Presentation.....	108
5.4 Results	109
5.4.1 General Depth Dependency of Cd Isotope Composition	109
5.4.2 North Pacific Water Column Profiles.....	110
5.4.3 Arctic Ocean Water Column Profile	112
5.5 Discussion.....	113
5.5.1 Biological Fractionation of Cd Isotopes.....	113
5.5.2 Variability of Cd Isotope Systematics.....	116
5.5.3 Constant Cd Isotope Composition of Deep Water	120
5.6 Conclusions	122
6. General Conclusions and Outlook	127
6.1 Conclusions	128
6.1.1 Cd/Ca Ratios of in-situ Collected Foraminiferal Tests	128
6.1.2 Cadmium Isotope Variations in Seawater	130
6.2 Outlook.....	132
6.2.1 Cd/Ca Ratios of Foraminiferal Tests	132
6.2.2 Cadmium Isotope Variations in Seawater	133
References	135
Acknowledgements	149
Curriculum Vitae.....	151

Abstract

The geochemistry of cadmium in seawater has attracted significant attention over the past 30 years. This interest is based on the marine distribution of the trace element Cd, which resembles that of the macronutrient phosphate. This suggests that the variable abundance of both elements in seawater is due to uptake by marine phytoplankton near the surface and particle recycling in deeper waters. Phosphate is only poorly preserved in marine sediments whereas Cd is recorded in fossil tests of planktonic and benthic foraminifera from deep-sea sediments. Hence, the Cd/Ca ratios of foraminiferal shells have been used in numerous paleoceanographic studies, as a water mass tracer and to investigate past changes in nutrient utilization. A number of results, however, have raised questions regarding the reliability of Cd as a paleoceanographic proxy. In addition, the factors that control the uptake of Cd by marine microorganisms are only poorly understood.

This thesis comprises two independent but nonetheless related investigations that address such questions and that aim to further our basic understanding of the behaviour of Cd in the marine environment. The first part of the thesis focuses on Cd/Ca ratios of *in-situ* collected planktonic foraminifera whereas the second part deals with variations in the stable isotope composition of Cd in the oceans. Both investigations were analytically challenging because they required (i) the development of new analytical techniques and (ii) precise Cd concentration and isotope composition measurements for samples where the amount of Cd available for analyses was limited in many cases.

The excellent accuracy and precision of the new Cd/Ca method reflects the application of an isotope dilution (ID) protocol for both Cd and Ca and isotopic analysis by multiple collector inductively coupled plasma mass spectrometry (MC-ICPMS). The determination of the Cd abundances involves simultaneous measurements of ^{110}Cd and ^{111}Cd with a dual ion counting system, whereas the ID analyses for the major element Ca were carried out by multiple collection with Faraday cups. Repeated analyses of spiked *Orbulina universa* tests yielded a reproducibility of $\pm 0.7\%$ for the Cd/Ca ratio, based on measurements that each consumed about 5 pg and 700 ng of natural Cd and Ca, respectively. The method is characterized by a total procedural Cd blank of 112 ± 44 fg (1s.d.), which results in a detection limit of 131 fg (3s.d.). This demonstrates that the new technique is superior to published methods for the determination of foraminiferal Cd/Ca, particularly with regard to the acquisition of precise and accurate data for samples of limited size.

Using this newly developed method, novel Cd/Ca data for *in-situ* sampled planktonic foraminifers of the species *Globigerinoides ruber*, *Globigerinoides sacculifer* and *Globigerina bulloides* from the Arabian Sea and the North Atlantic were acquired. The Cd/Ca ratios obtained for *G. ruber* sampled from the live habitat during different monsoon seasons generally show a correlation with seawater phosphate. No such trend is observed for *G. sacculifer*, however, and this indicates that vital effects and/or different ecological niches may be responsible for the different Cd/Ca systematics of *G. ruber* and *G. sacculifer*. Analyses of live specimens and sedimentary tests of *G. ruber*, *G. sacculifer*, and *G. bulloides* yielded consistently higher Cd/Ca values for tests from surface sediments. A post-depositional alteration of the tests is unlikely to be responsible for these differences. Rather, the latter appears to reflect a combination of factors, including the formation of calcite crusts with high Cd contents, the different time scales that are represented by *in-situ* and sedimentary tests, and the dominance of tests from periods of high productivity in sediments. Our results also reveal higher Cd/Ca ratios for live *G. ruber* than for settling shells of the same species. This indicates a preferential loss of Cd and/or selective dissolution of Cd-enriched calcite phases during settling of the tests through the water column. Sedimentary tests, however, are less effected by dissolution processes, as they are mainly deposited in mass sinking events. The latter are associated by higher sinking velocities compared to individually, slowly settling tests.

For the accurate and precise determination of the stable Cd isotope composition of seawater, a new technique has been developed, that utilizes a ^{110}Cd - ^{111}Cd double spike, and involves separation of Cd from seawater by column chromatography and isotopic analyses by MC-ICPMS. As a by-product the double spike technique also generates precise Cd seawater concentration data. The novel procedure is characterized by a reproducibility of about ± 1.0 to ± 1.6 $\epsilon^{114/110}\text{Cd}$ (2s.d.) for standard and seawater measurements that each consumed about ~8 ng of natural Cd ($\epsilon^{114/110}\text{Cd}$ is the deviation of the $^{114}\text{Cd}/^{110}\text{Cd}$ isotope ratio of a sample from the standard in parts per 10,000). Even samples with as little as 1 to 5 ng of seawater derived Cd can be analyzed with a precision of about ± 2 to ± 6 $\epsilon^{114/110}\text{Cd}$ (2s.d.). This demonstrates that the new double spike technique is superior to published methods of Cd isotope analyses, with regard to the acquisition of precise data for samples of limited size.

The Cd isotope data that were acquired for seawater samples from four major ocean basins reveal, for the first time, large and well-resolved Cd isotope fractionations in the marine

environment. A large group of seawater samples exhibits a clear relationship of Cd isotope composition and concentration, whereby the most Cd-depleted samples show the most fractionated Cd isotope compositions (up to $\epsilon^{114/110}\text{Cd} \approx 38 \pm 6$). This suggests that Cd fractionation is due to kinetic isotope effects that are generated during closed system uptake of dissolved seawater Cd by phytoplankton. A small set of samples do not follow this trend, as they displays extremely low Cd contents (<0.008 nmol/kg) but nearly un-fractionated Cd isotope compositions. Such complexities, which are not mirrored by the Cd concentration data, require that the Cd distribution was affected by additional processes, such as water mass mixing, atmospheric inputs, and/or adsorption. Finally, Cd-rich water samples from ≥ 900 m depth display nearly constant $\epsilon^{114/110}\text{Cd}$ values of about $+3.3 \pm 0.5$ (1s.d.) although their Cd concentrations show the expected increase along the global flow path of deep water from the Atlantic to the Pacific Ocean. This indicates that phytoplankton organic matter, which increases the Cd content of deeper water masses upon remineralization, is also characterized by a constant Cd isotope composition of $\epsilon^{114/110}\text{Cd} \approx +3$. This observation can be explained by a near-quantitative closed system uptake of Cd by phytoplankton from surface waters.

Seite Leer /
Blank leaf

Kurzfassung

Die Geochemie des Spurenelementes Cadmium im Meerwasser ist seit über 30 Jahren Gegenstand wissenschaftlicher Untersuchungen. Das wissenschaftliche Interesse basiert auf der ozeanischen Verteilung von Cd, die der von Phosphat, einem bedeutendem Nährstoff für marine Lebewesen, stark gleicht. Die Korrelation zwischen Phosphat und Cd legt nahe, dass die Verteilung beider Elemente im Ozean durch die gleichen Prozesse geprägt wird: Aufnahme von Phosphat und Cd durch marines Phytoplankton im Oberflächenwasser sowie Freisetzung von Phosphat und Cd durch Recycling und Lösung von toter Biomasse im tieferen Bereich der Wassersäule. Phosphat wird überwiegend in organischem Material gebunden und wird daher nur schlecht in Sedimenten überliefert. Cadmium hingegen wird auch in die Gehäuse von planktischen und benthischen Foraminiferen eingebaut, die einen Grossteil mariner Sedimente stellen. Diese Tatsache haben sich zahlreiche paläoozeanographische Studien zu nutze gemacht, um anhand von Cd/Ca in fossilen Foraminiferengehäusen Rückschlüsse auf Wassermassenverteilung und Nährstoffschwankungen in der Vergangenheit zu ziehen. Einige Ergebnisse stellen jedoch die Verwendung von Cd/Ca als paläoozeanographischen Proxy in Frage. Hinzu kommt, dass die Faktoren, welche die Aufnahme von Cd durch marine Mikroorganismen kontrollieren, nur unzureichend verstanden werden.

Die vorliegende Dissertation beinhaltet zwei Teilstudien, welche auf die oben genannten Problemstellungen Bezug nehmen und darüber hinaus darauf abzielen, das grundlegende Verhalten von Cd im ozeanischen Bereich besser zu verstehen. Während sich der erste Teil der Dissertation detailliert mit Cd/Ca in Gehäusen von *in-situ* gefangenen planktischen Foraminiferen beschäftigt, behandelt der zweite Teil Variationen der Isotopenzusammensetzung von Cd im Meerwasser. Beide Untersuchungen stellten analytische Herausforderungen dar und erforderten (i) die Entwicklung neuer analytischer Methoden und (ii) präzise Messungen von Cd-Konzentration und Isotopie an Proben deren Cd-Gehalt häufig limitiert war.

Die exzellente Präzision der neuen Cd/Ca Methode basiert auf der Verwendung der Isotopenverdünnungstechnik (ID) und Konzentrationsmessungen mittels Multikollektor induktiv gekoppelter Plasma Massenspektrometrie (MC-ICPMS). Die Bestimmung der Cd-Konzentrationen beinhaltet die simultane Messung von ^{110}Cd und ^{111}Cd mittels zweier Ionenzähler, wohingegen die ID Analyse des Hauptelements Ca mit Hilfe von Faraday Cups

durchgeführt wird. Wiederholte Messungen von planktischen Foraminiferen der Art *Orbulina universa* lieferten eine Cd/Ca Reproduzierbarkeit von $\pm 0.7\%$. Diese Messungen benötigten jeweils nur etwa 5 pg natürliches Cd und 700 ng natürliches Ca. Die Methode ist gekennzeichnet durch einen Gesamtcadmiumblank von 112 ± 44 fg (1s.d.), woraus sich eine Nachweisgrenze von 131 fg (3 s.d.) ergibt. Diese Ergebnisse demonstrieren, dass die entwickelte Methode, auch für kleinste Probenmengen, eine deutlich höhere Präzision bietet als bereits veröffentlichte Verfahren für die Bestimmung von Cd/Ca in Foraminiferengehäusen.

Mit Hilfe dieser neu entwickelten Methode wurde Cd/Ca an Gehäusen planktischer Foraminiferen der Arten *Globigerinoides ruber*, *Globigerinoides sacculifer* und *Globigerina bulloides* gemessen, welche aus der Wassersäule im Arabischen Meer und im Nord-Atlantik entnommen wurden. Die Ergebnisse demonstrieren, dass lebend aus dem Habitat gefangene *G. ruber* in der Regel eine Korrelation von Cd/Ca mit dem Phosphatgehalt des Meerwassers zeigen. Eine solche Korrelation wird jedoch nicht für *G. sacculifer* beobachtet, was auf artspezifische Unterschiede bezüglich des Einbaus von Cd in die Gehäuse von *G. ruber* und *G. sacculifer* schliessen lässt. Der Cd/Ca Gehalt von sedimentären Gehäuse von *G. ruber*, *G. sacculifer* und *G. bulloides* ist signifikant höher als jener lebend gefangener Organismen. Es ist unwahrscheinlich, dass eine nach der Ablagerung im Sediment erfolgte Alteration der Schalen für diese Beobachtung verantwortlich ist. Der Unterschied in Cd/Ca lässt sich vielmehr auf eine Kombination verschiedener Faktoren zurückführen: (i) Bildung von Cd-reichen Kalzit Krusten, (ii) Lebend gefangene und sedimentäre Foraminiferengehäuse spiegeln unterschiedliche Zeitspannen wieder (iii) Schalen, die zu Zeiten hoher Nährstoffgehalte kalzifizierten dominieren in Sedimenten.

Des weiteren zeigen lebend im Habitat gefangene *G. ruber* höhere Cd/Ca Werte als abgesunkene Gehäuse. Dieses Ergebnis weist darauf hin, dass einzeln sinkende Schalen toter Individuen während des Absinkens partiell angelöst werden. Gehäuse aus Sedimenten sind von diesen Lösungsprozessen weniger betroffen, da diese Schalen in der Regel in Massen-Absink-Ereignissen abgelagert werden. Letztere haben eine deutlich höhere Sinkgeschwindigkeit als einzeln, nicht in einem solchen Verband sinkende Gehäuse.

Das neue Verfahren zur präzise Bestimmung der Isotopenzusammensetzung von Cd im Meerwasser beinhaltet als wesentliche Elemente die Verwendung eines ^{110}Cd - ^{111}Cd Doppelspikes, die Abtrennung von Cd von der Meerwassermatrix mittels Säulenchemie und die anschliessende Isotopenmessung am MC-ICPMS. Des weiteren liefert die Doppelspike-Methodik präzise Cd-Konzentrationsdaten. Wiederholte Messungen von Cd-Referenzmaterial und Meerwasser ergaben eine Reproduzierbarkeit von etwa ± 1.0 bis $\pm 1.6 \text{ } \epsilon^{114/110}\text{Cd}$ (2 s.d.) für Messungen die jeweils ~ 8 ng natürliches Cd benötigten. Sogar kleinste Mengen von Cd im Meerwasser (1-5 ng) können noch mit einer Präzision von ± 2 bis $\pm 6 \text{ } \epsilon^{114/110}\text{Cd}$ (2 s.d.) gemessen werden. Dies belegt eine höhere Präzision der neuen Doppelspikemethode gegenüber bereits bestehenden Verfahren und zeichnet diese Methodik besonders aus für Isotopenmessungen an Proben mit geringem Cd Gehalt.

Die Cd-Isotopie wurde für Meerwasserproben aus der Arktis, dem Nordatlantik, der Antarktis und dem Nordpazifik bestimmt. Die Daten dokumentieren erstmals eine eindeutige und starke Fraktionierung von Cd im ozeanischen Bereich. Ein grosser Teil der Proben zeigt einen klaren Zusammenhang zwischen der Isotopie und der Konzentration von Cd, wobei die am stärksten an Cd verarmten Proben die stärkste Fraktionierung aufweisen (bis zu $\epsilon^{114/110}\text{Cd} \approx 38 \pm 6$). Diese Beobachtung weist darauf hin, dass die Fraktionierung von Cd durch kinetische Isotopeneffekte bestimmt wird, welche bei der Aufnahme von gelöstem Cd durch Phytoplankton wirken. Einige wenige Flachwasserproben zeigen jedoch eine Abweichung von diesem Trend. Diese Proben sind durch einen extrem geringen Cd-Gehalt (< 0.008 nmol/kg) gekennzeichnet, weisen allerdings eine nahezu unfraktionierte Isotopenzusammensetzung auf. Dieses Ergebnis setzt voraus, dass die Cd-Isotopie dieser Proben durch zusätzliche Prozesse beeinflusst wurde, wie z.B. durch die Mischung unterschiedlicher Wassermassen, durch atmosphärischer Eintrag und/oder durch Adsorbierungsprozesse. Cadmiumreiche Wasserproben aus Tiefen grösser als 900 m zeigen nahezu konstante $\epsilon^{114/110}\text{Cd}$ Werte von etwa $+3.3 \pm 0.5$ (1s.d.), obwohl ihre Konzentrationen den erwarteten Anstieg entlang der globalen Tiefenwasserzirkulation vom Atlantik zum Pazifik aufweisen. Diese Tatsache deutet an, dass organisches Material von Phytoplankton, dessen Remineralisierung eine erhöhte Cd-Konzentration tieferer Wassermassen bewirkt, ebenfalls durch eine konstante Cd-Isotopenzusammensetzung von $\epsilon^{114/110}\text{Cd} \approx +3$ gekennzeichnet ist. Eine mögliche Erklärung hierfür ist die nahezu vollständige Aufnahme von Cd durch Phytoplankton im Oberflächenwasser.

Seite Leer /
Blank leaf

CHAPTER 1

Introduction

The global oceanic thermohaline circulation system affects the Earth's climate, e.g., on a glacial-interglacial time-scale, through changes in heat and salt transport (Broecker, 1997). In addition, atmospheric carbon dioxide concentrations are linked to the marine carbon system, which hence is an important factor in climate oscillations. Because the open marine biological productivity, and carbon turnover, is limited by the availability of nutrients, records of nutrient-linked properties are essential if we are to understand the mechanisms that drive global changes in the Earth's climate.

1.1 CADMIUM IN SEAWATER

The interest of oceanographers in the trace element cadmium (Cd) is based on the observation that its oceanic distribution is closely correlated with those of the major nutrient phosphate (Boyle et al., 1976; Bruland, 1980). Both Cd and phosphate exhibit a depletion in surface waters due to uptake of these elements by marine phytoplankton. The Cd/P ratio of seawater decreases with decreasing phosphate content, suggesting a preferential uptake of Cd by phytoplankton relative to phosphate (Elderfield and Rickaby, 2000). Consequently, Cd concentrations in most depleted surface waters are as low as ~ 0.001 nmol/kg (Bruland, 1983). After organisms die, they sink through the water column and undergo decomposition or dissolution in deeper waters, where Cd concentrations are up to ~ 1 nmol/kg (Bruland, 1983). Through this process, Cd and phosphate are regenerated into the dissolved form (Bender and Gagner, 1976; Boyle et al., 1976; Bruland, 1980), Cd being regenerated preferentially relative to phosphate from decomposing particles (Knauer and Martin, 1981; Collier and Edmond, 1984).

The oceanic circulation modifies this vertical distribution pattern. As Cd and phosphate display a relatively low level of scavenging in deep water (Bruland and Lohan, 2003), their concentrations increase along the global flow path of deep water from the North Atlantic, through the Southern Ocean to the North Pacific and this creates water masses with distinct chemical signatures.

The main input of Cd into the ocean is from rivers and atmospheric dust deposition to the surface water. Subsequently, the element is involved in many internal cycles of assimilation into biogenic particulate matter and remineralization as described above, prior to ultimate burial in sediments. Consequently Cd displays an intermediate residence time in the ocean of about 10 to 100 kyr, similar to that of phosphorus (Bewers and Yeats, 1977; Martin and Whitfield, 1983; Ruttenger, 2003). The Cd flux out of the ocean takes place by the

incorporation of Cd into marine sediments (Collier and Edmond, 1984; Rosenthal et al., 1995; White, 1998).

1.2 CADMIUM IN PLANKTONIC FORAMINIFERS

Foraminifers are unicellular organisms with a shell (test) that encompasses the organism and separates the cytoplasm from the surrounding seawater. The application of Cd as a paleoceanographic proxy builds on the observation of Boyle (1981) that Cd is incorporated into the tests of foraminifera in proportion to the Cd concentration of the surrounding seawater. The close correlation of seawater Cd and phosphate and the preservation of these tests in marine sediments provide an indirect record of past phosphate levels. Such a record is useful because phosphate itself is mainly incorporated into organic matter and therefore only poorly preserved.

In the last 15 years, numerous studies have used Cd/Ca ratios of benthic foraminifers (seafloor dwelling species) to infer changes in ocean circulation patterns and deep-water phosphate levels on glacial/interglacial time-scales (e.g., Boyle and Keigwin, 1982; Boyle and Keigwin, 1985/86; Boyle and Keigwin, 1987; Lynch-Stieglitz and Fairbanks, 1994; Bertram et al., 1995; Lynch-Stieglitz et al., 1996; Oppo and Horowitz, 2000; Zahn and Stüber, 2002). Virtually all early Cd/Ca studies focused on the analysis of benthic foraminiferal tests. The advantage of this approach is that benthic species have larger shells with higher Cd concentrations (0.02-0.25 $\mu\text{mol per mol Ca}$) than the tests of surface dwelling, planktonic foraminifera (0.002-0.1 $\mu\text{mol per mol Ca}$; Lea, 1999). Using improved analytical techniques, more recent studies have extended the application of Cd/Ca to planktonic foraminifera (e.g., Rickaby and Elderfield, 1999; Rickaby et al., 2000). Such measurements are of particular interest because the Cd content in planktonic foraminifera is believed to be a proxy for surface water phosphate utilization, which in turn is linked to productivity (Rickaby and Elderfield, 1999; Elderfield and Rickaby, 2000).

Planktonic foraminifers are abundant and diverse in surface and subsurface waters of all modern open oceans, but are less frequent in shelf areas and shallow marginal seas (Schiebel and Hemleben, 2001). Their maximum abundance is found in euphotic near-surface waters (~10-50 m; Bé, 1977), which reflects the main environmental controls of planktonic foraminifers: light, temperature, salinity and nutrients. Especially symbiont-bearing species such as *Globigerinoides ruber*, *Globigerinoides sacculifer* and *Orbulina universa* are bound to the euphotic zone (Schiebel et al., 2001; Schiebel et al., 2004), whereas some species

without an algal symbiosis (e.g., *Globorotalia truncatulinoides*) live in the deeper ocean for most of the year (Schiebel and Hemleben, 2005).

The life cycle of planktonic foraminifera is characterized by a vertical migration through the water column (e.g., Hemleben et al., 1989; Schiebel and Hemleben, 2005). Juvenile individuals ascend into surface waters, whereas with maturity they descend into deeper subsurface waters to reproduce. This ends the life of the parent cell and the empty tests sink to the ocean floor. The life span of planktonic foraminifers varies between 14 days and a year and reproduction is triggered by the lunar cycle in most cases (Erez et al., 1991; Schiebel and Hemleben, 2001; Schiebel and Hemleben, 2005).

Growth of foraminifera is accompanied by sequentially adding new chambers, which results in the precipitation of carbonate. Some species may develop spines (spinose species) that allow the cytoplasm to stretch out of the test and to carry prey and symbionts (Schiebel and Hemleben, 2001). Test of planktonic foraminifers consist of about 99% pure calcite and trace elements (e.g., Mg, Ba, and Cd) comprise the remaining 1%. The latter are incorporated from seawater into the lattice of the foraminiferal tests during shell calcification. As noted above, Cd concentrations in planktonic foraminiferal shell calcite are extremely low (0.002–0.1 $\mu\text{mol per mol Ca}$; Lea, 1999) reflecting the low surface water Cd concentrations from which the shells are precipitated. The relationship between foraminiferal shell Cd and seawater Cd can be expressed by the partition coefficient $D_{\text{Cd}} = (\text{Cd/Ca})_{\text{foram}} / (\text{Cd/Ca})_{\text{sw}}$ (e.g., Rickaby and Elderfield, 1999). Laboratory culturing studies have become important for the investigation of the Cd partition coefficient. Delaney (1989) reported a D_{Cd} of ~2 to 4 for *G. sacculifer*, *G. ruber* and *O. universa*, whereas Mashiotto et al. (1997) suggested a significantly lower D_{Cd} of 0.095 for the symbiont bearing species *O. universa* compared to the non-symbiont bearing *G. bulloides* ($D_{\text{Cd}} \approx 1.9$), which they attributed to sequestration of Cd by the symbiotic dinoflagellate algae.

1.3 CADMIUM STABLE ISOTOPE GEOCHEMISTRY

Stable isotope geochemistry deals with variations in the isotopic composition of elements originating from physicochemical processes rather than from radioactive decay. Investigations of mass-dependant variations in stable isotope compositions have traditionally centred on a few light elements due to the analytical difficulty of resolving extremely small natural mass dependant variations in isotope composition of elements heavier than 40 amu. Since the end of the 1990's, the technique of multiple collector inductively coupled plasma mass

spectrometry (MC-ICPMS) has opened up new avenues of research. MC-ICPMS measurements benefit from the high ionisation efficiency and excellent sensitivity as well as from the flat-topped peaks and multiple ion beam collection, which allow for high precision isotope ratio determination (e.g., Halliday et al., 2000; Rehkämper et al., 2001). In addition, the instrumental mass bias of MC-ICPMS can be well monitored and corrected for by external normalization, standard-sample bracketing or double-spike techniques (Rehkämper et al., 2004). Overall, these advantages permit very precise stable isotope measurements also of “heavy” elements that could previously not be analyzed with sufficient precision. One of the elements that fall into this category is Cd (with a mass of 112 amu).

Cadmium has eight stable isotopes with relative abundances that vary from less than 1.5% (^{106}Cd , ^{108}Cd) to approximately 25% (^{112}Cd , ^{114}Cd). The remaining Cd isotopes have intermediate abundances of about 7.5% (^{116}Cd) and 12.5% (^{110}Cd , ^{111}Cd , ^{113}Cd). In a strict sense ^{113}Cd is not a stable isotope, as it decays to ^{113}In with a very long half-life of 9×10^{15} years. Throughout this study, variations in the stable isotopes of Cd in a sample are reported relative to results obtained for a standard with an ϵ -notation:

$$\epsilon^{114/110}\text{Cd} = \left(\frac{(^{114}\text{Cd}/^{110}\text{Cd})_{\text{sample}}}{(^{114}\text{Cd}/^{110}\text{Cd})_{\text{std}}} - 1 \right) \times 10,000$$

where $(^{114}\text{Cd}/^{110}\text{Cd})_{\text{sample}}$ and $(^{114}\text{Cd}/^{110}\text{Cd})_{\text{std}}$ denote the isotope ratio of ^{114}Cd and ^{110}Cd of the sample and the standard, respectively.

There exist a few published studies about natural variations in Cd stable isotope compositions. Large Cd isotope effects were determined in extraterrestrial samples caused by evaporation and/or condensation processes (e.g., Rosman and De Laeter, 1976; Rosman and De Laeter, 1988; Wombacher et al., 2003; Wombacher et al., 2007). In contrast, only minor Cd stable isotope variations ($\epsilon^{114/110}\text{Cd}$ between -4 and +4.8) were detected in natural terrestrial samples, including Cd-minerals, sediments and igneous rocks (Wombacher et al., 2003). Slightly larger Cd isotope effects ($\epsilon^{114/110}\text{Cd}$ between -6.4 and +3.6) were reported for anthropogenic samples, including dust and slag from a lead smelter (Cloquet et al., 2005). The Cd isotope variations of these terrestrial and anthropogenic samples are caused by inorganic processes. Biological processes typically generate larger isotope fractionations than purely inorganic reactions (other than evaporation or condensation) as shown for elements such as Fe, Cu, and Zn (Zhu et al., 2002).

1.4 MOTIVATION OF THIS STUDY

1.4.1 Cd/Ca Ratios of in-situ Collected Planktonic Foraminifers

Even though the Cd/Ca ratios of foraminifera have become an important tool in paleoceanography, there are still questions and concerns regarding the reliability of this tracer.

A rigorous cleaning of sedimentary tests is required to remove adsorbed and adhering phases from the surface of the shells (Boyle, 1981; Boyle and Keigwin, 1985/86; Boyle, 1988). The removal of such authigenic coatings is an important part of the foraminiferal cleaning procedure, especially because they can have significantly higher (orders of magnitude) Cd concentrations than the calcite tests (Boyle, 1988). However, successful removal of these Cd-rich coatings has hitherto been assessed only by indirect evidence (Boyle, 1988).

It has also been suggested that the dissolution of shells following deposition on the ocean floor may significantly alter the Cd/Ca ratios of foraminiferal tests (McCorkle et al., 1995). Dissolution effects have, for example, been called upon to explain the anomalous distribution behaviour of Cd between seawater and foraminiferal tests at depths below 2500 m (Elderfield et al., 1996).

The use of the Cd/Ca proxy is furthermore complicated by the life cycle of planktonic foraminifers during which they migrate through the water column (Hemleben et al., 1989; Schiebel et al., 1997; Schiebel et al., 2004). In addition, some planktonic species precipitate a gametogenic calcite crust during reproduction and/or secondary calcite crusts in subsurface waters (Orr, 1967; Bé, 1980; Duplessy et al., 1981; Hemleben et al., 1989; Schiebel et al., 1997). For *G. sacculifer*, compositional differences between the primary calcite that forms the chambers and the secondary calcite have been documented for $\delta^{18}\text{O}$ and Mg (Duplessy et al., 1981; Spero and Lea, 1993; Nürnberg et al., 1996; Eggins et al., 2004). Surface veneers that are enriched in Mg, Ba, Mn and Zn have also been found on tests of *G. ruber* (Eggins et al., 2004). Therefore, also the Cd composition of individual parts of the shells may vary in accordance to the different seawater conditions experienced by a foraminifer during its life span.

Further complications arise from the putative temperature dependence of the Cd partition coefficient, as shown by a recent study for *G. bulloides* for a temperature range of 4 to 16 °C (Rickaby and Elderfield, 1999). These results suggest that Cd incorporation into the calcite lattice of planktonic foraminifers is not only controlled by dissolved seawater Cd

concentration but also by seawater temperature and the acquired Cd/Ca ratios require a correction for the seawater temperature prevailing during shell calcification. In addition, there are a number of major discrepancies between $\delta^{13}\text{C}$ and Cd/Ca data for sedimentary records that are difficult to explain at present (Boyle, 1992).

In order to address some of these questions, we performed Cd/Ca analyses of planktonic foraminifers collected from the water column and from surface sediments. The first part of the thesis addresses the following questions: (i) Do live foraminifers that were sampled from the species-specific habitats show identical Cd/Ca ratios as empty tests of sinking (dead) specimens obtained well below the habitat? (ii) Do the shells of planktonic foraminifera extracted from sediment core-tops display identical Cd/Ca ratios as the tests collected from the water column? (iii) Is the incorporation of Cd into the calcite lattice of planktonic foraminifers species-specific? (iv) Do the Cd concentrations of *in-situ* sampled planktonic foraminifers mirror seawater phosphate concentrations? In summary, answers to these questions may help to assess the reliability of planktonic foraminiferal Cd/Ca ratios as a proxy for nutrient levels in surface seawater.

1.4.2 Cadmium Isotope Variations in Seawater

The uptake of phosphate by marine organisms is clearly governed by its role as an essential macronutrient. Cadmium, however, is generally regarded as toxic for organisms at higher concentrations (Brand et al., 1986; Sunda, 1987; Lane and Morel, 2000) and the factors that regulate Cd uptake by phytoplankton and control the Cd versus phosphate relationship are not fully understood. More recently, it was found that Cd can substitute for zinc in carbonic anhydrase when Zn-availability is limited (Price and Morel, 1990; Morel et al., 1994; Sunda and Huntsman, 2000; Lane et al., 2005). Carbonic anhydrase is a Zn-metalloenzyme that is ubiquitous in the bacteria, plant and animal kingdoms, and which catalyses the reversible conversion of CO_2 and water into carbonic acid and HCO_3^- ions (Lionetto et al., 2005). It plays a fundamental role in a number of physiological processes, such as respiration, ionic transport, acid-base regulation and calcification (Henry, 1996). The substitution of Zn by Cd was also suggested for other Zn-metalloenzymes, such as alkaline phosphatase, which allows phytoplankton to acquire phosphate from organic compounds (Morel and Price, 2003). These results indicate that the nutrient-like behaviour of Cd in the oceans is probably a consequence of true biological demand for Cd during growth of marine phytoplankton. However, it has also been proposed that the nutrient-like distribution of Cd

may be due to efficient scavenging onto living or nonliving particulate material (Collier and Edmond, 1984; Yee and Fein, 2001; Dixon et al., 2006).

Isotopic analyses have previously provided a wealth of information on the marine cycling of nutrient elements, such as nitrogen (Sigman et al., 1999) and silicon (De La Rocha et al., 1998; Reynolds et al., 2006). Further insight into the processes that govern the marine distribution of Cd may therefore be provided by Cd isotope measurements. Biological processes typically generate kinetic isotope effects, and the phytoplankton is therefore expected to be enriched in the light isotopes of Cd. The residual Cd-depleted seawater should thus show a complementary signature, characterized by an enrichment of the heavy Cd isotopes.

Recent culturing experiments demonstrated that freshwater phytoplankton cells preferentially take up the light isotopes of Cd (Lacan et al., 2006), which is expected to leave an isotopic fingerprint also in the residual Cd-depleted seawater. To date, there is only one published study of Cd isotope variations in seawater (Lacan et al., 2006), however, the measured isotopic variations were barely larger than the analytical uncertainties.

The second part of the thesis investigates (i) if the uptake of Cd from seawater by marine organisms is accompanied by analytically resolvable isotope fractionations and (ii) if isotopic differences of dissolved seawater Cd correlate with variations in Cd concentration. Such a correlation may be expected if Cd isotopes are fractionated by the same process that controls the Cd abundances and Cd/P ratios of seawater. Identification of such a correlation would thus provide unique constraints on the behaviour of Cd in the marine environment.

1.5 OUTLINE OF THE THESIS

Chapter 2 is concerned with the development and verification of a new method for Cd/Ca analyses of planktonic foraminiferal tests. Because the Cd content of these shells is extremely low (down to 0.002 μmol per mol Ca), determination of Cd/Ca is a challenging task. Cd/Ca studies of fossil shells may overcome this problem by using larger sample sizes, however, for *in-situ* collected planktonic foraminifers the sample material is generally strongly limited. Any successful method must therefore yield precise and accurate results (better than about $\pm 5\%$) even for samples with as little as 1-5 pg of Cd. Such measurements are not standard at present. Previously published methods for Cd/Ca determination in foraminiferal tests either had an insufficient precision for such small Cd amounts or were able to achieve the required precision, but for significantly larger amounts of Cd. The required precision and accuracy of

our new method are achieved by application of an isotope dilution technique in conjunction with a MC-ICPMS instrument that is equipped with a multiple ion counting system.

A dataset of Cd/Ca ratios of planktonic foraminiferal shells that were collected from the water column (*in-situ*) and from surface sediments are presented and discussed in *Chapter 3*. The foraminiferal Cd/Ca ratios were acquired using the methods described in the previous chapter. The Cd/Ca ratios are discussed in relation to (i) their correlation with surface water phosphate, (ii) species-specific-differences, (iii) variations between different *in-situ* samples, and (iv) variations between sedimentary tests and those obtained from the water column.

Chapter 4 describes the second major methodological development during the course of this thesis. A new technique for the accurate and precise determination of Cd isotope composition in seawater is introduced and verified. It utilizes a Cd double spike and it involves separation of Cd from seawater by column chromatography and isotopic analysis by MC-ICPMS. As a by-product the method also provides precise Cd concentration data. The superior precision of the new approach compared to previously published methods enabled us to unambiguously resolve Cd isotope fractionation in seawater for the first time.

A dataset of Cd isotope variations and concentrations for seawater samples determined with the double-spike technique are presented in *Chapter 5*. The seawater samples were collected from four major ocean basins and cover a wide range of Cd concentrations. The results reveal large and well resolved Cd isotope fractionations in the marine environment.

Chapter 6 presents a brief summary and the main conclusions of this thesis. In addition, it gives suggestions for further research.

CHAPTER 2

A Highly Sensitive MC-ICPMS Method for Cd/Ca Analyses of Foraminiferal Tests

Published as: Ripperger S. and Rehkämper M. (2007) A highly sensitive MC-ICPMS method for Cd/Ca analyses of foraminiferal tests. *Journal of Analytical Atomic Spectrometry*, DOI:10.1039/b704267a.

Abstract

A new highly sensitive technique for the precise and accurate determination of Cd/Ca ratios in foraminiferal shells is presented and validated. The excellent accuracy and precision of the method reflects the application of an isotope dilution (ID) protocol for both Cd and Ca and isotopic analysis by multiple collector inductively coupled plasma mass spectrometry. The determination of the Cd abundances involves simultaneous measurements of ^{110}Cd and ^{111}Cd with a dual ion counting system, whereas the ID analyses for the major element Ca were carried out by multiple collection with Faraday cups.

The performance of the method was verified by analyzing multiple samples of the planktonic foraminifer *Orbulina universa* that were handpicked from a sediment core taken in the North Atlantic. Analyses of unspiked samples that consumed as little as ~200 ng Ca, indicate that the Ca ID measurements are accurate to about $\pm 0.2\%$ (all errors are 1RSD). For the Cd ID analyses, the accuracy and precision is about $\pm 1.3\%$ and $\pm 3\%$ for measurements that consumed 3-12 pg and 0.5-1.5 pg of Cd, respectively. Repeated analyses of spiked *O. universa* tests yielded a reproducibility of $\pm 0.7\%$ for the Cd/Ca ratio, based on measurements that each consumed about 5 pg and 700 ng of natural Cd and Ca, respectively. The method is characterized by a total procedural Cd blank of 112 ± 44 fg (1s.d.), which results in a detection limit of 131 fg (3s.d.). This demonstrates that the new technique is superior to published methods for the determination of foraminiferal Cd/Ca, particularly with regard to the acquisition of precise data for samples of limited size.

2.1 INTRODUCTION

The trace element composition of calcite foraminiferal shells has become an important tool to reconstruct past oceanic conditions. This is based on the observation, that trace elements are incorporated directly from seawater into foraminiferal tests and therefore reflect the seawater conditions present during shell precipitation. Foraminiferal Cd has attracted particular attention over the past 25 years. This interest is based on the nutrient-type distribution of Cd in the oceans, which resembles that of the major nutrient phosphorus (Boyle et al., 1976; Bruland, 1980). Hence, foraminiferal Cd/Ca ratios have been used in numerous paleoceanographic studies to assess past nutrient utilization.

In the last decades, studies of Cd/Ca ratios of foraminifers have focused mainly on the analysis of benthic species, primarily for methodical reasons. The advantage of using benthic species is that they have larger shells with higher Cd contents (up to 0.25 μmol per mol Ca) than the tests of planktonic foraminifers (Lea, 1999; Rickaby et al., 2000) and therefore the number of specimens needed for analysis is smaller. Because of improved analytical techniques (e.g., sector field inductively coupled plasma mass spectrometry; Rosenthal et al., 1999, Marchitto, 2006) more recent studies have extended the application of Cd/Ca to planktonic foraminifers. Such measurements are of particular interest, because the Cd in planktonic foraminifera is believed to be a proxy for surface water phosphate utilization, which in turn is linked to productivity (Rickaby and Elderfield, 1999; Elderfield and Rickaby, 2000).

The precise determination of Cd/Ca ratios in planktonic foraminifers is a challenging task, however, because Cd abundances can be as low as 0.002 μmol per mol Ca (Lea, 1999). This becomes critical especially in cases where sample material is limited, for example for *in-situ* collected planktonic foraminifers. Such measurements are of particular interest because they can address concerns regarding the reliability of the Cd/Ca proxy (Boyle, 1988; McCorkle et al., 1995).

Therefore, the general goal of this study was to develop techniques, which are routinely able to provide Cd/Ca ratios for foraminiferal tests with a precision and accuracy of better than 5%, even for samples with as little as 1-5 pg of Cd. This goal was achieved by the application of the isotope dilution technique in conjunction with a multiple collector inductively coupled plasma mass spectrometer (MC-ICPMS) that was equipped with a multiple ion counting system. This instrumental setup is ideally suited for precise isotope

dilution measurements of trace elemental quantities, because it provides superior sensitivity and more efficient sample utilization during the analyses compared to quadrupole inductively coupled plasma mass spectrometry (Q-ICPMS) and single collector magnetic-sector ICP mass spectrometry.

2.2 LABORATORY METHODS AND REAGENTS

2.2.1 Laboratory Methods

All blank-critical laboratory work was carried out in Class 10 laminar flow workbenches within a Class 10,000 clean room facility. Hydrazine and its solutions were only handled in conventional exhaust hoods, however, due to the toxicity of this reagent (Mitchell et al., 1980). The mineral acids were purified once by sub-boiling distillation in quartz stills (6 M HCl, 14 M HNO₃) and the water was 18 MΩ-grade from a Millipore purification system. All reagents used for foraminiferal cleaning were of ultra pure quality. The reductive and oxidative cleaning solutions were prepared freshly on the day of use (Martin and Lea, 2002).

2.2.2 Standard Solutions

2.2.2.1 Cd Isotope Standard

A gravimetric “JMC Cd Zürich” solution (Ripperger and Rehkämper, 2007b) with a concentration of 1224.01 µg/g was prepared from 99.999% pure Cd metal pellets (Alfa Aesar Puratronic grade) that had been leached with 0.1 M HNO₃ and cleaned with water and ethanol to remove oxide coatings, prior to dissolution in 2 M HNO₃ (Table 2.1). Further dilutions of this primary solution were used for the calibration of Cd tracer solutions and as Cd isotope standards for MC-ICPMS analyses.

Table 2.1. Average Cd isotope compositions determined for the JMC Cd Zürich standard and the ¹¹⁰Cd-Spike-B.

Solution	n	¹¹⁰ Cd/ ¹¹¹ Cd	¹¹² Cd/ ¹¹¹ Cd	¹¹³ Cd/ ¹¹¹ Cd	¹¹⁴ Cd/ ¹¹¹ Cd
JMC Cd Zürich [§]	56	0.977047 (122)	1.878769 (126)	0.950117 (69)	2.22783 (278)
¹¹⁰ Cd-Spike-B [§]	4	72.7346 (3860)	1.14095 (396)	0.432102 (2712)	0.915444 (6861)

The uncertainties given in the parentheses denote 2 standard deviations (and refer to the last significant digits). n = number of measurements. [§] The isotope data for the JMC Cd Zürich standard were obtained over a period of 11 months by internal normalization relative to ¹¹⁰Cd/¹¹⁴Cd = 0.438564 (Ripperger and Rehkämper, 2007b) with the exponential law. [§] The isotopic data for the spike were obtained on four separate measurement days by external normalization to admixed Ag relative to a value of ¹¹⁰Cd/¹¹⁴Cd = 0.438564 for natural Cd.

2.2.2.2 Ca Isotope Standard

A gravimetric Ca solution (288.73 µg/g) was prepared from NIST SRM 915a Ca, which is a 99.97% pure CaCO₃ powder purchased from the National Institute of Standards & Technology (Table 2.2). Prior to dissolution in 2 M HNO₃, the Ca powder had been dried in an oven at 70°C for four hours and then stored in a desiccator to remove chemically bound water. The calibration of the Ca tracer and further MC-ICPMS analyses utilized solutions that were prepared from this primary stock solution.

Table 2.2. Average Ca isotope compositions determined for the NIST SRM 915a Ca standard and the ⁴³Ca-Spike-B.

Solution	n	⁴² Ca/ ⁴⁴ Ca	⁴³ Ca/ ⁴⁴ Ca
NIST SRM 915a Ca ^s	88	0.312210	0.064800 (63)
⁴³ Ca-Spike-B [§]	11	0.062563 (3228)	4.69550 (1549)

The uncertainties given in the parentheses denote 2 standard deviations (and refer to the last significant digits). n = number of measurements. ^s The isotopic data for the NIST SRM 915a Ca standard were obtained over a period of 4 months by internal normalization to ⁴²Ca/⁴⁴Ca = 0.312210 (Russell et al., 1978) with the exponential law. [§]The isotope data for the ⁴³Ca-Spike-B were acquired over a period of 2 months. The spike was measured relative to NIST SRM 915a Ca using an empirically optimized fractionation factor (see section 2.2.3.2).

2.2.3 Spike Solutions

2.2.3.1 ¹¹⁰Cd Spike Preparation

About 50 mg of ¹¹⁰Cd-enriched metal (95.6% purity; Isoflex Corp., USA) were dissolved in 200 ml of 2 M HNO₃ and the isotope composition and concentration of this solution (hereafter referred to as ¹¹⁰Cd-Spike-A) were determined by mass spectrometry. These results were used to plan the preparation of a more dilute ¹¹⁰Cd-Spike-B solution, which was made up from a suitable volume (~60 µl) of ¹¹⁰Cd-Spike-A that was weighed, dried, and redissolved in ~1000 ml of 2 M HNO₃. Repeated analyses were conducted on four separate days to define the Cd isotope composition of the ¹¹⁰Cd-Spike-B (Table 2.1) relative to the natural reference ratio of ¹¹⁰Cd/¹¹⁴Cd = 0.438564 (Wombacher and Rehkämper, 2004). These analyses used external normalization to added Ag with the exponential law for mass bias correction (Ripperger and Rehkämper, 2007b). The Cd concentration of the ¹¹⁰Cd-Spike-B was

determined by reverse isotope dilution using the gravimetric JMC Cd Zürich solution that was prepared in our laboratory. This solution is ideally suited for the calibration because its Cd concentration is known to within about $\pm 0.02\%$. Repeated analyses of four separate spike-standard mixtures yielded a Cd concentration of 13.189 ± 0.026 ng/g (2s.d.) for the tracer.

Finally, a very dilute ^{110}Cd -Spike-C solution was prepared for the spiking of small samples of foraminiferal tests. To this end, ~ 10 ml of the ^{110}Cd -Spike-B were weighed in and diluted with 2 M HNO_3 to obtain one litre of tracer solution with a Cd concentration of 153.90 pg/g.

2.2.3.2 ^{43}Ca Spike Preparation

About 6 mg of CaCO_3 , isotopically enriched in ^{43}Ca (49.5% purity; Isoflex Corp., USA) were dissolved in 150 ml 2 M HNO_3 . The isotopic composition and concentration of this solution (hereafter referred to as ^{43}Ca -Spike-A) were then roughly determined by MC-ICPMS. Further dilution of this concentrated stock solution served to produce ^{43}Ca -Spike-B. The Ca isotope composition of this solution (Table 2.2) was determined by repeated analyses on 3 separate days relative to the natural reference ratio of $^{42}\text{Ca}/^{44}\text{Ca} = 0.31221$ (Russell et al., 1978). The spike analyses used an optimised fractionation factor that was based on the mean of instrumental mass fractionation factors determined for multiple analyses of a NIST SRM 915a Ca solution conducted on the same day. A Ca concentration of 0.6582 ng/g ± 0.0021 (2s.d.) was determined by reverse isotope dilution for ^{43}Ca -Spike-B, based on replicate analyses of 4 individual spike-standard mixtures.

2.3 SAMPLES AND SAMPLE HANDLING

2.3.1 Samples

Planktonic foraminifers of the species *Orbulina universa* were used throughout this study for method validation. The specimens were picked from the >500 μm size fraction of homogenized sediment material from the Azores Front core KL 88 (34.78° N and 27.66° W, 2060 m water depth; Schiebel et al. 2000).

A number of analyses were carried out on unspiked foraminiferal tests. In this case, sample size ranged from a maximum of about 15 specimens (equivalent to an initial weight of ~ 900 μg CaCO_3) down to only 4 specimens (equivalent to ~ 240 μg CaCO_3). In addition, we performed analyses of 1 and 2 specimens (equivalent to ~ 60 -120 μg CaCO_3), that were first

leached and dissolved according to the standard sample preparation protocol (see section 2.3.2) and then split into 2 or 3 approximately equal aliquots.

The analyses of spiked foraminiferal shells utilized a large homogenized sample of 46 *O. universa* tests. The tests were first leached and dissolved according to the standard sample preparation protocol (section 2.3.2) and the solution was split into 4 approximately equal fractions. These fractions were then spiked and further processed and analyzed as four individual samples.

2.3.2 Cleaning of Foraminiferal Tests

Following picking, the foraminiferal tests were crushed with a Teflon needle, homogenized and transferred to pre-cleaned 1.5 ml centrifuge vials using a moistened brush. A cleaning procedure modified after Boyle and Keigwin (1985/86), Boyle and Rosenthal (1996), Martin and Lea (2002), and Weldeab et al. (2006) was then applied (Table 2.3). The minor modifications pertain to the volumes of cleaning solution that were used (which were adapted to the sample size) and the exact duration of the ultrasonication periods. It is possible, albeit unlikely, that the applied procedure will slightly alter the Cd/Ca ratios of the residual carbonate material (Martin and Lea, 2002; Weldeab et al., 2006). Any small alterations will not be problematic, however, as most laboratories now apply very similar leaching techniques. This ensures that the Cd/Ca data from various sources are comparable, even if the absolute ratios are slightly offset from the native values. Rigorously cleaned tests that are completely free of potentially contaminating phases (such as adhering detrital particles, Fe-Mn oxyhydroxide coatings or residues of organic tissue) are furthermore essential for paleoceanographic studies, which utilize the foraminiferal Cd/Ca ratios as a proxy of seawater nutrient utilization. Without such cleaning, residual contaminants can readily obscure the native Cd/Ca signal of the foraminiferal calcite and produce serious analytical artifacts and erroneous interpretations (e.g., Boyle, 1981; Boyle, 1983).

In a first step (Table 2.3), clays and fine-grained carbonates were removed by rinsing the shell fragments with distilled water and methanol. Each rinse included 30 s of ultrasonication before the supernatant was siphoned off. The shell fragments were then treated with a reductive cleaning solution containing 1 M buffered hydrazine to remove Mn-rich coatings. Following addition of this solution, the samples were placed in a warm (50°C) water bath for 30 min and ultrasonicated and flipped briefly every 5 min. Organic material, as well as any surface organics were removed with an oxidative cleaning solution, that was made up from

50 μl H_2O_2 (25%) and 5 ml NaOH (0.1 M). The treatment consisted of two oxidative cleaning steps, each including the addition of 250 μl cleaning solution, heating of the samples in a warm (50°C) water bath for 10 min as well as ultrasonication and a brief flipping of the centrifuge vials. Multiple water rinses were employed after the reductive and oxidative treatment to remove any suspended impurities and remaining reagents. After transferring the shell fragments to a fresh vial, any remaining organic material and contaminants adsorbed to the shell surfaces were removed by leaching the tests briefly with 0.001 M HNO_3 . In a final step, the shell fragments were rinsed with distilled water and dissolved in 500 μl 0.075 M HNO_3 .

The leaching procedure was typically associated with about 50% of the sample material being lost during cleaning, which is similar to the loss reported in a previous study of benthic foraminifers (Boyle, 1995). This is most likely due to partial dissolution of shell fragments during the reductive treatment and weak acid leach, as well as the loss of small shell particles during solution transfers.

Table 2.3. Procedure used for the cleaning of foraminiferal tests.

Initial Rinse	3 rinses with distilled water (500 µl), ultrasonicate for 30 s each time and pipette off supernatant
	3 rinses with methanol (500 µl), ultrasonicate for 30 s each time and pipette off supernatant
	2 rinses with distilled water (500 µl), ultrasonicate for 30 s each time and pipette off supernatant
Reductive Treatment	<i>Reductive cleaning solution ("RCS")</i> : 93.75 µl of 98.5% anhydrous hydrazine added to a mixture of 1.25 ml 0.25 M citric acid monohydrate and 1.5 ml 25% aqueous ammonium (prepared freshly on the day of use)
	Add 100 µl RCS, place samples in subboiling water bath (~50°) for 30 min, flip and briefly ultrasonicate every 5 min for 30 s and open caps
	Pipette off RCS
	3 rinses with distilled water where vial and cap are filled completely, pipette off supernatant
	2 rinses with distilled water (500 µl), ultrasonicate for 30 s each time and pipette off supernatant
Oxidative Treatment	<i>Oxidative cleaning solution ("OCS")</i> : 50 µl of 25% H ₂ O ₂ to 5 ml 0.1 M NaOH solution (prepared freshly on the day of use)
	Carry out twice: add 250 µl OCS and heat for 10 min, flip and ultrasonicate twice for 30 s and pipette off supernatant
	3 rinses with distilled water where vial and cap are filled completely, pipette off supernatant
	2 rinses with distilled water (500 µl), ultrasonicate for 30 s each time and pipette off supernatant
Sample Transfer	Carry out 3 times: add 100 µl distilled water and immediately transfer suspension to a new vial
	Pipette off excess water from sample in new vial
Weak Acid Leach	Add 250 µl of 0.001 M HNO ₃ , ultrasonicate for 30 s and pipette off supernatant
	2 rinses with distilled water (500 µl), ultrasonicate for 30 s each time, and pipette off supernatant
	Carefully remove any remaining water
Dissolution	Dissolve test fragments in 500 µl of 0.075 M HNO ₃
	Ultrasonicate as long as CO ₂ production increases
	Centrifuge for 5 min at 10,000 g and remove residual particles

2.3.3 Spiking of Samples

The sample solutions in 0.075 M HNO₃ were transferred to 2.5 ml Savillex beakers and split in two parts, whereby the minor aliquot (5%) was spiked with ⁴³Ca-Spike-B and the major aliquot (95%) with ¹¹⁰Cd-Spike-C. To this end, a suitable mass of the ⁴³Ca tracer (~350 mg) was weighed into an empty Savillex beaker and 25 µl of the sample solution were added. The remaining 475 µl of solution were then spiked with a suitable volume (~80 mg) of the ¹¹⁰Cd tracer. The spiked samples were then left on a hot plate to equilibrate for one day prior to evaporation to dryness.

The Ca aliquot did not require further processing and the residue was simply redissolved in ~30 µl 14 M HNO₃ for storage. Just prior to use, the Ca fraction was evaporated to near complete dryness and redissolved in an appropriate volume of 0.1 M HNO₃ to obtain a solution suitable for mass spectrometric analysis. The Cd aliquot was dried with a few drops of 10 M HCl to convert the residue into the chloride form, dried again with one drop 1 M HCl, and finally taken up in 50 µl of 1 M HCl for column chemistry.

2.3.4 Column Chemistry

An ion-exchange chromatography procedure, modified after Rickaby et al. (2000) was used to isolate Cd from the major element Ca as well as from minor matrix elements such as Na, K, Mg, Sr, and others. Biorad AG 50W-X8, 200-400 mesh cation-exchange resin was used in Teflon columns, with 250 µl resin beds and 3.5 ml sample reservoir volumes (Table 2.4). Following loading of the sample solutions, Cd was eluted from the resin with 1 M HCl.

Table 2.4. Column chemistry procedure for the separation of Cd from the calcite matrix.

Bio Rad AG 50W-X8 resin, 200-400 mesh 250 µl resin in shrink-fit Teflon columns	
14 ml 6 M HCl	Resin cleaning
1 ml 1 M HCl	Equilibration
50 µl sample solution in 1 M HCl	Sample loading & Cd collection
150 µl 1 M HCl	Cd collection
150 µl 1 M HCl	Cd collection

The Cd eluates were then evaporated to dryness, dried again with one drop 14 M HNO₃ to remove any residual chloride and finally taken up in ~30 µl 14 M HNO₃ for storage. Just prior to use, the solutions were evaporated to near complete dryness and dissolved in an appropriate volume of 0.1 M HNO₃ to obtain the desired Cd concentration for mass spectrometric analysis. This separation method typically achieved yields of > 90% for Cd.

2.3.5 Mass Spectrometry

All mass spectrometric analyses were carried out with Nu Plasma MC-ICPMS instruments at the ETH Zürich. The isotope dilution (ID) concentration measurements were performed using a multiple ion counting system for Cd and multiple Faraday collectors equipped with 10¹¹ Ω resistors for Ca. All analyses employed a CETAC MCN 6000 desolvator for sample introduction, in conjunction with T1H nebulizers (CETAC) that operated at flow rates of about 100-120 µl/min.

2.3.5.1 Cd Concentration Measurements

The Cd ID measurements utilized 2 data acquisition cycles (Table 2.5). In the first cycle, the ¹⁰⁵Pd ion beam was monitored to correct for the isobaric interference from ¹¹⁰Pd. The second cycle served to simultaneously determine the ion currents of ¹¹⁰Cd and ¹¹¹Cd. Data collection for both cycles comprised 20 integrations of 5 s each. Each Cd analysis was preceded by an on-peak zero determination. This involved an ion beam intensity measurement with the data acquisition routine described above, whilst 0.1 M HNO₃ was aspirated. The Cd analyses were followed by a thorough (5-10 min) washout, whereby the sample introduction system was flushed first with 1 M HNO₃ and then with 0.1 M HNO₃.

Several measurements of a JMC Cd Zürich standard solution were conducted at the beginning of each analytical session, to confirm that the instrument was performing properly. In addition, a mixed Cd-Pd standard solution, which yielded a ¹¹⁰Pd/¹¹⁰Cd ratio of about 0.05 was analyzed, to optimise the parameters of the Pd interference correction (see section 2.3.6.1).

A Cd ID analysis with 40 data acquisition cycles required about 4 min, during which about 400-500 µl of sample solution were consumed. The analyses of spiked samples utilized solutions with total Cd concentrations of ~16 pg/ml (ppt) and thus they consumed about 5 pg of foraminiferal Cd. Such solutions generally yielded ion beam intensities of about 56 x 10³ and 13 x 10³ cps for ¹¹⁰Cd and ¹¹¹Cd, respectively.

Table 2.5. Collector configurations and major molecular interferences for the Cd and Ca isotope dilution analyses

Mass	42	43	43.5	44	55	105	110	111
<i>Cd Analyses</i>								
Cycle 1						IC1		
Cycle 2							IC1	IC0
<i>Ca-Mn Analyses</i>								
Main Run	L4	L1	H1	H4				
Mn run, cycle 1					Ax			
Mn run cycle 2	L4	L1	H1	H4				
<i>Abundances of Cd, Ca and Mn isotopes and isobaric nuclides (in %)</i>								
Cd							12.49	12.80
Pd						22.33	11.72	
Ca (and Mn)	0.67	0.135		2.086	(100)			
<i>Major molecular interferences for Ca, Pd and Cd</i>								
$M^{40}Ar^+$						^{65}Cu	^{70}Zn ^{70}Ge	^{71}Ga
$M^{16}O^+$	^{26}Mg	^{27}Al		^{28}Si		^{89}Y	^{94}Zr ^{94}Mo	^{95}Mo
$M^{14}N^+$	^{28}Si	^{29}Si		^{30}Si		^{91}Zr	^{96}Zr ^{96}Mo ^{96}Ru	^{97}Mo

2.3.5.2 Ca Concentration Measurements

The Ca ID analyses were modified from techniques established for high-precision Ca isotope composition measurements by MC-ICPMS (Halicz et al., 1999). The acquisition of the Ca ID data ("main run") comprised 20 integrations of 5 s each, whereby the ion beam intensities of ^{42}Ca , ^{43}Ca , and ^{44}Ca were measured simultaneously with the Faraday cups of the instrument (Table 2.5). Additionally, $^{87}Sr^{2+}$ was monitored at 43.5 u to enable interference corrections for the doubly charged ions $^{84}Sr^{2+}$, $^{86}Sr^{2+}$ and $^{88}Sr^{2+}$, which have nearly the same mass/charge ratios as $^{42}Ca^+$, $^{43}Ca^+$ and $^{44}Ca^+$, respectively.

For each sample, the main run was immediately followed by a second measurement ("Mn run") that comprised two data acquisition cycles for the determination of Mn/Ca ratios (see section 2.3.6.4). The first cycle served to measure the ion current of ^{55}Mn , whereas the second cycle was used to monitor the ion beam intensities at positions corresponding to 42 u, 43 u,

43.5 u, and 44 u (Table 2.5). The data acquisition sequence comprised 4 integrations of 15 s each for both cycles.

Prior to each main run, on-peak zeros were measured at mass positions 42 u, 43 u, 43.5 u, 44 u and 55 u, whilst 0.1 M HNO₃ was aspirated ("acid run"). These on-peak zero measurements were necessary to correct for baseline aberrations from scattered ⁴⁰Ar⁺ and ⁴⁰Ca⁺ ions. Electronic baselines were furthermore determined for 15 s at the beginning of each measurement (main run, Mn run, acid run), whilst the ion beam was deflected in the electrostatic analyser. Each Mn run was followed by a thorough (~10 min) washout, whereby the sample introduction system was flushed first with 1 M HNO₃ and then with 0.1 M HNO₃.

A complete analysis (including Ca main run and Mn run) required about 6.5 min, during which ~650 µl of sample solution were aspirated, whilst a Ca measurement alone needed only 3 min and ~300 µl of solution. The foraminiferal samples were generally analyzed as solutions with total Ca concentrations of about 1-3 µg/ml (ppm). Calcium solutions with concentrations of ~2 ppm generally yielded total ion beam intensities of about 300×10^{-11} A.

2.3.6 Data Processing

2.3.6.1 Cd Isotope Dilution Data

The raw uncorrected Cd intensity data were processed by an off-line data reduction scheme. First, the measured on-peak zero values were subtracted from the ion beam intensities of ¹⁰⁵Pd, ¹¹⁰Cd and ¹¹¹Cd. This yielded "background-corrected" ¹¹⁰Cd/¹¹¹Cd ratios that were then adjusted to account for the isobaric interference from ¹¹⁰Pd. The correction involved the use of the ¹⁰⁵Pd intensities to calculate ¹¹⁰Pd/¹¹¹Cd ratios, which were corrected for mass discrimination with a power law technique (Wombacher and Rehkämper, 2003) and an empirically optimised mass fractionation factor of ~1.5% per amu mass difference.

A gain correction factor was then applied to all ¹¹⁰Cd/¹¹¹Cd data. This factor was based on the mean ¹¹⁰Cd/¹¹¹Cd ratio obtained for analyses of the JMC Cd Zürich solution during each measurement session, relative to the reference value of ¹¹⁰Cd/¹¹¹Cd = 0.977047 (Table 2.1). In a last step, the mass fractionation factor of the Pd interference correction was optimised, such that the Pd-doped Cd standard yielded gain-corrected ¹¹⁰Cd/¹¹¹Cd data that were indistinguishable from those obtained for the essentially Pd-free JMC Cd Zürich standard.

As long as the ¹¹⁰Pd/¹¹⁰Cd ratios obtained for samples are smaller than those of the Pd-doped Cd standards, it can be assumed that the ¹¹⁰Cd/¹¹¹Cd ratios are properly corrected for contributions from ¹¹⁰Pd. This was the case for all spiked foraminiferal samples, as they

yielded $^{110}\text{Pd}/^{110}\text{Cd}$ ratios that were approximately three times lower (at ~ 0.015) compared to the Pd-doped Cd standards ($\sim 0.04\text{--}0.05$).

2.3.6.2 *Ca Isotope Dilution Data*

The raw Ca isotope data from the mass spectrometric analyses were also processed with an off-line data reduction scheme. This involved the following steps: (1) Subtraction of the “electronic baselines” from the raw ion beam intensities determined during the acid run and the main run; (2) Subtraction of the on-peak zero values obtained during the acid run from the Ca ion beam intensities determined in the main run; (3) This set of raw intensity data was used to obtain Ca isotope ratios for standards that were corrected for interferences from doubly charged ions ($^{84}\text{Sr}^{2+}$, $^{86}\text{Sr}^{2+}$ and $^{88}\text{Sr}^{2+}$) and (4) instrumental mass fractionation. For standards the latter utilized an exponential law normalization relative to $^{42}\text{Ca}/^{44}\text{Ca} = 0.312210$ (Table 2.2). An optimised fractionation factor was used for the instrumental mass bias correction of samples. This factor corresponds to the mean of the instrumental mass fractionation determined for multiple analyses of a NIST SRM 915a Ca solution measured on the same day.

2.3.6.3 *Calculation of Cd and Ca Concentrations and Cd/Ca Ratios*

The Cd and Ca concentrations were determined using a spreadsheet-based ID calculation. For Ca, these calculations were based on the $^{43}\text{Ca}/^{44}\text{Ca}$ ratio, and the $^{42}\text{Ca}/^{44}\text{Ca}$ ratio was used to correct for minor offsets of the data from the spike-sample mixing line by application of a secondary mass fractionation correction. The Cd ID calculation utilized the $^{110}\text{Cd}/^{111}\text{Cd}$ isotope ratio and the data were corrected for the contribution of the procedural blank (see section 2.4.1).

The final Cd/Ca results are reported in units of $\mu\text{mol/mol}$, with a “total uncertainty” that was determined by propagating the individual uncertainties:

$$\text{total uncertainty} = R \cdot \sqrt{\sigma_{\text{B}}^2 + \sigma_{\text{Cd}}^2 + \sigma_{^{43}\text{Ca}}^2 + \sigma_{^{42}\text{Ca}}^2} \quad (2.1)$$

where R is the Cd/Ca ratio of the spiked sample in $\mu\text{mol/mol}$ and σ_{B} , σ_{Cd} , $\sigma_{^{43}\text{Ca}}$, and $\sigma_{^{42}\text{Ca}}$ denote the relative errors from the uncertainty of the Cd blank correction, and from the uncertainties of the Cd and Ca concentrations, based on the within-run statistics of the measured $^{110}\text{Cd}/^{111}\text{Cd}$, $^{43}\text{Ca}/^{44}\text{Ca}$ and $^{42}\text{Ca}/^{44}\text{Ca}$ isotope ratios. The uncertainties of the weights, isotope compositions and concentrations of the isotopically enriched Cd and Ca

tracer solutions can be neglected in this error propagation because they generally have only a very minor (1 to 10%) effect on the total uncertainty of the Cd/Ca data obtained for samples.

2.3.6.4 Mn/Ca Ratios

The Mn/Ca ratios of cleaned foraminifera shells are determined on routine basis in most Cd/Ca studies, to detect samples with high residual Mn contents from incomplete removal of ferromanganese oxyhydroxides (e.g., Boyle, 1983; Martin and Lea, 1998; Rickaby et al., 2000). In our study, the Mn/Ca ratios of the samples were quantified relative to a calibration line defined by three Ca standard solutions doped with different amounts of Mn. The calculations utilized the measured and known $^{55}\text{Mn}/^{44}\text{Ca}$ ratios of the standards and the measured $^{55}\text{Mn}/^{44}\text{Ca}$ ratios of samples, following subtraction of spike-derived ^{44}Ca .

Generally, Mn/Ca values below 100 $\mu\text{mol/mol}$ are considered indicative of sufficient removal of secondary Mn-oxide overgrowth (Boyle, 1983; Martin and Lea, 1998). In this study, Mn/Ca ratios of less than 8 $\mu\text{mol/mol}$ were determined for all analyzed foraminiferal samples, and this demonstrates that our methods are sufficiently effective in removing Mn-rich phases from the carbonate shells.

2.4 RESULTS

2.4.1 Procedural Blanks and Detection Limit

Blank samples (that initially consisted only of distilled acid) were routinely processed alongside “real” samples through the complete procedure that was used to prepare foraminiferal tests for analysis (including cleaning, spiking and column chemistry). The blank samples were then analyzed by ID-MC-ICPMS with the same (or very similar) techniques that were applied for samples. Repeated measurements indicate that the procedural Cd blank of the method was about 112 ± 44 fg (1s.d., $n = 12$) and all concentration data were corrected for this contribution. For samples with 1 pg of Cd, a blank correction of this magnitude generates an uncertainty of about $\pm 4\%$ (1 RSD) for the Cd concentration. The uncertainty of the Cd blank furthermore yields a detection limit of 131 fg (3s.d.).

The Ca blank, which comprises 17 ± 6 ng (1s.d., $n = 3$) has a negligible effect on the measured Ca contents because it constitutes only $\sim 0.2\%$ of the indigenous Ca present in spiked sample solutions. The uncertainty of the blank provides a method detection limit of 18 ng (3s.d.) for Ca.

2.4.2 Analyses of Standard Solutions

Multiple analyses of Cd and Ca standard solutions were carried out on each measurement session prior to the actual ID analyses. The within-day reproducibility obtained for these standard measurements provide an estimate of the precision that can be achieved for sample measurements that are conducted at similar conditions. Note that all quoted uncertainties are 1RSD, unless otherwise stated.

2.4.2.1 Results for JMC Cd Zürich Standards

For solutions with Cd concentrations of 30 to 70 ppt, the standard analyses yielded within-day reproducibilities of about ± 0.1 to ± 0.3 % for the $^{110}\text{Cd}/^{111}\text{Cd}$ ratio (Table 2.6). In this case, a single measurement consumed about 11 to 30 pg of Cd. To evaluate the precision for samples with extremely low Cd contents, we performed analyses of standard solutions with Cd concentrations of about 1 and 5 ppt. The within-day reproducibility for such solutions was somewhat worse at about 1 and 0.4%, but these measurements consumed only 0.5 and 2 pg of Cd, respectively (Table 2.6).

Table 2.6. Within-day reproducibility of the $^{110}\text{Cd}/^{111}\text{Cd}$ ratio obtained for multiple analyses of a JMC Cd Zürich standard solution at various concentration levels.

Concentration (ppt)	n	Range of reproducibility (RSD %)	Natural Cd consumed per analysis (pg)
70	3	$\sim 0.12 \pm 0.08$	$\sim 25\text{-}30$
50	2	$\sim 0.21 \pm 0.05$	~ 20
30	9	$\sim 0.25 \pm 0.07$	~ 12
5	1	~ 0.4	~ 2
1	1	~ 1.0	~ 0.5

n = number of independent measurement sessions.

2.4.2.2 Results for NIST SRM 915a Ca Standards

The majority of the analyses utilized Ca solutions with concentrations of about 2 to 3 ppm, such that the measurements consumed about 600-900 ng Ca. These analyses yielded within-day reproducibilities of about 0.05 to 0.10% for $^{43}\text{Ca}/^{44}\text{Ca}$. The precision of the $^{42}\text{Ca}/^{44}\text{Ca}$ data was slightly worse at about 0.2 to 0.4%, because the baseline is significantly noisier at mass 42.

2.4.3 Accuracy of Isotopic Data - Analyses of Unspiked Foraminiferal Tests

The accuracy of the analytical technique was verified by analyzing multiple samples of unspiked *O. universa* tests that were individually processed in the laboratory. Such measurements constitute a rigorous test for the accuracy of the method because the isotopic analyses of such samples should yield the (known) natural isotope ratios for $^{110}\text{Cd}/^{111}\text{Cd}$ and $^{43}\text{Ca}/^{44}\text{Ca}$, $^{42}\text{Ca}/^{44}\text{Ca}$, whereas any systematic deviation would indicate the presence of analytical artefacts, for example from spectral interferences (Rehkämper et al., 2001).

2.4.3.1 Results for Cadmium

Cadmium isotope data ($^{110}\text{Cd}/^{111}\text{Cd}$) were acquired for 12 unspiked samples of *O. universa* (Fig. 2.1). Measurements that consumed about 3-12 pg Cd showed deviations from the reference value (Table 2.1) of less than 1.3 % and the $^{110}\text{Cd}/^{111}\text{Cd}$ ratios displayed a precision of $\pm 0.5\%$. In addition, we also analyzed samples with only ~ 0.5 to 1.5 pg Cd and found that even such small amounts can be analyzed with an accuracy of better than about $\pm 3\%$ (Fig. 2.1). Most of these low-Cd samples featured $^{110}\text{Cd}/^{111}\text{Cd}$ ratios that were slightly higher than the reference value. This indicates that the deviations are probably due to small residual spectral interferences on the ^{110}Cd ion beam. Further evidence for this conclusion is provided by the observation that the low-Cd samples required relatively large Pd corrections of 20-45% (equivalent to $^{110}\text{Pd}/^{110}\text{Cd}$ ratios of 0.20-0.45), due to decreased Cd contents in relation to the approximately constant levels of Pd present in the sample solutions. In contrast, Pd corrections of only 1-8% were observed for the samples with 3-12 pg of Cd.

Analyses of “real” (spiked) samples will be less affected by these problems. Such samples typically have $^{110}\text{Cd}/^{111}\text{Cd}$ ratios of between 5 and 30, and the latter are significantly larger than the natural value of $^{110}\text{Cd}/^{111}\text{Cd} \approx 1$ due to the addition of the ^{110}Cd tracer (Table 2.1). Measurements of sub-picogram quantities of Cd for “real” samples will thus exhibit ^{110}Cd ion beam intensities that are similar to those, which are obtained for unspiked samples with more than ~ 3 pg Cd.

Over a wide range of spike-sample ratios ($^{110}\text{Cd}/^{111}\text{Cd} \approx 5-30$), the error magnification factor (Riepe and Kaiser, 1966; Colby et al., 1981) of the Cd ID data reduction is less than 2. This means that an uncertainty of about $\pm 1\%$ on the $^{110}\text{Cd}/^{111}\text{Cd}$ ratio translates into an error of about $\pm 1-2\%$ for the Cd concentration. This demonstrates that the accuracy and precision of the analytical data for small spiked samples, with ≤ 1 pg Cd, is governed primarily by the uncertainty of Cd blank correction.

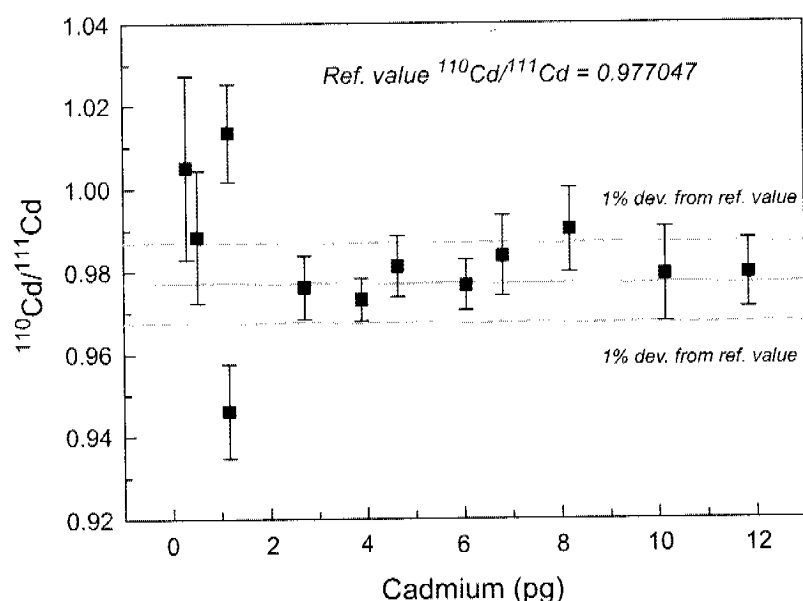


Fig. 2.1. $^{110}\text{Cd}/^{111}\text{Cd}$ ratios obtained for unspiked samples of *O. universa* versus the amount of Cd consumed during analysis. The results show that most measurements which utilized ~3 to 12 pg Cd yielded offsets of less than 0.7% from the reference value (solid line). Deviations of up to 3% were only observed for analyses that consumed less than 1 pg of Cd. The error bars denote the 1σ mean within-run statistics of the isotopic measurements. The dashed lines denote a 1% deviation from the reference value $^{110}\text{Cd}/^{111}\text{Cd} = 0.977047$ (Table 2.1).

2.4.3.2 Results for Calcium

For Ca, we determined the $^{43}\text{Ca}/^{44}\text{Ca}$ and $^{42}\text{Ca}/^{44}\text{Ca}$ ratios of 12 individually processed unspiked samples of *O. universa*. The isotope data were obtained in measurements that utilized sample solutions with Ca concentrations of 0.7 ppm and 3 ppm, such that the analyses consumed about 200 ng and 900 ng Ca, respectively.

The $^{43}\text{Ca}/^{44}\text{Ca}$ ratios obtained for 3 ppm Ca solutions indicate a maximum deviation from the reference value (Table 2.2) of less than 0.05% and the individual data are characterized by a precision of $\pm 0.02\%$ (Fig. 2.2). For analyses of solutions with concentrations of 0.7 ppm Ca, the deviation from the reference value was somewhat larger at about 0.12%, but the RSD value was similar at $\pm 0.01\%$ (Fig. 2.2). The majority of the measured $^{42}\text{Ca}/^{44}\text{Ca}$ ratios showed deviations of less than 0.5% from the reference value and the data provided a RSD of $\pm 0.1\%$.

Over a wide range of spike-sample ratios (that yield $^{43}\text{Ca}/^{44}\text{Ca} \approx 0.2\text{--}2.4$ for samples), errors of $\pm 0.1\%$ and $\pm 0.5\%$ on $^{43}\text{Ca}/^{44}\text{Ca}$ and $^{42}\text{Ca}/^{44}\text{Ca}$, respectively, yielded Ca concentrations that are erroneous by about $\pm 0.2\%$. This indicates that the Ca ID abundance data are also expected to have an accuracy of about $\pm 0.2\%$.

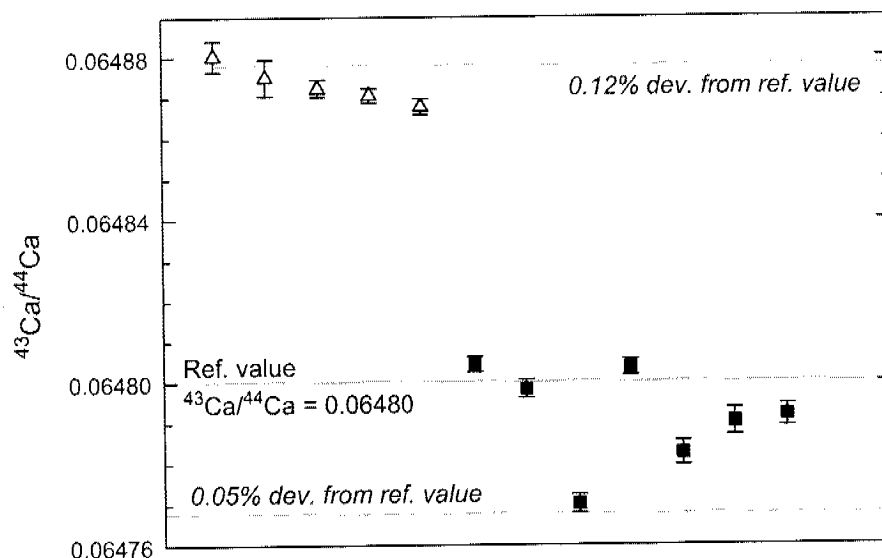


Fig. 2.2. $^{43}\text{Ca}/^{44}\text{Ca}$ ratios acquired for unspiked foraminiferal tests of *O. universa*. The samples were treated and analysed using the standard analytical protocol for Ca but without addition of the ^{43}Ca tracer. The results show that samples display deviations of less than 0.05% from the reference value for analyses, which consumed ~ 900 ng of Ca (filled squares). Deviations of about 0.12% were observed for measurements that consumed only about 200 ng Ca (open triangles). The error bars denote the 1σ mean within-run statistics of the isotope analyses.

2.4.4 Evaluation of Molecular Interferences

Repeated mass scans of sample solutions aliquots were performed to identify elements that are able to generate diatomic oxide-, nitride- or argide-based molecular ions that can interfere with the Ca and Cd ID measurements (Table 2.5). The mass scans focused on the mass ranges 23 to 45 u (for Ca) and 60 to 120 u (for Cd). These analyses revealed only traces of Mg, Al, Si, Cu, Zn, Ge, Zr, Mo, and Ru. In a previous study, Ripperger and Rehkämper (2007b) evaluated the formation rates of these diatomic ions for a wide range of elements at instrumental operating conditions that were nearly identical to those of the present study. They found that the formation rates were generally less than 4×10^{-3} for oxide ions (including the refractory oxides YO^+ and ZrO^+), less than 3×10^{-5} for nitrides and other oxides, and less than 5×10^{-4} for argides. No data are presently available for Mg, Si, and Al but it is not unreasonable to assume that the oxide, nitride, and argide formation rates of these elements

are also adequately described by the maximum values determined for the suite of elements previously investigated by Ripperger and Rehkämper (2007b).

The severity of a molecular interference for a particular analysis can be described by the interference ratio R_I , which is defined as:

$$R_I = \frac{I_x \times \alpha}{I_y} \quad (2.2)$$

where I_x refers to the ion beam intensity of an isotope that forms a molecular interference, α is the formation rate of the molecular ion, and I_y is the intensity of the corresponding Ca, Cd, or Pd ion beam, which is affected by the interference. For all analyzed foraminiferal samples, R_I was found to be less than 10^{-4} for $I_y = {}^{42}\text{Ca}$ and ${}^{110}\text{Cd}$, less than 10^{-5} for $I_y = {}^{43}\text{Ca}$, ${}^{44}\text{Ca}$, and ${}^{111}\text{Cd}$ and less than 10^{-2} for $I_y = {}^{105}\text{Pd}$. At this level, the interferences are far too insignificant to alter the measured Ca and Cd concentrations by more than 0.1%. These results, and the previously discussed measurements of unspiked *O. universa* shells, thus demonstrate that our sample preparation techniques yield solutions, which enable essentially interference-free (and hence accurate) ID concentration analyses of foraminiferal Cd/Ca ratios.

2.4.5 Reproducibility of Cd/Ca Ratios

The reproducibility of the method was evaluated by analyses of four individually spiked aliquots of a single dissolution of *O. universa* tests. The data that were acquired in these measurements, which each utilized about 5 pg and 700 ng of natural Cd and Ca, respectively, are summarized in Table 2.7.

Table 2.7. Reproducibility of Cd/Ca ratios obtained for multiple analyses of *O. universa* tests from the sediment core KL 88.

Sub-Sample	n	Cd/Ca ($\mu\text{mol/mol}$)	Uncertainty ($\mu\text{mol/mol}$)
1/1	1	0.0270	0.0003
1/2	1	0.0269	0.0003
1/3	1	0.0271	0.0003
1/4	1	0.0274	0.0003
Average	4	0.0271 \pm 0.0002 (RSD = 0.7%)	

The average value was calculated as unweighted mean of n independent measurements and the quoted uncertainty denotes 1 standard deviation. The uncertainty of the individual results was calculated as described in section 2.3.6.3.

The analyses yielded an average Cd/Ca ratio of 0.0271 $\mu\text{mol/mol}$ and a reproducibility of about ± 0.0002 $\mu\text{mol/mol}$ (1s.d.), which is equivalent to an uncertainty of $\pm 0.7\%$. This result demonstrates that our method can provide Cd/Ca ratios that have a precision of better than 1%, even for foraminiferal samples with low Cd contents of less than 10 pg.

2.5 DISCUSSION

Previously published methods for the determination of Element/Ca ratios by various ICP-MS techniques and TIMS (thermal ionisation mass spectrometry) are summarized in Table 2.8. Sector field and quadrupole ICP-MS instruments have rapid mass scanning capabilities and they are thus well suited for the simultaneous determination of several Element/Ca ratios, including Li/Ca, Mg/Ca, Sr/Ca, Ba/Ca, Zn/Ca, Cd/Ca, U/Ca and others (Table 2.8). Hence, they have become an important and routine tool for paleoceanographic studies, which utilize and interpret the Element/Ca ratios of foraminiferal calcite, corals, and other carbonate samples. These techniques typically achieve a precision of about 2% for Cd/Ca when more than 15 to 20 pg of Cd are available for analysis (Table 2.8).

Both Lea and Martin (1996) and Yu et al. (2005) also carried out Cd/Ca analyses with only ~ 5 pg of Cd and quoted reproducibilities of about 2 to 5% for these measurements. In comparison, our technique yields data that are precise to about 1% at similar conditions (Tables 2.7, 2.8). Our methods are slightly less precise (but still superior to other techniques) when even smaller amounts of Cd (~ 1 pg or less) are analyzed (Table 2.8) because the reproducibility is then essentially limited by the uncertainty of the blank correction, which is ± 44 fg (1s.d.).

Our total procedural blank is non-negligible because Cd is separated from the calcite matrix by ion-exchange chromatography. This separation also has advantages, however, because it eliminates elements that can generate molecular interferences during mass spectrometry (Table 2.5) and such interferences are likely to be most problematic for samples with low Cd contents. As a result, we have been able to demonstrate that our analyses generate accurate Cd isotope dilution data even for natural calcite samples with < 1 pg Cd (Fig. 2.1), but such rigorous tests have yet to be carried out for the other methods summarized in Table 2.8. This lack of documentation demonstrates that there is a need to establish well-characterized and widely available reference materials that can be used to validate the accuracy (and precision) of Element/Ca ratio measurements for natural carbonates.

The results of this study demonstrate that our technique provides particular advantages for the accurate and precise determination of Cd/Ca ratios for samples with very low Cd contents and/or which are available only in limited quantities. This includes, for example, planktonic foraminifera collected in sediment traps and tows. The methods will also be of interest to isotope laboratories, which already have access to MC-ICPMS instrumentation but not to a quadrupole or sector field ICP-MS instrument. The technique can furthermore be extended to additional elements, such as Li, Mg, Sr, Ba, Zn, and U, which can be (a) spiked with a suitable enriched tracer and (b) sequentially eluted at high yield from the cation-exchange columns that are used for the Cd separation.

Table 2.8. Comparison of various methods used for the determination of Cd/Ca ratios.

	Method* Metal/Ca ratios determined for:	Cd/Ca ($\mu\text{mol/mol}$)	RSD [§] (%)	Sample [§]	Cd (pg) ⁺
This study	ID-MC-ICPMS Cd, Mn	0.027 ~0.005	0.7 ~4	Plankt. F. Cd, Ca Std	~5 ~1
<i>Marchitto, 2006</i>	SF-ICP-MS Li, Mg, Sr, Mn, Fe, Zn, Cd, U	0.096-0.26	1.4-2.7	ME-Std	~13-72
<i>Rosenthal et al., 1999</i>	SF-ICP-MS Mg, Sr, Mn, Cd, U	~0.14	1.7	ME-Std	~16
<i>Lea and Martin 1996</i>	ID-Q-ICP-MS Sr, Ba, Cd	~0.15	~2	ME-Std	~4-30
<i>Harding et al., 2006</i>	Q-ICP-MS Mg, Sr, Mn, Zn, Cd, U	~0.14	1.7	ME-Std	~20
<i>Yu et al., 2005</i>	Q-ICP-MS Li, B, Mg, Sr, Al, Mn, Zn, Cd, U	0.01-0.07 0.07-0.24	4.8 2.4	ME-Std	1-4 4-15
<i>Rickaby et al., 2000</i>	ID-TIMS (Cd), AAS (Ca) Cd		~0.5-1	Cd, Ca Std	~50

* AAS: atomic absorption spectrometry, ID: isotope dilution, MC: multiple collector, Q: quadrupole, SF: sector field. [§] precision of the Cd/Ca analyses. [§] Plankt. F.: planktonic foraminifers, ME-Std: multi-element standard. ⁺ natural Cd consumed for an individual analysis.

2.6 SUMMARY AND CONCLUSIONS

A new method for the determination of the Cd/Ca ratios of foraminiferal tests is presented and validated. The results demonstrate that our analytical techniques permit the determination of foraminiferal Cd/Ca with an accuracy and reproducibility of about $\pm 1\%$, for samples with 3 to 12 pg of natural Cd. Even very small samples of foraminiferal tests with as little as 1 pg of natural Cd can be analysed. In this case, the accuracy and reproducibility is about $\pm 4\%$, mainly due to the uncertainty of the Cd blank correction.

These performance characteristics demonstrate that our method is superior to previously published procedures for the determination of Cd/Ca ratios in foraminiferal tests, with respect to both the quantification limit and the accuracy and reproducibility of the results (Boyle and Keigwin, 1985/86; Lea and Martin, 1996; Rosenthal et al., 1999; Rickaby et al., 2000; Yu et al., 2005; Harding et al., 2006; Marchitto, 2006). Our method is therefore the best available technique for determining Cd/Ca when only limited sample material with low Cd contents is available. This includes, for example, Cd/Ca analyses of *in-situ* sampled planktonic foraminifers (Wichtlhuber et al., 2004).

Acknowledgements

We are grateful to R. Schiebel for kindly sharing sample material and for help with the foraminiferal samples. H. Baur, U. Menet, D. Niederer, F. Oberli, C. Stirling, H. Williams and S. Woodland are thanked for keeping the clean labs and mass specs running. This project has profited from discussions with and the support of A. N. Halliday, J. McKenzie, R. Schiebel and D. Schmidt and the constructive comments of two anonymous reviewers. Financial aid for the study was provided by a grant from the Schweizerische Nationalfond (SNF).

CHAPTER 3

The Cd/Ca Ratios of in-situ Collected Planktonic Foraminiferal Tests

Submitted to *Paleoceanography* as: Ripperger S., Schiebel R., Rehkämper M. and Halliday A.
N. The Cd/Ca ratios of in-situ collected planktonic foraminiferal tests.

Abstract

The Cd/Ca ratios of planktonic foraminiferal tests have been used to reconstruct surface water nutrient utilization and paleoproductivity. The reliability of this proxy has hitherto not been comprehensively studied, however. To fill this gap, we present novel Cd/Ca data for *in-situ* sampled and sedimentary planktonic foraminifers of the species *Globigerinoides ruber*, *Globigerinoides sacculifer*, *Globigerina bulloides*, *Orbulina universa*, and *Globorotalia truncatulinoides* from the Arabian Sea and the North Atlantic. The Cd/Ca ratios obtained for *G. ruber* sampled from the live habitat generally display a correlation with seawater phosphate content but no such trend is observed for *G. sacculifer*. This distinct behaviour may reflect different ecological niches or species-specific incorporation of Cd into the calcite shells of the organisms. The Cd/Ca ratios of *G. ruber*, *G. sacculifer* and *G. bulloides* from surface sediments are consistently higher than those obtained for live collected specimens of the same species. Post-depositional alteration of the tests is unlikely to be responsible for these systematic differences. Rather, they appear to reflect a combination of factors, including the formation of calcite crusts with high Cd contents, the different timescales that are represented by *in-situ* and sedimentary foraminiferal tests, and the dominance of tests from periods of high productivity in sediments. Our results also reveal higher Cd/Ca ratios for live *G. ruber* than for settling tests of the same species. This suggests that planktonic foraminiferal shells are partially dissolved while they individually settle through the water column. Sedimentary tests, however, will be less affected by dissolution processes because they are primarily deposited in mass sinking events, which feature much higher settling velocities than those experienced by single settling shells.

3.1 INTRODUCTION

The geochemistry of cadmium in seawater has attracted significant attention over the past 30 years. This interest is based on the marine distribution of Cd, which resembles that of the macronutrient phosphate (e.g., Boyle et al., 1976; Bruland, 1980). Cadmium is furthermore incorporated into the tests of foraminifera in proportion to the Cd concentration of the ambient seawater (Boyle, 1981). Hence, the Cd/Ca ratios of foraminiferal shells have been used in numerous paleoceanographic studies, as a water mass tracer and to investigate past changes in nutrient utilization. Measurements of Cd in planktonic foraminifers are of particular interest, because such data can provide information on surface water phosphate utilization, which in turn is linked to phytoplankton productivity (Rickaby and Elderfield, 1999; Elderfield and Rickaby, 2000).

A number of results, however, have raised questions regarding the reliability of the Cd/Ca proxy. Artefacts from the contamination of the tests by ferromanganese coatings and other Cd-rich phases have hitherto been assessed only by indirect evidence (Boyle, 1988). It has also been suggested that the dissolution of shells following deposition on the ocean floor may significantly alter the Cd/Ca ratios of foraminiferal tests (McCorkle et al., 1995), analogous to the Mg/Ca values (e.g., Rosenthal and Boyle, 1993).

The use of foraminiferal proxies is furthermore affected by the life cycle during which planktonic foraminifers migrate vertically through the water column. Juvenile individuals of shallow-dwelling species ascend into surface waters, whereas with maturity they descend into deeper waters to reproduce (Hemleben et al., 1989; Schiebel et al., 1997; Schiebel and Hemleben, 2005). Planktonic foraminifers grow their tests by sequentially forming new chambers (primary calcite) and some species also precipitate a gametogenic calcite crust during reproduction and/or secondary calcite crusts in subsurface waters (Bé, 1980; Duplessy et al., 1981; Hemleben et al., 1989; Schiebel et al., 1997). For *G. sacculifer*, compositional differences between primary test walls and secondary calcite crust have been documented for $\delta^{18}\text{O}$ and Mg in specimens retrieved from plankton tows and lab culturing experiments (Duplessy et al., 1981; Spero and Lea, 1993; Nürnberg et al., 1996; Eggins et al., 2003). Surface veneers that are enriched in Mg, Ba, Mn and Zn have also been documented for live sampled tests of *G. ruber* (Eggins et al., 2003). Consequently, different parts of a shell could display distinct Cd contents, which reflect the variable seawater conditions experienced by a foraminifer during its life cycle.

The above concerns regarding the Cd/Ca proxy could be addressed by analyses of planktonic foraminifers that are sampled from the live habitat and comparison of these data with results obtained for samples from the deeper water column and from surface sediments collected at the same location. However, the precise determination of Cd/Ca ratios for *in-situ* collected planktonic foraminifers is technically challenging, because (i) the amount of sample material available for analysis is generally limited and (ii) planktonic foraminiferal calcite has extremely low Cd contents of ~0.002 to 0.1 μmol per mol Ca (Lea, 1999).

In this study, we have carried out such comprehensive analyses. To this end, we used a recently developed method (Ripperger and Rehkämper, 2007a) to obtain Cd/Ca data for *in-situ* sampled *Globigerinoides ruber*, *Globigerinoides sacculifer* and *Globigerina bulloides* from the Arabian Sea and the North Atlantic. For comparison, we also analyzed the same species from core top samples taken at the same location. Our results reveal previously unidentified differences in Cd/Ca ratios between cytoplasm bearing tests ("live specimens"), empty settling tests ("dead specimens"), and shells from surface sediments, as well as species-specific variations.

3.2 SAMPLES

3.2.1 In-situ Samples

The *in-situ* collected planktonic foraminifers were sampled with plankton tows (Schiebel et al., 1995) from both surface (0-100 m water depth, mainly "live" foraminifera) and subsurface waters (100-2500 m water depth, mainly empty settling tests) in the Arabian Sea and North Atlantic (Table 3.1).

The samples from the western Arabian Sea station (WAST) at 16°N, 60°E were collected in March, August and September 1995 during the Meteor cruises M31/3, M32/5 and M33/1, as well as Sonne cruise SO119 in May 1997 (Hiller, 1996; Schiebel and Bayer, 1996; Schiebel et al., 2004). The North Atlantic was sampled in September 1996 during Meteor cruise M36/5 at the BIOTRANS area at 47°N, 20°W (Schiebel et al., 2001).

Table 3.1. Sampling locations and associated seawater parameters for *in-situ* collected planktonic foraminifers analyzed in this study.

Sample	Cruise	Location	Station #	Date	Latitude	Longitude	Net #	Water depth (m)	Species	#	Test size (µm)
5r/1/2/3/4	M 31/3	Arabian Sea	111/2	13.03.95	16.09°N	59.69°E	912	0-200	<i>G. ruber</i>	35	>200
4r/3/4	M 31/3	Arabian Sea	110/4	13.03.95	16.20°N	60.30°E	914	0-100	<i>G. ruber</i>	40	>200
4s/1/2	M 31/3	Arabian Sea	110/4	13.03.95	16.20°N	60.30°E	914	0-100	<i>G. sacculifer</i>	40	>250
4r/1	M 31/3	Arabian Sea	110/4	13.03.95	16.20°N	60.30°E	915	300-500	<i>G. ruber</i>	40	250-315
4r/2	M 31/3	Arabian Sea	110/4	13.03.95	16.20°N	60.30°E	915	500-700	<i>G. ruber</i>	20	250-315
3r	SO 119	Arabian Sea	WAST 7	24.05.97	16.20°N	60.31°E	1284	20-40	<i>G. ruber</i>	25	>315
7r	SO 119	Arabian Sea	WAST 7	25.05.97	16.20°N	60.31°E	1287	0-40	<i>G. ruber</i>	64	>250
7s	SO 119	Arabian Sea	WAST 7	25.05.97	16.20°N	60.31°E	1287	20-40	<i>G. sacculifer</i>	14	>500
1r/1	M 32/5	Arabian Sea	430	01.08.95	17.11°N	60.01°E	979	60-80	<i>G. ruber</i>	20	250-315
1r/2	M 32/5	Arabian Sea	430	01.08.95	17.11°N	60.01°E	979	60-80	<i>G. ruber</i>	14	>315
1s	M 32/5	Arabian Sea	430	01.08.95	17.11°N	60.01°E	979	60-80	<i>G. sacculifer</i>	15	>315
2r/1	M 33/1	Arabian Sea	WAST 601	30.09.95	16.15°N	60.48°E	1007	20-40	<i>G. ruber</i>	40	250-315
2r/2	M 33/1	Arabian Sea	WAST 601	30.09.95	16.15°N	60.48°E	1009	2000-2500	<i>G. ruber</i>	40	250-315
6b	M 36/5	N. Atlantic	354/72	30.09.96	48.60°N	22.38°W	1173	40-80	<i>G. bulloides</i>	41	250-315

Station # = shipboard site number. WAST = western Arabian Sea station. net # = multinet number. # = number of specimen

Globigerinoides ruber (white), *Globigerinoides sacculifer* (without sac chamber), and *Globigerina bulloides* were picked from the >200 μm size fraction to exclude juvenile specimens, and facilitate comparison of the new data with previously published results on, for example, stable isotope ratios. Depending on availability and shell size, 14 to 40 tests were analyzed, which is equal to an initial sample weight of about 200 to 500 μg of CaCO_3 . Only one independent measurement was performed for the majority of *in-situ* samples, because more material was not available for further analyses.

3.2.2 Surface Sediment Samples

The same planktonic foraminifer species were analyzed from the top surfaces of the sediment cores SL 3011-1 (Arabian Sea; Ivanova et al., 2003) and MC 575 (North Atlantic; Kurbjewcit, 2000). Sediment samples were obtained using a multicorer at the same locations as the *in-situ* collected samples from the water column (Table 3.2). The samples were sieved over a 250- μm screen and handpicked to obtain aliquots that comprised about 20 to 300 individuals, which is equivalent to an initial sample weight of about 0.8-4 mg CaCO_3 . Two independent sample fractions were analyzed for each of the three species that were investigated.

Additional specimens of *Orbulina universa* and *Globorotalia truncatulinoides* were analyzed from the North Atlantic core MC 575 (Table 3.2). Forty and 37 tests were picked from the size fraction >250 μm , resulting in initial sample weights of about 1.6 and 3 mg for *O. universa* and *G. truncatulinoides*, respectively.

Mainly sedimentary planktonic foraminifers were used to validate the long-term reproducibility of the methods because *in-situ* collected specimens were too rare to permit repeated analyses. Samples for method validation (*O. universa*) were picked from the size fraction >500 μm from the 0-40 cm interval of the Azores Front core KL 88 (Table 3.2, Schiebel, et al., 2000). The samples comprised 10-23 specimens, which is equivalent to an initial sample weight of about 0.6 to 1.4 mg CaCO_3 .

Table 3.2. Sampling locations for sediment core samples analyzed in this study.

Sample	Core #	Location	Latitude	Longitude	Water depth (m)	Core depth (cm)	Species	Specimens	Test size (μm)
1	KL 88	North Atlantic	34.78°N	27.66°W	2060	0-40	<i>O. universa</i>	46	>500
2/3/4	KL 88	North Atlantic	34.78°N	27.66°W	2060	0-40	<i>O. universa</i>	10	>500
5	KL 88	North Atlantic	34.78°N	27.66°W	2060	0-40	<i>O. universa</i>	12	>500
6/7/8	KL 88	North Atlantic	34.78°N	27.66°W	2060	0-40	<i>O. universa</i>	23	>500
9	SL 3011-1	Arabian Sea	16.53°N	55.33°E	2636	3	<i>G. ruber</i>	50	>250
10	SL 3011-1	Arabian Sea	16.53°N	55.33°E	2636	3	<i>G. ruber</i>	122	>250
11	SL 3011-1	Arabian Sea	16.53°N	55.33°E	2636	3	<i>G. sacculifer</i>	20	>500
12	SL 3011-1	Arabian Sea	16.53°N	55.33°E	2636	3	<i>G. sacculifer</i>	26	>500
13	MC 575	North Atlantic	47.18°N	19.57°W	4577	0-0.5	<i>G. bulloides</i>	50	>300
14	MC 575	North Atlantic	47.18°N	19.57°W	4577	0-0.5	<i>G. bulloides</i>	300	>250
15	MC 575	North Atlantic	47.18°N	19.57°W	4577	0-0.5	<i>O. universa</i>	40	>250
16	MC 575	North Atlantic	47.18°N	19.57°W	4577	0-0.5	<i>G. truncatulinoides</i>	37	>250

3.3 OCEANOGRAPHIC SETTING OF THE SAMPLING AREAS

Physical properties and nutrient distribution in the Arabian Sea are largely influenced by the seasonal oscillation of the monsoon winds (Webster et al., 1998). The summer monsoon (southwest monsoon, SWM) is characterized by strong upwelling and high nutrient concentrations along the Oman margin from May to October (Bauer et al., 1991). Upwelling ceases during October, and the winter monsoon (northeast monsoon, NEM) affects the hydrography of the Arabian Sea from November to March. Relatively calm conditions prevail during the intermonsoon (IMS) in spring, from March to May. The surface water nutrient concentrations are lower during the NEM and IMS than during the SWM because the former periods feature less vigorous water mixing (Garcia et al., 2006).

The BIOTRANS area (47°N, 20°W) in the eastern North Atlantic is situated between the North Atlantic Current (NAC) and the Azores Current (AzC) (Stramma, 2001). Phytoplankton productivity peaks in spring when the upper water column is thoroughly mixed. In summer, a well stratified surface water column causes nutrient depletion and less productive conditions than in spring (Zeitzschel et al., 1998). During autumn the mixed layer deepens again forced by storms. This process is accompanied by the entrainment of nutrients into the mixed layer and stimulation of phytoplankton and zooplankton production (Sellmer et al., 1998; Schiebel et al., 2001).

3.3.1 Seawater Parameters for in-situ Collected Planktonic Foraminifers

Dissolved seawater phosphate concentrations and temperatures that prevailed during the calcification periods of the live collected foraminifers are listed in Table 3.3. At two of the six sampling sites seawater phosphate contents and temperatures were determined during sample collection from seawaters that were sampled along with planktonic foraminifers (hereafter referred as "in-situ" seawater phosphate and temperature). These phosphate concentrations deviate significantly from the average monthly values given in the World Ocean Atlas 2005 (Garcia et al., 2006; Locarnini et al., 2006), but the relative differences between different months are similar. For consistency, we therefore used the phosphate and temperature data from the World Ocean Atlas 2005 throughout this study, if not explicitly stated otherwise. To this end, we calculated the mean phosphate and temperature values for the uppermost 75 m of the water column for each calcification month, to account for the overall depth habitat (~0-80 m) occupied by *G. ruber*, *G. sacculifer* and *G. bulloides* (Schiebel et al., 1997; Schiebel et al.,

2004). Note that the calcification month does not necessarily correspond to the sampling date, because the calcification period is one month for *G. sacculifer* and *G. bulloides*, and two weeks for *G. ruber* (Bijma et al., 1990; Erez et al., 1991; Schiebel and Hemleben, 2005).

Table 3.3. Seawater phosphate contents and temperatures for the calcification months of analyzed *in-situ* foraminifers.

Sample	Species	Calcification Month	Sampling Depth (m)	P 0-75	T 0-75	P in-situ 0-60	T in-situ 0-60	Season
4s/1	<i>G. sacculifer</i>	Feb. / March, 1995	0-100	0.47	25.05	-	-	wNEM / IMS
4r/3, 5r	<i>G. ruber</i>	March, 1995	0-200	0.49	25.23	-	-	wNEM / IMS
7s	<i>G. sacculifer</i>	April / May, 1997	20-40	0.46	26.99	0.12	28.43	IMS / eSWM
3r, 7r	<i>G. ruber</i>	May, 1997	0-40	0.43	27.56	0.12	28.43	IMS / eSWM
1r, 1s	<i>G. ruber, G. sacculifer</i>	July, 1995	60-80	0.77	25.75	0.38	26.64	SWM
2r/1	<i>G. ruber</i>	September, 1995	20-40	0.99	24.67	-	-	ISWM
6b	<i>G. bulloides</i>	September, 1996	40-80	0.29	15.58	0.10	15.26	

P: seawater phosphate concentration in $\mu\text{mol/l}$. T: seawater temperature in $^{\circ}\text{C}$. 0-75: mean phosphate and temperature values for the uppermost 75 m of the water column (Garcia et al., 2006; Locarnini et al., 2006). In-situ 0-60: mean phosphate concentration and temperature for the uppermost 60 m determined during the time of sampling (Zeitischel et al., 1998; Schiebel et al., 2004). Season denotes the Indian Ocean monsoons: wNEM = weak NE monsoon, IMS = intermonsoon, eSWM = early SW monsoon, ISWM = late SW monsoon.

3.3.2 Seawater Parameters for Surface Sediment Samples

The seawater phosphate and temperature data for the sediment core top samples were also derived from the World Ocean Atlas 2005 (Garcia et al., 2006; Locarnini et al., 2006). For the shallow-dwelling species *G. ruber*, *G. sacculifer*, *G. bulloides* and *O. universa* (Schiebel et al., 1997; Schiebel et al., 2001; Schiebel et al., 2004), the seawater parameters were averaged for the uppermost 75 m of the water column of the corresponding most productive time period ("bloom months", Table 3.4). For the long-lived and deep dwelling species *G. truncatulinoides* (Schiebel and Hemleben, 2005), we used the annual mean phosphate and temperature values at 400 m depth.

Table 3.4. Seawater phosphate contents and temperatures for the bloom months of analyzed foraminifers from surface sediments.

Sample	Species	bloom month	P <i>b.m.</i> ($\mu\text{mol/l}$)	T <i>b.m.</i> ($^{\circ}\text{C}$)	P annual ($\mu\text{mol/l}$)	T annual ($^{\circ}\text{C}$)
SL 3011-1	<i>G. ruber</i>	July-Sept.	1.16	21.29	0.95	24.02
SL 3011-1	<i>G. sacculifer</i>	March-May	0.60	25.93	0.95	24.02
MC 575	<i>G. bulloides</i>	May-June	0.32	13.54	0.33	14.04
MC 575	<i>O. universa</i>	July-August	0.23	15.51	0.33	14.04
MC 575	<i>G. truncatulinoides</i>	-	0.72	11.23	0.72	11.23

P *b.m.* and T *b.m.* denote the phosphate concentration and temperature for the bloom month. P and T annual denote the mean annual phosphate content and temperature at the sampling site. All phosphate and temperature values were taken from the World Ocean Atlas 2005 (Garcia et al., 2006; Locarnini et al., 2006) and are average values for the uppermost 75 m, except for *G. truncatulinoides* where the seawater parameters correspond to 400 m water depth.

3.4 ANALYTICAL METHODS

3.4.1 General

A detailed description of the analytical techniques is provided by Ripperger and Rehkämper (2007a). Only a brief summary is thus given here, plus more comprehensive accounts of procedures that are specific to this study.

Following handpicking, the foraminiferal tests were crushed and cleaned with a leaching procedure (Table 3.5) that is similar to techniques used in previous Cd/Ca studies (Boyle and Keigwin, 1985/86; Boyle and Rosenthal, 1996; Martin and Lea, 2002).

Table 3.5. Procedure used for the cleaning of foraminiferal tests.***Initial Rinse***

3 rinses with distilled water (500 μ l), ultrasonicate for 30 s each time and pipette off supernatant

3 rinses with methanol (500 μ l), ultrasonicate for 30 s each time and pipette off supernatant

2 rinses with distilled water (500 μ l), ultrasonicate for 30 s each time and pipette off supernatant

Reductive Treatment

Reductive cleaning solution ("RCS"): 93.75 μ l of 98.5% anhydrous hydrazine added to a mixture of 1.25 ml 0.25 M citric acid monohydrate and 1.5 ml 25% aqueous ammonium (prepared freshly on the day of use)

Add 100 μ l RCS, place samples in sub-boiling water bath ($\sim 50^\circ$) for 30 min, flip and briefly ultrasonicate every 5 min for 30 s and open caps

Pipette off RCS

3 rinses with distilled water where vial and cap are filled completely, pipette off supernatant

2 rinses with distilled water (500 μ l), ultrasonicate for 30 s each time and pipette off supernatant

Oxidative Treatment

Oxidative cleaning solution ("OCS"): 50 μ l of 25% H_2O_2 to 5 ml 0.1 M NaOH solution (prepared freshly on the day of use)

Carry out twice: add 250 μ l OCS and heat for 10 min, flip and ultrasonicate twice for 30 s and pipette off supernatant

3 rinses with distilled water where vial and cap are filled completely, pipette off supernatant

2 rinses with distilled water (500 μ l), ultrasonicate for 30 s each time and pipette off supernatant

Sample Transfer

Carry out 3 times: add 100 μ l distilled water and immediately transfer suspension to a new vial

Pipette off excess water from sample in new vial

Weak Acid Leach

Add 250 μ l of 0.001 M HNO_3 , ultrasonicate for 30 s and pipette off supernatant

2 rinses with distilled water (500 μ l), ultrasonicate for 30 s each time, and pipette off supernatant

Carefully remove any remaining water

Dissolution

Dissolve test fragments in 500 μ l of 0.075 M HNO_3

Ultrasonicate as long as CO_2 production increases

Centrifuge for 5 min at 10,000 g and remove residual particles

About 50% of the foraminiferal material was lost during cleaning of sediment core samples, but when applied to *in-situ* collected foraminiferal shells the losses were typically larger at up to 80%. The latter observation appears to reflect that *in-situ* sampled tests are more readily shattered into extremely small pieces during crushing and cleaning with ultrasonication. These small fragments either dissolved more readily during the treatment or were otherwise lost during solution transfers. In addition, the initial sample sizes were generally smaller for the *in-situ* collected foraminifers than for the sediment samples, which may enhance the effect of calcite dissolution during leaching (Boyle, 1995).

Following cleaning, the tests were dissolved in dilute HNO₃ and split in two aliquots. The major (95%) and minor (5%) aliquots were then spiked with a ¹¹⁰Cd and ⁴³Ca tracer, respectively. The Ca aliquot did not require further processing. Following evaporation to dryness it was simply re-dissolved in an appropriate volume of 0.1 M HNO₃ to obtain a solution suitable for mass spectrometric analysis. Cadmium was separated at high yield (>90%) from the matrix elements by cation-exchange chromatography prior to the mass spectrometry.

Repeated measurements indicate that the method is characterized by a total procedural Cd blank of 112 ± 44 fg (1s.d., $n = 12$), and a detection limit of 131 fg (3s.d. of blank). All Cd concentration data were corrected for this blank contribution. For samples with 1 pg of Cd, a blank correction of this order of magnitude generates an uncertainty of about 4% for the Cd concentration. The Ca blank of 17 ± 6 ng (1s.d., $n = 3$) has a negligible effect on the measured Ca contents as it constituted only ~0.2 % of the indigenous Ca present in the sample solutions.

The isotope dilution concentration measurements were carried out with Nu Plasma MC-ICPMS instruments at ETH Zurich, using a multiple ion counting system for Cd, and multiple Faraday collectors equipped with $10^{11} \Omega$ resistors for Ca. Sample introduction employed a CETAC MCN 6000 desolvator, which was used in conjunction with T1H nebulizers (CETAC) that were operated at flow rates of about 100-120 μ l/min. A single Cd concentration measurement required about 4 min, during which about 400-500 μ l of sample solution were consumed. The majority of *in-situ* samples were analyzed as solutions with total Cd concentrations of ~3-15 pg/ml (ppt). Such analyses generally consumed about 0.5-2.5 pg of natural Cd and yielded total ion beam intensities of about $(3-9) \times 10^4$ cps and $(2-6) \times 10^5$ cps for ¹¹⁰Cd and ¹¹¹Cd, respectively, depending on the spike-sample ratio. Each Ca analysis required about 6.5 min, during which ~650 μ l of sample solution were consumed. *In-situ* samples were analyzed as solutions with total Ca concentrations of about 1-2 μ g/ml (ppm), which yielded total ion beam intensities of about 150 to 300×10^{11} A.

3.4.2 Examination of Foraminiferal Cleaning Procedure

The removal of secondary ferromanganese (Fe-Mn) oxide coatings and organic matter represent important steps to obtain reliable foraminiferal Cd/Ca records. Cleaning procedures therefore include both a reductive and an oxidative cleaning step (Table 3.5). In principle, foraminiferal tests that were collected directly from the water column are not expected to have any Fe-Mn oxide coatings that would need to be removed by reductive cleaning. It is furthermore reasonable to assume that such samples may require more stringent oxidative cleaning because *in-situ* collected foraminifers typically bear more organic matter than foraminifers from sediment cores (e.g., Anand et al., 2003). We therefore carried out experiments, which investigated whether different cleaning procedures are necessary for *in-situ* collected and sedimentary foraminifers.

The effect of the reductive cleaning procedure on *in-situ* collected *G. ruber* and *G. sacculifer* was evaluated by analyses of four individually processed samples from 0-100 m water depth (Table 3.1, samples 4s/1/2 and 4r/3/4). One sample of each species (4s/1 and 4r/3) was subjected to the full cleaning procedure (Table 3.5), whilst the other two samples (4s/2 and 4r/4) were cleaned according to the standard cleaning protocol but without the reduction step. An intensified oxidative treatment was applied to all four samples, which consisted of five (normally two; Table 3.5) leaching steps.

Two experiments were performed to investigate the potential impact of organic matter on the total Cd content of foraminifers. (i) The Cd concentrations of the oxidative cleaning solutions, which had been used to leach the samples 4s/1/2 and 4r/3/4 (Table 3.1), were determined. (ii) The Cd/Ca ratios of *in-situ* collected tests were determined after they had been subjected to 2, 3, 4 or 5 oxidative cleaning steps. Four individually processed sample fractions, each containing 35 specimens of *G. ruber* from 0-200 m depth, were used in this second experiment (Table 3.1, samples 5r/1/2/3/4).

3.4.3 Data Presentation

All Cd/Ca and Mn/Ca data are reported in $\mu\text{mol/mol}$. The quoted uncertainties for the Cd/Ca data were obtained as follows. (i) If only a single analysis was available for a sample, the “total uncertainty” (t.u.) was obtained by propagating the individual uncertainties:

$$\text{total uncertainty} = R \cdot \sqrt{\sigma_B^2 + \sigma_{\text{Cd}}^2 + \sigma_{^{43}\text{Ca}}^2 + \sigma_{^{42}\text{Ca}}^2} \quad (3.1)$$

where R is the Cd/Ca ratio of the spiked sample in $\mu\text{mol/mol}$ and σ_B , σ_{Cd} , $\sigma_{^{43}\text{Ca}}$, and $\sigma_{^{42}\text{Ca}}$ denote the relative errors from the Cd blank uncertainty and from the uncertainty of the Cd and Ca concentrations, based on the within-run statistics of the $^{110}\text{Cd}/^{111}\text{Cd}$, $^{43}\text{Ca}/^{44}\text{Ca}$ and $^{42}\text{Ca}/^{44}\text{Ca}$ isotope data, respectively. (ii) When several measurements were performed for a sample, the error denotes either 1 standard deviation (1s.d.) or the total range of the individual data (hereafter abbreviated as r.i.), depending on the number of independent analyses.

The inter-specimen variability of Cd/Ca data for foraminiferal samples is generally larger than the within-day uncertainty of the measurements (Boyle, 1995). For this study, the best estimate of the inter-specimen variability for surface sediments and *in-situ* samples is given by the relative standard deviation (RSD) obtained for multiple analyses of (i) *O. universa* picked from the sediment core KL 88, and (ii) *in-situ* sampled *G. ruber* (4r/3, 5r), respectively (see section 3.5.2).

3.5 RESULTS

3.5.1 Evaluation of Leaching Procedure

3.5.1.1 Experiments that Monitor the Removal of Fe-Mn Coatings

The leaching experiments yielded similar Mn/Ca ratios for *G. sacculifer* ($\sim 3\text{--}4 \mu\text{mol/mol}$; Table 3.6) regardless of whether the cleaning procedure (Table 3.5) included the reductive cleaning step or not. For *G. ruber*, the sample without reductive cleaning (sample 4r/4) even yielded a significantly lower Mn/Ca ratio compared to that obtained for the reductively cleaned tests (sample 4r/3).

Table 3.6. Effect of the reductive cleaning procedure on Mn/Ca and Cd/Ca ratios.

Sample	Species	RCS	Mn/Ca ($\mu\text{mol/mol}$)	Cd/Ca ($\mu\text{mol/mol}$)
4s/1	<i>G. sacculifer</i>	yes	3	0.0192 ± 0.0002
4s/2	<i>G. sacculifer</i>	no	4	0.5032 ± 0.0127
4r/3	<i>G. ruber</i>	yes	66	0.0109 ± 0.0006
4r/4	<i>G. ruber</i>	no	4	0.3915 ± 0.0117

RCS: reductive cleaning step included in cleaning procedure or not. The uncertainty of the Cd/Ca ratios denotes the total uncertainty (see section 3.4.3).

In general, Mn/Ca values below 100 $\mu\text{mol/mol}$ are considered indicative of sufficient removal of secondary Mn-oxide overgrowths (Boyle, 1983; Martin and Lea, 1998) and all four samples display Mn/Ca ratios (of $<66 \mu\text{mol/mol}$) below this threshold. This indicates that the *in-situ* collected foraminifers have little or no Fe-Mn oxide coating, although the samples were collected from the well oxygenated euphotic zone (0-100 m), where Mn would most likely form insoluble Mn-oxide, that can precipitate onto organic particulate matter (Oasim, 1982; Pomies et al., 2002).

It is noteworthy, however, that foraminiferal tests that were not subjected to a reductive cleaning display Cd/Ca ratios that are more than an order of magnitude larger compared to reductively cleaned samples (Table 3.6). This is most readily explained by (i) contamination of the tests with a Cd-bearing phase, which is not removed by acid or oxidative leaching, or (ii) partial dissolution of Cd-rich organic matter during the reductive cleaning. It cannot be excluded, however, that the low Cd/Ca ratios of samples that have been subjected to a reductive cleaning (4s/1, 4r/3) reflect partial dissolution of the calcite tests, as was previously suggested by Barker et al. (2003) to explain aberrant foraminiferal Mg/Ca data.

3.5.1.2 *Experiments that Monitor the Removal of Organic Material*

In the first experiment, we monitored the Cd/Ca ratios of successive oxidative cleaning solutions that were siphoned off from the samples after leaching. These supernatants yielded decreasing Cd contents with increasing leach number for tests that had not been subjected to a previous reductive cleaning step (Fig. 3.1a). In contrast, consistently low Cd contents of less than 1 pg were recorded for the supernatants of samples, which were cleaned according to our standard procedure, which includes reductive leaching (Table 3.5). The observation that the oxidative cleaning solutions of non-reductively treated samples contain much more Cd (even after five successive 10 min leaches) than reductively cleaned tests, strengthens the conclusion that organic matter is at least partially removed by the reducing agent.

In the second experiment, we monitored the Cd/Ca ratios of samples subjected to two, three, four or five oxidation steps. A low Cd/Ca ratio of 0.0083 ± 0.0013 (t.e.) was obtained for the tests that were treated with three oxidative cleaning steps, but the remaining fractions yielded a nearly constant (4% RSD) Cd/Ca ratio of $0.0129 \mu\text{mol/mol}$ (Fig. 3.1b). This suggests that no improvement in cleaning is gained by the application of more than two oxidation steps. The slightly lower Cd/Ca ratio obtained for the sample that was leached 3

times can be attributed to inter-specimen variability, as the sample fractions had not been homogenized before cleaning.

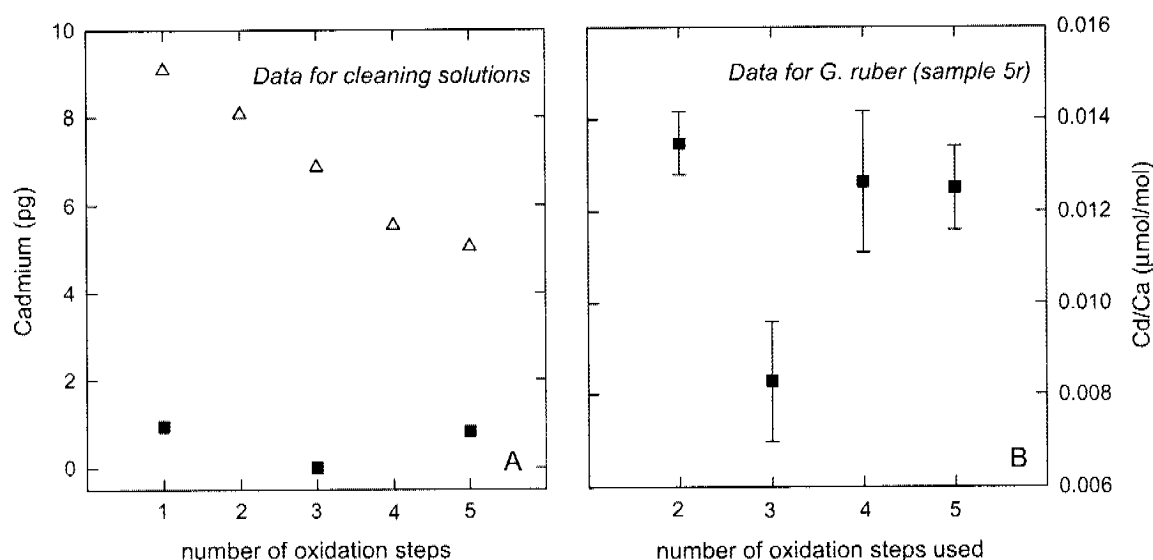


Fig. 3.1. (a) Shown are the Cd contents of oxidative cleaning solutions, after they had been used for leaching of *in-situ* collected foraminifers. Each oxidative treatment lasted for 10 minutes (Table 3.5), after which a fresh batch of cleaning solution was used. Filled squares: data for samples subjected to the full cleaning procedure, including the reductive treatment (Table 3.5). Open triangles: data for samples, which underwent the standard cleaning protocol, but without the reductive step. The error bars for the Cd data are smaller than the symbol size. (b) Measured Cd/Ca ratios for tests of *G. ruber* picked from a plankton net catch at 0-200 m depth. Each sample was treated with a different number of oxidative cleaning steps, each lasting for 10 minutes. Error bars represent the total uncertainty (see section 3.4.3).

3.5.1.3 Summary of the Leaching Experiments

The results of the leaching experiments indicate that the standard cleaning protocol (Table 3.5) is also suitable for cleaning of *in-situ* collected tests. This conclusion is supported by the Mn/Ca ratios that were determined for all collected tests analyzed in this study. For this large group of samples, the Mn/Ca ratios varied between 3 and 108 $\mu\text{mol/mol}$, which does not significantly exceed the threshold value of 100 $\mu\text{mol/mol}$ (Boyle, 1983; Martin and Lea, 1998). A major advantage of using a cleaning procedure that is essentially identical to the standard Cd/Ca leaching protocol, is that this facilitates the comparison of data acquired for *in-situ* collected samples with results for sedimentary foraminifers from this and previous studies.

3.5.2 Analytical Reproducibility and Natural Variability of Cd/Ca Ratios

The long-term reproducibility of foraminiferal Cd/Ca data is based on multiple analyses, conducted over a period of two years, for *O. universa* tests picked from the sediment core KL 88 (Table 3.7). A total of 11 analyses were carried out and these used 8 independent sample fractions that were cleaned and processed separately. The measurements consumed about 5-11 pg and 0.5-1 µg of natural Cd and Ca, respectively, and yielded an average Cd/Ca ratio of 0.0307 ± 0.0038 (1s.d.). This uncertainty, which is equivalent to an RSD value of $\pm 12\%$, is more than an order of magnitude larger than the analytical reproducibility of $\pm 0.7\%$ that was determined in a previous study (Ripperger and Rehkämper, 2007a). Our result is comparable to the reproducibility of about 8% reported by Rickaby et al. (2000) for 4 and 6 replicate picks of foraminiferal tests from a sediment core. Taken together, these data support the finding of Boyle (1995), who concluded that the reproducibility of foraminiferal Cd/Ca ratios is limited by the inter-specimen variability within a sediment sample ("natural variability"), if precise methods are available for the measurements.

Table 3.7. Reproducibility of Cd/Ca ratios (µmol/mol) obtained for multiple analyses of *O. universa* picked from the sediment core KL 88.

Sample	n	Cd/Ca (µmol/mol)	total uncertainty (µmol/mol)
1 [§]	4	0.0271	0.0002*
2	1	0.0261	0.0002
3	1	0.0333	0.0003
4	1	0.0309	0.0002
5	1	0.0362	0.0004
6	1	0.0295	0.0003
7	1	0.0275	0.0004
8	1	0.0348	0.0006
Average KL 88 <i>O. universa</i>	8	0.0307 ± 0.0038 (RSD 12%)	

The average value was calculated as unweighted mean of n independent measurements and the quoted uncertainty denotes 1 standard deviation. Total uncertainty as defined in section 3.4.3. *1 standard deviation. [§] From Ripperger and Rehkämper (2007a).

Repeated analyses were also performed for *in-situ* collected foraminifers from a water depth of 0-200 m. A total of five analyses were carried out for *G. ruber* (sample 5r and 4r/3, Table 3.8), and these utilized five independent sample fractions. The measurements yielded an average Cd/Ca ratio of 0.0116 ± 0.0020 (1s.d.) and a RSD of $\pm 18\%$. This RSD value is similar to but slightly worse than the reproducibility obtained for tests from sediment core sample KL 88 (Table 3.7), but the majority of analyses for *in-situ* collected foraminifers consumed only ~ 0.5 to 0.8 pg of natural Cd.

3.5.3 Cd/Ca Ratios of *in-situ* Collected Planktonic Foraminifers

The Cd/Ca records that were acquired for the *in-situ* collected planktonic foraminifers are summarized in Table 3.8. These analyses focused mainly on the spinose species *G. ruber* and *G. sacculifer* from the Arabian Sea. In order to compare the Cd/Ca ratios of live collected (cytoplasm-bearing) foraminifers to those of dead specimens (settling, empty tests), the results were divided into three categories according to the depth range from which the foraminifers were collected. Category A samples were taken from the respective species-specific natural habitats and are hence expected to consist almost exclusively of live specimens. Category B samples include foraminifera collected from depth ranges that extend to levels marginally below the actual live habitats (0-200 m). Therefore, it can be assumed that these samples consist of live individuals and recently deceased specimens. As the ratio of living-to-dead individuals is estimated to be $\sim 10:1$ at 100 m water depth (Schiebel, 2002), it is reasonable to combine the discussion of Category A and B samples. Samples of Category C were taken well below the natural habitat at depths of 300 to 2500 m and therefore contain mainly dead specimens.

3.5.3.1 Live Foraminifers - Category A (0-80 m) and B (0-200 m)

The live habitats of the analyzed species span a nearly identical depth range of ~ 0 -60 m for *G. sacculifer* and *G. bulloides* and ~ 0 -80 m for *G. ruber* (Schiebel et al., 1997; Schiebel et al., 2004). Samples of *G. ruber* and *G. sacculifer* were obtained during different monsoon seasons (Table 3.3), and the analyzed foraminifers are thus assumed to have calcified under different ecological (e.g., nutrient levels) and physical (e.g., light, temperature) conditions.

Table 3.8. Cd/Ca records obtained for samples of *in-situ* collected planktonic foraminifers.

Sample	Species	Sampling date	Water depth (m)	n	Cd (pg)	Cd/Ca ($\mu\text{mol/mol}$)	total uncertainty	Blank corr. (%)
Category A (0-80 m water depth)								
3r	<i>G. ruber</i>	24.05.97	20-40	1	0.26	0.0040	0.0007	32
7r	<i>G. ruber</i>	25.05.97	0-40	1	1.1	0.0039	0.0002	9
	Average			2		0.0039 \pm 0.0001 (r.i.)		
7s	<i>G. sacculifer</i>	25.05.97	20-40	1	3.8	0.0175	0.0002	3
1r/1	<i>G. ruber</i>	01.08.95	60-80	1	1.3	0.0320	0.0012	8
1r/2	<i>G. ruber</i>	01.08.95	60-80	1	3.0	0.0470	0.0010	4
	Average			2		0.0395 \pm 0.0075 (r.i.)		
1s	<i>G. sacculifer</i>	01.08.95	60-80	1	2.2	0.0198	0.0005	5
2r/1	<i>G. ruber</i>	30.09.95	20-40	1	0.71	0.0162	0.0010	14
6b	<i>G. bulloides</i>	30.09.96	40-80	1	0.40	0.0085	0.0009	23
Category B (0-200 m water depth)								
5r/1*	<i>G. ruber</i>	13.03.95	0-200	1	1.8	0.0135	0.0004	6
5r/2*	<i>G. ruber</i>	13.03.95	0-200	1	0.59	0.0083	0.0007	16
5r/3*	<i>G. ruber</i>	13.03.95	0-200	1	0.76	0.0126	0.0008	13
5r/4*	<i>G. ruber</i>	13.03.95	0-200	1	1.3	0.0125	0.0005	8
4r/3*	<i>G. ruber</i>	13.03.95	0-100	1	0.77	0.0109	0.0006	13
	Average			5		0.0116 \pm 0.0020		
4s/1*	<i>G. sacculifer</i>	13.03.95	0-100	1	5.2	0.0192	0.0002	2
Category C (300-2500 m water depth)								
4r/1	<i>G. ruber</i>	13.03.95	300-500	1	0.22	0.0034	0.0007	35
4r/2	<i>G. ruber</i>	13.03.95	500-700	1	0.27	0.0048	0.0008	29
2r/2	<i>G. ruber</i>	30.09.95	2000-2500	1	0.78	0.0041	0.0002	13

The average Cd/Ca ratios were calculated as unweighted mean of n independent measurements. Total uncertainty as defined in section 3.4.3. Cd (pg) denotes the amount of natural Cd determined in the sample solution by isotope dilution. *Samples that were treated with the standard cleaning protocol, but using three (5r/2), four (5r/3) or five (5r/4, 4r/3, 4s/1) oxidation steps, respectively.

The seasonal variations in ecological conditions (Fig. 3.2a) are generally mirrored by the Cd/Ca ratios of the analyzed tests of live *G. ruber* (Fig. 3.2b). Samples of *G. ruber* (4r/3 and 5r) that were collected in March 1995 during the late NEM and beginning of the IMS, which constitutes a period that is generally characterized by low (near-) surface seawater phosphate concentrations ($\sim 0.4 \mu\text{mol/l}$; Fig. 3.2a), exhibit an average Cd/Ca ratio of 0.0116 ± 0.0020 (1s.d, Fig. 3.2b.). Live *G. ruber* (3r, 7r/1) collected towards the end of the IMS period and the onset of the SWM in May 1997 yielded an average Cd/Ca value of 0.0040 ± 0.0001 (1s.d.), which is the lowest value obtained for live specimens from the Arabian Sea. In contrast, samples of live *G. ruber* (1r) taken during the fully developed SWM in August 1995, where the uppermost water column is characterized by a significantly higher phosphate content ($\sim 0.8 \mu\text{mol/l}$; Fig. 3.2a) exhibit the highest Cd/Ca ratio of 0.0395 ± 0.0075 (r.i.) determined for an *in-situ* collected sample (Fig. 3.2b).

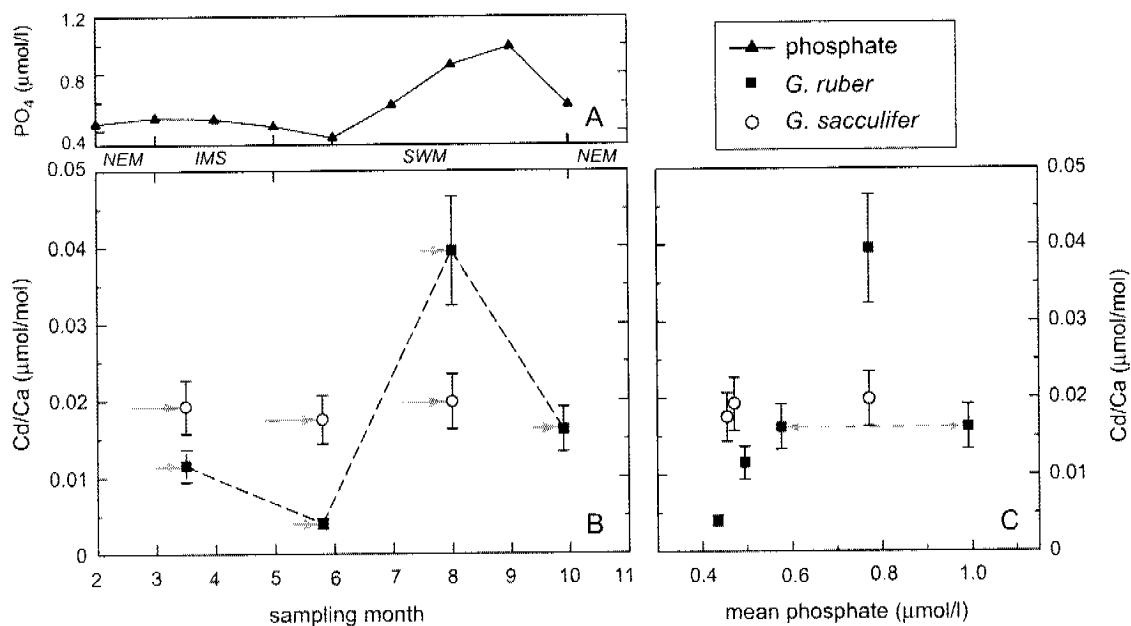


Fig. 3.2. (a) Seawater phosphate concentration for the uppermost 75 m of the water column at 16°N and 60°E , derived from the World Ocean Atlas 2005 (Garcia et al., 2006). (b) Cd/Ca ratios of live *G. ruber* (filled squares) and *G. sacculifer* (open circles) collected in the Arabian Sea versus the sampling month. The arrows denote the life span (calcification period) of the two species, which is a fortnight for *G. ruber* and a full synodic lunar cycle for *G. sacculifer*. The different monsoon seasons are indicated in the upper part of the figure. (c) Cd/Ca ratios of live *G. ruber* (filled squares) and *G. sacculifer* (open circles) versus mean seawater phosphate concentration for the upper 75 m of the water column. The dashed arrows denote the seawater phosphate concentration during September (higher value) and October (lower value) that may be appropriate for the given sample (see text). The uncertainty of the Cd/Ca data is given by the RSD value of $\pm 18\%$ obtained for multiple analyses of *G. ruber* tests of Category B (see section 3.4.3 and Table 3.8).

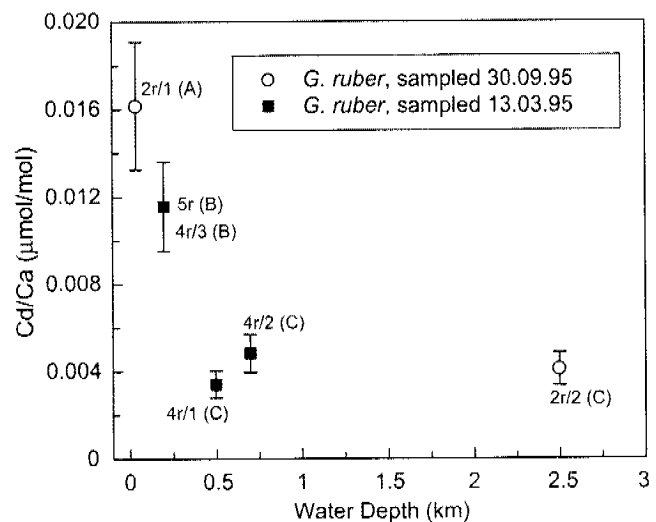
An intermediate Cd/Ca of 0.0162 ± 0.0010 (t.u.) was found for live *G. ruber* (2r/1) sampled during the late SWM, at end of September 1995. The majority of results obtained for *G. ruber* therefore exhibit a correlation of Cd/Ca with surface water phosphate concentrations (Fig. 3.2c). No seasonal trend was observed for the Cd/Ca data obtained for live *G. sacculifer* (Fig. 3.2b) even though the specimens were collected in the Arabian Sea together with *G. ruber*, in March (4s/1), August 1995 (1s), and May 1997 (7s). Tests of *G. sacculifer* from March and August display nearly identical Cd/Ca ratios of 0.0192 ± 0.0002 (t.u.) and 0.0198 ± 0.0005 (t.u.), respectively. A slightly lower value of 0.0175 ± 0.0002 (t.u.) was obtained for the live *G. sacculifer* sampled in May (Fig. 3.2b).

A Cd/Ca value of 0.0085 ± 0.0009 (t.u.) was determined for live specimens of *G. bulloides* (sample 6b) collected in September 1996 from the North Atlantic, where phosphate concentrations are generally lower than in the Arabian Sea (Garcia et al., 2006). However, a comparison of this result with the data for the Arabian Sea samples is not straightforward, due to the different oceanographic settings.

3.5.3.2 Empty Tests of Settling Planktonic Foraminifers - Category C (300-2500 m)

Category C samples are comprised only of *G. ruber* tests from the Arabian Sea. These samples display consistently lower Cd/Ca ratios than their counterparts sampled from the live habitat on the same day (Table 3.8).

Fig. 3.3. Cd/Ca ratios obtained for tests of *in-situ* collected *G. ruber* versus sampling depth. The symbols are plotted at the deepest level of the depth interval over which the samples were collected and are labelled with sample number and category (Table 3.8). Samples taken on the same day are shown as identical symbols (open circles: 30.09.95, filled squares: 13.03.95). The Cd/Ca ratios obtained for *G. ruber* collected from the live habitat (Category A) and from depth intervals extending slightly below the live habitat (Category B) are significantly higher than those obtained for *G. ruber* tests taken well below the live habitat (Category C). The uncertainty of the average Cd/Ca value for the category B sample denotes 1 standard deviation (Table 3.8). The RSD value of $\pm 18\%$ obtained for multiple analyses of this sample was also used to characterize the uncertainty of Category A and C samples, for which only one analysis was performed per sample (see section 3.4.3).



In particular, tests collected from 300-500 m (4r/1) and 500-700 m depth (4r/2) have Cd/Ca ratios of 0.0034 ± 0.0007 (t.u.) and 0.0048 ± 0.0008 (t.u.), respectively, which are about a factor of 2-3 lower than the average value obtained for samples collected from 0-200 m water depth (4r/3 and 5r; Fig. 3.3). A decrease of Cd/Ca ratio with depth is also evident from a comparison of results obtained for live *G. ruber* from 20-40 m (sample 2r/1) and empty shells (sample 2r/2) from the deepest sampling interval (2000-2500 m depth). The latter tests exhibit a Cd/Ca ratio that is about 5 times lower at 0.0041 ± 0.0002 (t.u.) compared to the live specimens (Fig. 3.3).

3.5.4 Cd/Ca Ratios of Planktonic Foraminiferal Shells of Surface Sediments

To facilitate a comparison of Cd/Ca ratios determined for *in-situ* collected and sedimentary tests of planktonic foraminifers, we analyzed several sets of samples from similar locations (Tables 3.1, 3.2). The Cd/Ca data for these surface sediment samples are summarized in Table 3.9. Tests of *G. ruber* and *G. sacculifer* from the top of sediment core SL 3011-1 yielded essentially identical average Cd/Ca ratios of 0.0603 ± 0.010 (r.i.) and 0.0568 ± 0.0084 (r.i.), respectively.

Table 3.9. Results obtained for different species of planktonic foraminifers picked from sediment core tops.

Sample	Species	n	Cd (pg)	Cd/Ca ($\mu\text{mol/mol}$)	total uncertainty	Blank corr. (%)
9	<i>G. ruber</i>	1	5.2	0.0502	0.0006	2
10	<i>G. ruber</i>	1	39	0.0704	0.0008	0.3
Average SL 3011-1, <i>G. ruber</i>		2		0.0603 ± 0.0101		
11	<i>G. sacculifer</i>	1	4.6	0.0484	0.0009	2
12	<i>G. sacculifer</i>	1	17	0.0652	0.0007	0.7
Average SL 3011-1, <i>G. sacculifer</i>		2		0.0568 ± 0.0084		
13	<i>G. bulloides</i>	1	2.1	0.0461	0.0011	5
14	<i>G. bulloides</i>	1	44	0.0488	0.0007	0.3
Average MC 575, <i>G. bulloides</i>		2		0.0475 ± 0.0014		
15	<i>O. universa</i> MC 575	1	27	0.0274	0.0002	0.4
16	<i>G. truncatulinoides</i> MC 575	1	63	0.0718	0.0010	0.2

The average values were calculated as unweighted mean of n independent measurements and the quoted uncertainties denote the total range of the individual data. Total uncertainty as defined in section 3.4.3. Cd (pg) denotes the amount of natural Cd determined in the sample solution by isotope dilution.

Three different species were analyzed from the top of sediment core MC 575 from the North Atlantic. The lowest Cd/Ca of 0.0274 ± 0.0002 (t.u.) was determined for *O. universa* and this result is identical, within the error, to the Cd/Ca data obtained for the same species from sediment core KL 88 (Table 3.7). A somewhat higher Cd/Ca value of 0.0475 ± 0.0014 (r.i.) was measured for *G. bulloides*. The deep dwelling species *G. truncatulinoides* yielded the highest Cd/Ca ratio of 0.0718 ± 0.0010 (t.u.).

3.6 DISCUSSION

3.6.1 Incorporation of Cd into the Shell Calcite of Live Foraminifers

The incorporation of Cd from seawater into the tests of foraminifers can be described by a partition coefficient D_{Cd} (e.g., Lea, 1999). However, different species collected at the same time and location may bear different Cd/Ca ratios as a result of different ecologic demands and characteristics of shell calcification. We therefore investigated whether the measured Cd/Ca ratios of planktonic foraminifers sampled from the water column show any correlation with seawater phosphate concentrations and estimated the partition coefficient for the different species.

3.6.1.1 Correlation of Foraminiferal in-situ Cd/Ca Ratios with Seawater Phosphate

Catalogued monthly average values of seawater phosphate derived from the World Ocean Atlas 2005 were used in the following (see section 3.3.1). In most cases, uncertainties are not specified for the monthly phosphate values (Garcia et al., 2006), but an indication of the magnitude of possible deviations can be obtained for the samples from the M 32/5 and SO 119 cruises (Table 3.1). In this case, the *in-situ* phosphate concentrations are about a factor of 2 to 4 lower than the monthly mean values (Table 3.3). Such deviations of measured phosphate contents from the monthly averages are expected to be especially severe, if seawater phosphate displays large spatial or temporal gradients, as are typical for the Arabian Sea (Webster et al., 1998).

Despite of these uncertainties, the majority of Cd/Ca ratios obtained for live *G. ruber* display a good correlation with seawater phosphate (Fig. 3.2c). Only one sample collected in late September 1995 (2r/1) does not unequivocally follow this trend. However, the seawater phosphate concentrations derived from the World Ocean Atlas 2005 (Garcia et al., 2006) decrease by about a factor of two between September and October. The timing of this strong seasonal change in nutrient levels varies from year to year and the actual phosphate content at

the time of sampling might therefore be better represented by the lower October phosphate concentration ($\sim 0.58 \mu\text{mol/l}$; Garcia et al., 2006), which is plotted alongside the September value (Fig. 3.2c). Application of the October value places this Cd/Ca ratio on the trend defined by the other *G. ruber* data (Fig. 3.2c) and a linear fit to this correlation suggests a relationship of $\text{Cd/Ca} \approx 0.10 * [\text{P}] - 0.04$.

The results obtained for live *G. sacculifer* exhibit a different Cd/Ca to phosphate relationship than the *G. ruber* specimens from the same multinet samples. Inspection of Fig. 3.2c reveals that *G. sacculifer* display nearly constant Cd/Ca values for phosphate contents between 0.4 and 0.8 $\mu\text{mol/l}$. The observed differences in Cd/Ca between *G. ruber* and *G. sacculifer* point towards species-specific mechanisms for the incorporation of Cd into foraminiferal tests, or possibly different ecological niches of these two species. An alternative explanation follows from the observation that *G. sacculifer* has a life span of approximately four weeks (Bijma et al., 1990; Schiebel et al., 2004), whereas the average reproduction cycle of *G. ruber* is two weeks only (Almogi-Labin, 1984; Bijma et al., 1990; Schiebel and Hemleben, 2001). The different Cd/Ca values of *G. ruber* and *G. sacculifer* might therefore reflect differences in the conditions of the ambient seawater during calcification of the shells.

3.6.1.2 Cadmium Partition Coefficients for the *in-situ* Collected Species

It has been suggested, that the incorporation of Cd into shells of *G. bulloides* varies strongly with temperature, and this relationship was defined for temperatures of 4 to 16 °C (Rickaby and Elderfield, 1999). Our results for live *G. bulloides* yield $D_{\text{Cd}} \approx 6$ at a temperature of about 15 °C (see Appendix and Table 3.3). This matches well with the equation $D_{\text{Cd}} = 0.637 * \exp 0.15T$ of Rickaby and Elderfield (1999), which predicts $D_{\text{Cd}} \approx 6$ at 15 °C. The relationship, however, does not hold for live *G. ruber* and *G. sacculifer*, which display D_{Cd} values of about 2 to 8 at significantly higher temperatures of 26.5 to 28.5 °C (Table 3.3). Due to the small number of samples analyzed, the limited availability of *in-situ* phosphate data, and the narrow temperature range, we cannot rule out or establish a temperature dependence of D_{Cd} for *G. ruber* and *G. sacculifer*. This implies, that any temperature-driven differences for the incorporation of Cd into foraminiferal shells will only be of minor importance for the *in-situ* collected tests from the Arabian Sea (Table 3.1), as the variations in temperature are very small (Table 3.3).

3.6.2 Cd/Ca Ratios of Settling Shells

The vertical sinking velocity of large foraminiferal shells ($>200\text{ }\mu\text{m}$) is up to 500 m per day (Schiebel and Hemleben, 2001). Consequently, the settling time for the analyzed tests of *G. ruber* (Category C, Table 3.8) between the live habitat in the upper 80 m and 2500 m is about 5 days. It can hence be assumed that both live specimens and empty tests, which were collected well below the live habitat on the same day, calcified under similar ecological conditions. Both types of samples should therefore display similar Cd/Ca ratios.

Inspection of Fig 3.3 reveals, however, that settling shells (Category C) of *G. ruber* collected from depths $>300\text{ m}$, display significantly lower Cd/Ca ratios than their counterparts from the live habitat. Preferential loss of Cd and/or selective dissolution of Cd-enriched calcite phases during sinking of the tests through the water column may be responsible for this observation. This assumption is supported by earlier findings, which suggest that the dissolution of calcite shells occurs primarily in the twilight zone, between 100 m and 1000 m water depth (Schiebel, 2002; Schiebel et al., 2007).

A preferential enrichment of Cd at sites in the calcite structure of the shells, which are more susceptible to dissolution could account for the preferential loss of Cd relative to the major element Ca. This could be explained by different distribution coefficients of Cd into the different parts of the calcareous test wall (e.g., microgranular versus cubedral; Hemleben, et al., 1989, and references therein). It is conceivable, that the incorporation of Cd into the outer calcite wall is less pronounced than into the inner wall, as the latter is placed closer to the foraminiferal cytoplasm (which may contain higher Cd concentrations than the shell). The inner test wall might also be more prone to dissolution effects, because of the random crystallographic orientation of the calcite crystals and because partial dissolution of tests could be related to changes in the microenvironment (e.g., decreasing pH) within the foraminiferal shells during bacterial remineralization of remaining cytoplasm (Schiebel et al., 2007). Alternatively, Cd could be enriched at crystal edges and/or lattice dislocations in the shell, which are likely to be more effected by dissolution processes.

3.6.3 Cd/Ca Ratios of in-situ Collected and Sedimentary Foraminiferal Tests

A comparison of the Cd/Ca data reveals that foraminiferal tests from surface sediments have consistently higher Cd/Ca ratios than *in-situ* collected specimens (Fig. 3.4). In the following, we discuss this difference for both live foraminifers and settling shells, and we evaluate if the Cd/Ca ratios of sedimentary tests are biased by secondary alteration. Such an

evaluation is of particular significance, as secondary alteration might render the Cd/Ca data of planktonic foraminiferal shells unsuitable for proxy studies.

3.6.3.1 Comparison of Cd/Ca Ratios obtained for Live Foraminifers and Surface Sediments

For the same species, foraminiferal tests from surface sediments exhibit Cd/Ca ratios that are about a factor of 1.5 to 15 higher compared to the shells of live foraminifers (Fig. 3.4). It is possible that this difference reflects post-depositional alteration of the tests, for example by precipitation of Cd-rich mineral phases from pore waters. Pore waters of surface sediments (0-0.5 cm) have Cd contents of 0.7-1.6 nmol/kg (e.g., Tachikawa and Elderfield, 2002), which are about an order of magnitude higher than surface water Cd concentrations of the North Atlantic and Arabian Sea (Saager et al., 1992; e.g., Ripperger et al., 2007).

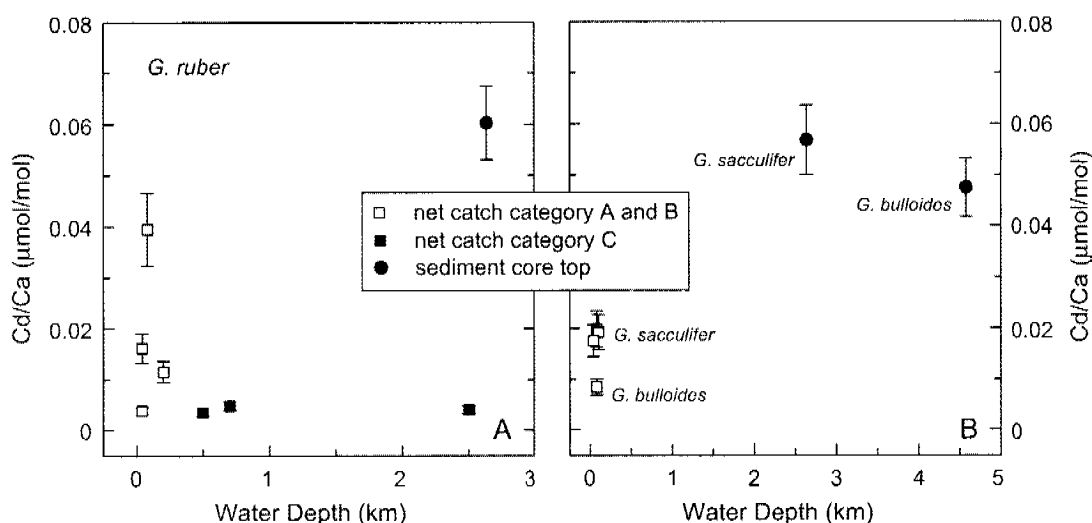
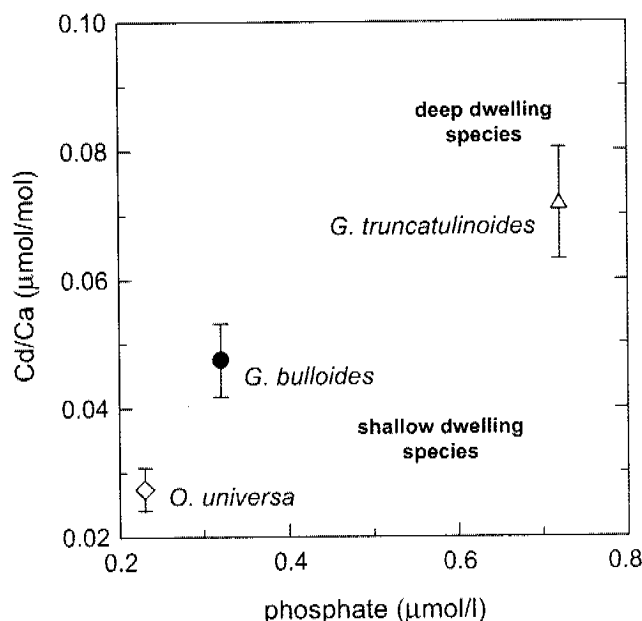


Fig. 3.4. Cd/Ca ratios obtained for different species of foraminifera from plankton net tows (squares) and sediment core tops (filled circles) versus sampling depth. The *in-situ* collected samples and corresponding sediment core tops are from approximately the same location. The symbols for the *in-situ* collected samples are plotted at the deepest level of the depth interval over which the samples were collected (Table 3.8). (a) Cd/Ca ratios obtained for *G. ruber* tests from a sediment core top and from plankton net tows conducted in different months versus water depth (for detailed information see Table 3.8). (b) Cd/Ca ratios determined for *G. sacculifer* and *G. bulloides* versus water depth. The uncertainty of the Cd/Ca data obtained for fossil shells and *in-situ* collected samples denotes the RSD obtained for multiple analyses of *O. universa* from sediment core KL 88 ($\pm 12\%$) and *in-situ* sampled *G. ruber* ($\pm 18\%$, samples 4r/3, 5r), respectively (for detailed information see section 3.4.3).

The results obtained for the sediment core MC 575 reveal, however, that planktonic foraminiferal species with different seasonal occurrences and depth habitats bear different sedimentary Cd/Ca ratios, which follow seawater phosphate concentrations (Tables 3.4 and 3.9, Fig. 3.5). This indicates that the Cd/Ca ratios of tests from surface sediments are not

significantly overprinted by sedimentary pore waters but reflect primary (shell formation) processes.

Fig. 3.5. Sedimentary Cd/Ca ratios obtained for three different species analyzed from the sediment core top MC 575 versus seawater phosphate concentration. The latter was derived from the World Ocean Atlas 2005 (Garcia et al., 2006) and corresponds to the mean phosphate concentration prevailing during the species-specific bloom month and at the species-specific habitat.



In particular, for most of the year *G. truncatulinoides* lives and calcifies its shell in deeper waters (Schiebel et al., 2002; Schiebel and Hemleben, 2005) that are characterized by higher Cd concentrations than surface waters (e.g., Bruland, 1980; De La Rocha, 2003). This signal is preserved in sedimentary tests of *G. truncatulinoides*, which display significantly higher Cd/Ca ratios than shells of the shallow-dwelling species *G. bulloides* and *O. universa* from the same core top (Table 3.9, Fig. 3.5). The Cd/Ca ratio of *O. universa* tests was furthermore observed to be about 40% lower compared to *G. bulloides*. This offset may reflect the different ecological and trophic demands of these two species. *O. universa* is a tropical to subtropical species that generally calcifies after the spring bloom in North Atlantic (Schiebel and Hemleben, 2000), when surface waters are warm, well stratified and depleted in phosphate (Table 3.4). In contrast, *G. bulloides* is most frequent when vigorous mixing of the upper water column occurs and advection of phosphate-rich subsurface waters is observed (Schiebel and Hemleben, 2000). It is also possible, however, that the different Cd/Ca ratios of *O. universa* and *G. bulloides* tests reflect a lower partition coefficient D_{Cd} for the symbiont-bearing species *O. universa* (Mashiotta et al., 1997). In any case, these relatively small primary differences between *G. truncatulinoides*, *G. bulloides* and *O. universa* tests from the same core top (Fig. 3.5) would probably not be visible, if the Cd/Ca ratios had been significantly modified by secondary alteration. In summary, we therefore regard secondary

alteration as an unlikely explanation for the observed offsets of Cd/Ca data for *in-situ* collected and sedimentary foraminiferal tests (Fig. 3.4). The further discussion therefore focuses on three "primary" mechanisms that can account for these offsets and which have less severe consequences for the proxy application of Cd/Ca ratios.

(i) Tests of live and sedimentary planktonic foraminifers may bear different calcite phases. It has been suggested that shells of planktonic foraminifers, such as *G. bulloides*, *G. sacculifer* and *G. ruber*, that underwent reproduction consist of two calcite types: a primary calcite that forms the chamber walls and a gametogenic (GAM) calcite crust, which is precipitated during reproduction (Bé, 1980; Lohmann, 1995; Schiebel et al., 1997). Such a layer of GAM calcite can add about 30% in weight to the primary calcite of a test, as shown for *G. sacculifer* (Bé, 1980). The reproduction of the analyzed species typically takes place near the thermocline (~60-100 m; Schiebel and Hemleben, 2005) where the Cd concentrations are somewhat higher than in shallow surface waters (e.g., Boyle et al., 1976; Saager et al., 1992; De La Rocha, 2003). A GAM calcite crust or any other secondary calcite that forms at subsurface waters is therefore likely to be enriched in Cd relative to the primary calcite, based on the (reasonable) assumption that both types of calcite feature similar distribution coefficients for the incorporation of Cd.

The shells from surface sediments analyzed in this study are assumed to bear both primary and GAM calcite phases, as the majority of tests are from adult (i.e., large tests sizes; Hemleben et al., 1989, Bijma et al., 1990) specimens that likely underwent reproduction. The presence of GAM calcite crusts on tests of live foraminifers can also be assumed for adult (large) specimens. For *G. bulloides*, the reproduction rate of specimens with tests larger 150 μm is nearly 100% (Schiebel et al., 1997), whereas for *G. sacculifer* the reproduction rate increases exponentially between a test size of ~300-400 μm and is about 80 to 100% for tests as large as about 500 μm (Bijma and Hemleben, 1994).

Taking into account the test size of the analyzed live specimens we can hence assume that the majority of *G. bulloides* specimens from sample 6b and most *G. sacculifer* specimens from samples 1s, 7s (test size >315 μm and >500 μm , respectively) underwent reproduction. In addition, spines were not observed on most of these large *G. bulloides* and *G. sacculifer* tests. This supports the conclusion that the majority of the specimens underwent gametogenesis, as spines are generally resorbed during reproduction (Bé, 1980; Hemleben et al., 1989). Although these live collected *G. bulloides* and *G. sacculifer* tests are therefore likely to bear GAM crusts the Cd/Ca ratios of these samples are nonetheless about a factor of three to five lower compared to sedimentary tests (Fig. 3.4). The same offset in Cd/Ca was

observed for the live *G. sacculifer* tests of sample 4s/1 (Fig. 3.4), but these shells are smaller ($>250\ \mu\text{m}$) and some (but not all) of the specimens were observed to bear spines. This indicates that this sample is comprised of tests both with and without GAM calcite (cf., Bijma and Hemleben, 1994).

Taken together, our data thus indicate that the formation of GAM calcite crusts does not account for the observed offsets in Cd/Ca between the analyzed sedimentary and live *G. bulloides* and *G. sacculifer* tests. A more general conclusion should not be drawn from these data, however, given that the formation of GAM calcite and other secondary calcite crusts is species-specific. The *G. sacculifer* results must furthermore be viewed with caution, as the Cd/Ca ratios of these samples were not observed to correlate with seawater phosphate (Fig. 3.2).

(ii) Both sets of samples cover different time periods. Planktonic foraminifers from surface sediments represent sedimentation over time periods of several hundred to thousands of years (Manighetti et al., 1995; Barker et al., 2007), and the Cd/Ca ratios of such samples thus integrate over long-term changes in Holocene climate, hydrography and the trophic state of surface waters. This includes periods of enhanced monsoon activity as well as variable seawater nutrient concentrations (Burns et al., 2002; Mayewski et al., 2004).

(iii) Foraminiferal shells that were calcified during seasons of enhanced planktonic bio-productivity are expected to dominate in surface sediments. In the Arabian Sea, *G. ruber* and *G. sacculifer* are most abundant during the late SWM and during late NEM to spring IMS, respectively (Schiebel, 2002; Schiebel et al., 2004). In the North Atlantic *G. bulloides* is most frequent during the spring (Schiebel and Hemleben, 2000; Schiebel et al., 2001). In all three cases, the maximum abundances of the foraminifers occur at times of enhanced nutrient, and by inference Cd, concentrations (Garcia et al., 2006) that are characterized by phytoplankton blooms and associated with mass sinking events (Fowler and Knauer, 1986; Schiebel, 2002; De La Rocha, 2003).

Most of the analyzed live collected samples, however, did not calcify during seasonal peaks of seawater phosphate and Cd contents and hence they do not reflect the conditions that prevail during periods of mass production. In particular, this is true for (i) the tests of live *G. sacculifer* (sample 1s) that were collected in August in the Arabian Sea (Table 3.3), and (ii) the tests of live *G. bulloides* from the North Atlantic (sample 6b), which calcified in late September when the seawater phosphate concentrations are lower than during peak production in spring (Garcia et al., 2006). In addition, we observed that the live *G. ruber* tests of sample 1r, which were collected in the Arabian Sea in August (Table 3.1) and that calcified

during the fully developed SWM in July (Table 3.3), display the smallest offset to the sedimentary Cd/Ca value (Fig. 3.4). The small offset may reflect that this single sample did not fully capture the maximum nutrient levels that prevailed during the bloom months of *G. ruber* from July to September (Table 3.3).

In contrast, the proposed mechanism is not in accord with the observation that the live *G. sacculifer* samples 4s/1 and 7s were both obtained during bloom months (March and May; Table 3.3) but display the same offset to the sedimentary Cd/Ca ratio (Fig. 3.4) as the *G. sacculifer* sample 1s, which is from a non-bloom period (Table 3.3). It is possible, however, that this discrepancy is due to the non-systematic behaviour of *G. sacculifer*, which forms tests that do not display a correlation of Cd/Ca ratio with the seawater phosphate content (Fig. 3.2).

In summary, this suggests that the dominance of tests from time periods with high nutrient levels in the sedimentary record may account for some but not for all of the observed discrepancy in Cd/Ca ratios between live specimens and tests from sediment core tops. This discrepancy is most likely caused by a combination the mechanisms that were discussed above.

3.6.3.2 Comparison of Cd/Ca Ratios Obtained for Settling Shells and Surface Sediments

The large difference in Cd/Ca between settling shells and tests from surface sediments (Fig. 3.4) indicates that sedimentary shells are less affected by the dissolution processes, which are thought to reduce the Cd/Ca ratios of slowly settling individual tests (see section 3.6.2). The deposition of surface sediments is dominated by mass sinking events following phytoplankton blooms (Schiebel, 2002). Such mass sinking events are accompanied by high sinking velocities and a substantial fraction of the phytoplankton therefore reaches the ocean floor as relatively well preserved particles (Fowler and Knauer, 1986; Schiebel, 2002).

The analyzed empty foraminiferal tests were not collected during such mass sinking events, however. In general, settling plankton blooms have only rarely been sampled with net hauls, due to their unpredictable and rapid occurrence (Schiebel, 2002). It is therefore reasonable to assume that the settling tests of this study were exposed to dissolution for a longer time, due to the much slower sinking velocities of single shells.

3.7 SUMMARY AND CONCLUSIONS

In order to further the basic understanding of the Cd/Ca proxy and its application to planktonic foraminifers, we have determined Cd/Ca ratios for tests of *G. ruber*, *G. sacculifer* and *G. bulloides* from both plankton net tows and sedimentary core tops that were taken at the same location.

Live (cytoplasm bearing) specimens of *G. ruber*, which were sampled in the Arabian Sea during different monsoon seasons, bear significantly different Cd/Ca ratios that appear to reflect seasonal changes in seawater phosphate concentrations. Such a correlation of Cd/Ca and seawater phosphate content is not observed for *G. sacculifer*. This indicates that vital effects or different ecological niches may be responsible for the different Cd/Ca systematics of *G. ruber* and *G. sacculifer*.

The Cd/Ca data obtained for *G. ruber* reveal differences between live specimens and empty tests that were sampled from subsurface waters. The latter exhibit Cd/Ca values that are about 50 to 80% lower compared to shells sampled from their live habitat. This suggests that the tests are partially dissolved while settling through the water column.

The observation that live specimens of *G. ruber*, *G. sacculifer* and *G. bulloides* have significantly lower Cd/Ca ratios than tests from surface sediments is unlikely to be due to post-depositional alteration of the shells, for example by Cd-enriched pore waters. This conclusion is supported by the observation that fossil tests of *G. bulloides*, *G. truncatulinoides* and *O. universa* from the same sediment core top show distinct differences in Cd/Ca that mirror the specific ecological demands of these species. Such differences are not expected to be discernible if modification of the Cd/Ca ratios by secondary alteration is an important process. A combination of different factors can, however, account for the distinct Cd/Ca systematics of sedimentary and live collected foraminiferal tests. (i) Samples from the water column and surface sediments may contain variable amounts of planktonic foraminifers that underwent reproduction and precipitated a gametogenic calcite crust within subsurface waters with elevated Cd concentrations. (ii) Surface sediment samples integrate over longer time periods and the foraminifers may thus record long-term changes in Holocene climate and monsoon strength. (iii) The majority of foraminiferal tests deposited in surface sediments were calcified during periods of high productivity and seawater nutrient concentrations (Fowler and Knauer, 1986; Schiebel, 2002), while most of the live collected samples are not representative of such bloom seasons.

The large difference in Cd/Ca that is evident for sedimentary and settling shells of *G. ruber* indicates that the former are significantly less affected by the dissolution processes, which take place during settling of the shells through the water column. This distinct behaviour is most readily explained by the different sinking velocities of the tests. The deposition of surface sediments takes place mainly during mass sinking events that follow phytoplankton blooms which are associated with high sinking velocities. Dissolution of rapidly settling tests is less pronounced than dissolution of individually, slowly sinking tests analyzed in the present study (cf., Schiebel, 2002).

Overall, the present investigation has enabled us to identify clear differences in foraminiferal Cd/Ca ratios for tests of live and deceased specimens, as well as surface sediments, but the identification of the exact mechanisms responsible for these variations remains speculative at present. Further studies are needed to firmly establish the observed trends and their causes. Further progress is expected by increasing the sampling density of live collected foraminifers during the species-specific blooms. Analyses of empty tests from mass sinking events, as well as investigations of gametogenic calcification in lab-culturing experiments are also expected to yield further insights. Distinct chamber and chamber-wall layer Cd contents may be resolvable with laser-ablation ICP-MS or ion probe analyses of individual shells, as has been demonstrated for other foraminiferal trace elements, such as Mg, Li, Mn, Ba, Zn and Sr (Eggins et al., 2003; Hathorne et al., 2003). If such measurements would reveal differences in Cd/Ca of different parts of the shell (e.g., outer and inner calcite layers; primary calcite and GAM calcite crusts), different element ratios could be attributed to effects of shell formation and dissolution.

Our data also support the conclusion that the Cd/Ca ratios of fossil foraminiferal shells can be used to reconstruct past seawater phosphate concentration at times of maximum productivity. In combination with knowledge of the ecological demands of particular species it may therefore be possible to make inferences on the extent of seasonal variations in nutrient utilization.

Appendix

For a trace element, the relationship between its concentration in the shell calcite of foraminifera and seawater can be described by a partition coefficient D (e.g., Lea, 1999). For the incorporation of Cd into foraminiferal calcite, the partition coefficient D_{Cd} is defined as (see Rickaby and Elderfield, 1999):

$$D_{Cd} = \frac{\left(\frac{Cd}{Ca}\right)_{\text{foram}}}{\left(\frac{Cd}{Ca}\right)_{\text{sw}}} = \frac{\left(\frac{Cd}{Ca}\right)_{\text{foram}}}{\left(\frac{Cd}{P}\right)_{\text{sw}} \cdot \frac{[PO_4]_{\text{sw}}}{[Ca]_{\text{sw}}}} \quad (\text{A3.1})$$

where $(Cd/Ca)_{\text{foram}}$ and $(Cd/Ca)_{\text{sw}}$ denote the Cd/Ca ratio of foraminifera and seawater, respectively; $[PO_4]_{\text{sw}}$ denotes the seawater phosphate concentration prevailing at the time of shell calcification. Here, we assumed a constant Ca^{2+} seawater concentration of $[Ca]_{\text{sw}} = 1.054 \times 10^4 \mu\text{mol/l}$ (see Rickaby and Elderfield, 1999).

The relationship of seawater Cd and P was modelled by Elderfield and Rickaby (2000) on the assumption of closed system Rayleigh fractionation:

$$\left(\frac{Cd}{P}\right)_{\text{sw}} = \left(\frac{Cd}{P}\right)_{\text{DSW}} \cdot \frac{1}{\alpha} \cdot \left(\frac{1-f^\alpha}{1-f}\right) \quad (\text{A3.2})$$

where $f = [P]_{\text{sw}} / [P]_{\text{DSW}}$ and $[P]_{\text{sw}}$, $[P]_{\text{DSW}}$ denote the phosphorus concentrations of seawater where the foraminifera calcified and of deep seawater ($\sim 3.3 \mu\text{mol/kg}$), respectively.

The fractionation factor α describes the preferential incorporation of Cd relative to P into particulate organic matter. A fractionation factor of 2.5 and 2 was used for the calculation of D_{Cd} for the North Atlantic and Arabian Sea samples, respectively (see Elderfield and Rickaby, 2000). The Cd and P concentrations of deep seawater were estimated as 1.2 nmol/kg and $3.3 \mu\text{mol/kg}$, respectively. To calculate the D_{Cd} values presented in section 3.6.1.2, mean in-situ seawater phosphate contents for the uppermost 60 m of the water column (see Table 3.3) were inserted for $[PO_4]_{\text{sw}}$ in equation (A3.1) and for $[P]_{\text{sw}}$ in equation (A3.2).

Acknowledgements

We wish to thank Captain and Crew of R/V SONNE cruise 119, and R/V METEOR cruises M31/3, M32/5, 33/1 and M36/5, for their help in obtaining the samples. The samples that were analyzed in this study are from the collection of R. Schiebel, which he acquired while he was a member of the working group of C. Hemleben at the University of Tübingen (Germany). This project has benefited from discussions with and the support of J. McKenzie and D. Schmidt. Financial aid for the study was provided by a grant from the Schweizerische Nationalfond (SNF).

CHAPTER 4

Precise Determination of Cadmium Isotope Fractionation in Seawater by Double Spike MC-ICPMS

Published as: Ripperger S. and Rehkämper M. (2007) Precise determination of cadmium isotope fractionation in seawater by double spike MC-ICPMS. *Geochimica Et Cosmochimica Acta*, **71**(3), 631-642.

Abstract

A new technique has been developed for the accurate and precise determination of the stable Cd isotope composition of seawater. The method utilizes a ^{110}Cd - ^{111}Cd double spike, and it involves separation of Cd from seawater by column chromatography and isotopic analyses by multiple collector inductively coupled plasma mass spectrometry. As a by-product it also generates precise Cd concentration data.

Repeated analyses of three pure Cd reference materials and three seawater samples yielded reproducibilities of about ± 1.0 to ± 1.6 $\epsilon^{114/110}\text{Cd}$ (2s.d.), based on measurements that each consumed about ~ 8 ng of natural Cd ($\epsilon^{114/110}\text{Cd}$ is the deviation of the $^{114}\text{Cd}/^{110}\text{Cd}$ isotope ratio of a sample from the standard in parts per 10,000). This demonstrates that the new double spike technique is superior to published methods of Cd isotope analyses, with regard to the acquisition of precise data for samples of limited size. Additional experiments showed that as little as 1 to 5 ng of seawater Cd could be analyzed with a precision of about ± 2 to ± 6 $\epsilon^{114/110}\text{Cd}$ (2s.d.). The accuracy of the seawater isotope data was ascertained by experiments in which a Cd-free seawater matrix was doped with small quantities of isotopically well-characterized Cd. Repeated mass scans that were carried out on purified Cd fractions of several samples furthermore demonstrated the absence of significant spectral interferences.

The isotope data that were acquired for the three seawater samples reveal, for the first time, small but resolvable Cd isotope fractionations in the marine environment. Cadmium-rich intermediate water from the North Pacific was found to have an isotope composition of $\epsilon^{114/110}\text{Cd} = 3.2 \pm 1.0$. In contrast, Cd-depleted seawater from the upper water column of the Atlantic and Arctic Oceans displayed isotope compositions of $\epsilon^{114/110}\text{Cd} = 6.4 \pm 1.1$ and 6.6 ± 1.6 , respectively. These observations are in accord with the interpretation that the isotope effects are due to the biological fractionation that occurs during the uptake of dissolved seawater Cd by phytoplankton.

4.1 INTRODUCTION

The geochemistry of Cd in seawater has attracted significant attention over the past 30 years. This interest is based on the nutrient-type distribution of this element, which closely resembles the distribution of phosphate (Boyle et al., 1976; Bruland, 1980; Bruland, 1983). As a consequence both Cd and P are estimated to have similar marine residence times of about 10 - 100 kyr (Bewers and Yeats, 1977; Martin and Whitfield, 1983; Ruttenberg, 2003). The low dissolved P concentrations of surface seawater are due to uptake by marine organisms, and this is in accord with the role of P as an essential macronutrient. The higher P abundances that are observed at greater depth in the oceans are thought to reflect oxidative regeneration of organic material (Bender and Gagner, 1976; Boyle et al., 1976; Bruland, 1980; Bruland, 1983). The reason why Cd displays a marine distribution that is akin to P is still disputed. It is possible that the similarity in behaviour reflects true biological demand for the micronutrient Cd (Price and Morel, 1990; Cullen et al., 1999) but it has also been proposed that this could be due to scavenging of Cd by biological particles (Collier and Edmond, 1984).

It is likely that Cd isotope data for seawater can provide further insights into the cycling of this element in the marine environment. This statement is justified because it has been shown that biological uptake can generate significant Cd isotope effects (Lacan et al., 2005), whereby the lighter isotopes are enriched in the organic material. In addition, it has been demonstrated that abiotic geological processes other than evaporation and condensation are unable to significantly fractionate Cd isotope compositions (Wombacher et al., 2003). Hence, it is possible that the Cd isotope composition of seawater may be a proxy for the Cd concentration and therefore, by inference, for nutrient utilization.

Isotopic studies of Cd in seawater face significant analytical challenges, however. These are related to the low dissolved Cd contents and high matrix to Cd ratios of such water samples, as well as the limited extent of isotope fractionation that is expected in many cases. It is unclear whether current methods for the determination of Cd stable isotope compositions, which utilize either a double spike protocol in conjunction with TIMS (thermal ionisation mass spectrometry, Rosman and De Laeter, 1976; Schmitt et al., 2006) or MC-ICPMS (multiple collector inductively coupled plasma mass spectrometry) without double spiking (Wombacher et al., 2003; Cloquet et al., 2005), are well suited for dealing with such difficulties. These techniques appear to require either large quantities of Cd for analysis or

generate data of limited precision. This conclusion is underlined by the MC-ICPMS study of Lacan et al. (2005), which was unable to resolve any differences in Cd isotope compositions for a number of seawater samples.

To address this shortcoming, the present study presents new methods of Cd isotope analyses that are suitable for the accurate and precise resolution of small Cd isotope effects in seawater. The novel procedure utilizes MC-ICPMS together with a double spike for the correction of the instrumental as well as any laboratory-induced mass fractionation.

4.2 METHODS

4.2.1 General

All critical sample preparation work was carried out in Class 10 laminar flow workbenches within a Class 10,000 clean room facility. The mineral acids were purified once by sub-boiling distillation in either quartz (6 M HCl, HBr, HNO₃) or Teflon stills (10 M HCl). The water was 18 M Ω grade from a Millipore purification system. The HNO₃-HBr mixture that is required for the anion-exchange chemistry was prepared freshly on the day of use (Rehkämper and Halliday, 1999).

4.2.2 Standard Solutions and Cd Isotope Notation

The Cd isotope data of samples are reported relative to results obtained for a standard with an ϵ -notation:

$$\epsilon^{114/110}\text{Cd} = \left(\frac{R_{\text{Sam}}}{R_{\text{Std}}} - 1 \right) \times 10,000 \quad (4.1)$$

where R_{Sam} and R_{Std} denote the $^{114}\text{Cd}/^{110}\text{Cd}$ isotope ratio of the sample and the standard, respectively.

Two standards with identical Cd isotope compositions were utilized in this study: a "JMC Cd Münster" solution, which was previously prepared by Wombacher and co-workers (Wombacher et al., 2003; Wombacher and Rehkämper, 2004), and the in-house standard "Alfa Cd Zürich" (Table 4.1). Both solutions were made up from commercial ICP standard solutions with 1000 $\mu\text{g g}^{-1}$ Cd in 5% HNO₃ that were purchased from Alfa Aesar (Johnson Matthey Company). Numerous measurements have shown that the Cd isotope compositions of JMC Cd Münster and Alfa Cd Zürich are identical to within better than $\pm 0.5 \epsilon^{114/110}\text{Cd}$ (2s.d.). These solutions are ideally suited as reference standards because their Cd isotope compositions are very similar to that of the bulk silicate Earth (Wombacher et al., 2003).

Three fractionated Cd isotope standard solutions were repeatedly analyzed during the course of this study (Table 4.1). These are the “Münster Cd” solution described by Wombacher and Rehkämper (2004), the “BAM-I012 Cd” isotope reference material, and a “JMC Cd Zürich” solution that was used to calibrate the concentration of the new Cd double spike. This solution was prepared by the authors from 99.999% pure Cd metal pellets (Alfa Aesar Puratronic grade) that had been leached with 0.1 M HNO₃ and cleaned with water and ethanol to remove oxide coatings, prior to dissolution in 2 M HNO₃.

Table 4.1. Cadmium isotope standards utilized in this study and the respective isotope compositions (reported as $\epsilon^{114/110}\text{Cd}$) as determined with the ^{110}Cd - ^{111}Cd double spike and by other techniques.

Standard	Source	This Study	Reference Data		
		Cd double spike ^a	Ext. norm. to Ag ^b	Ext. norm. to Ag ^c	Std.-sample bracketing ^d
JMC Cd Münster ^e	Alfa Aesar ICP std. solution, lot 502552A			$\equiv 0$	
Alfa Cd Zürich	Alfa Aesar ICP std. solution, lot 901463E			$\equiv 0$	
BAM-I012 Cd ^e	Proposed Cd SRM of BAM/Germany ^f	-12.9 ± 1.1 (n = 32)	-11.9 ± 1.5 (n = 2)	-10.8 ± 1.5 (n = 15)	
Münster Cd ^e	Fractionated Cd std. of Münster University	$+45.9 \pm 1.2$ (n = 6)	$+45.5 \pm 1.5$ (n = 2)	$+46.5 \pm 0.5$ (n = 3)	$+44.8 \pm 0.4$ (n = 5)
JMC Cd Zürich	Solution of Alfa Aesar Puratronic Cd metal	-17.0 ± 0.7 (n = 4)	-18.6 ± 1.5 (n = 2)		

n = number of independent measurements; std. = standard; SRM = standard reference material; ext. norm. = external normalization. ^a the uncertainties for the double spike data denote 2 standard deviations. ^b data of this study, acquired by MC-ICPMS at the ETH Zürich, using ext. norm. to admixed Ag as described by Wombacher et. al. (2003). The given uncertainties are based on the reproducibility obtained for multiple analyses of the zero-epsilon standard. ^c Wombacher and Rehkämper (2004). The uncertainties are 2 standard deviations. ^d Cloquet et al. (2005). The uncertainty denotes 2 standard deviations. ^e see Wombacher and Rehkämper (2004) for more information on this SRM. ^f BAM = Bundesanstalt für Materialwissenschaft und -prüfung, Germany.

4.2.3 Cadmium Double Spike

4.2.3.1 Double Spike Design

Cadmium has eight stable isotopes with relative abundances that vary from less than 1.5% (^{106}Cd , ^{108}Cd) to approximately 25% (^{112}Cd , ^{114}Cd). The remaining Cd isotopes have intermediate abundances of about 7.5% (^{116}Cd) and 12.5% (^{110}Cd , ^{111}Cd , ^{113}Cd) (Table 4.2). A double spike-technique involves the use of a spike that is artificially enriched in two isotopes of the target element. A precise correction for the instrumental mass bias can be obtained with such a spike by solving the relevant equations (Hofmann, 1971; Hamelin et al., 1985) in 3-dimensional isotope ratio space, whereby a single nuclide is the common denominator of all three isotope ratios. The following rationale was used in choosing the most suitable composition for the new Cd double spike:

- (1) The nuclides ^{106}Cd , ^{108}Cd , and ^{116}Cd were avoided because they suffer from isobaric interferences from either major Pd (^{106}Pd , ^{108}Pd : ~27%) or Sn (^{116}Sn : ~14%) isotopes. Such interferences are particularly problematic if MC-ICPMS is utilized for isotopic analysis because the ICP ion source of such instruments readily ionises these elements.
- (2) Of the remaining Cd isotopes, only ^{111}Cd is free from isobaric interferences. The isobars of ^{112}Cd and ^{114}Cd , however, are very minor Sn nuclides with relative abundances of less than 1% (Table 4.2). Based on this, these 3 isotopes were deemed to be suitable for the Cd double spike analyses. This necessitates that either ^{117}Sn or ^{118}Sn are monitored for the calculation of an interference correction (Table 4.2).
- (3) The remaining two Cd nuclides, ^{110}Cd and ^{113}Cd , suffer from potential interferences from Pd and In isotopes, respectively. As Cd is typically more readily separated from Pd than from In by ion-exchange chromatography (Wombacher et al., 2003), ^{110}Cd was thought to be a more suitable isotope for the double spike analyses than ^{113}Cd .
- (4) Once it had been decided that the double spike procedure would utilize ^{110}Cd , ^{111}Cd , ^{112}Cd , and ^{114}Cd , simple numerical methods, adapted from those outlined by Galer (1999), were used to identify a spike composition and isotope ratio space that would provide optimal (near 90°) intersection angles between the mass fractionation vectors of spiked and unspiked samples as well as minimal error magnification factors over a wide range of spike-sample ratios. These calculations demonstrated that a Cd double spike that is enriched in ^{110}Cd and ^{111}Cd with a ratio of $^{110}\text{Cd}/^{111}\text{Cd} \approx 0.5$ would provide the most favourable results if the equations are solved in $^{110}\text{Cd}/^{111}\text{Cd}$ - $^{112}\text{Cd}/^{111}\text{Cd}$ - $^{114}\text{Cd}/^{111}\text{Cd}$ isotope space. They also

showed that such a double spike is ideally used with a molar ratio of spike-derived Cd to sample-derived natural Cd of approximately 4. This ratio, denoted as S/N ratio hereafter, was derived for spiked samples from the measured $^{111}\text{Cd}/^{114}\text{Cd}$ isotope data.

Table 4.2. Collector configuration and major isobaric and molecular interferences for the Cd isotope analyses.

Mass	105	110	111	112	114	117
<i>Collector configuration</i>						
Main run		L5	L4	L3	H1	H6
Pd run	L4	H5	H6			
<i>Abundances of Cd isotopes and isobaric nuclides (in %)</i>						
Cd		12.5	12.8	24.1	28.7	
Pd	22.6	13.5				
Sn				0.97	0.65	7.68
<i>Main molecular interferences</i>						
M^{40}Ar^+	^{65}Cu	^{70}Zn ^{70}Ge	^{71}Ga	^{72}Ge	^{74}Ge ^{74}Se	^{77}Se
M^{16}O^+	^{89}Y	^{94}Zr ^{94}Mo	^{95}Mo	^{96}Zr ^{96}Mo ^{96}Ru	^{98}Mo ^{98}Ru	^{101}Ru
M^{14}N^+	^{91}Zr	^{96}Zr ^{96}Mo ^{96}Ru	^{97}Mo	^{98}Mo ^{98}Ru	^{100}Mo ^{100}Ru	^{103}Rh

4.2.3.2 Double Spike Preparation

The double spike was prepared as a mixture of individual concentrated spike solutions of isotopically enriched ^{110}Cd and ^{111}Cd . To this end, ~50 mg of ^{110}Cd metal (95.6% purity; Isoflex Corp., USA) and ~5.7 mg ^{111}CdO (96.4% purity; Oak Ridge National Laboratory, USA) were individually dissolved in 2 M HNO_3 and the Cd isotope compositions and concentrations of the two solutions were determined by mass spectrometry. These results were used to plan the preparation of the final double spike solution, such that this would achieve the desired composition. Suitable volumes of the individual spikes were then weighed in, mixed, dried down and redissolved in ~1000 ml of 2 M HNO_3 to obtain a double spike solution, which was characterized by $^{110}\text{Cd}/^{111}\text{Cd} \approx 0.5$ and a Cd concentration of about 150 ng/g.

The Cd isotope composition of the double spike was determined by repeated MC-ICPMS analyses that were conducted over a period of two months, using external normalization to added Ag with the exponential law for mass bias correction (Table 4.3). The Ag-based normalization that was applied in these analyses utilized a $^{107}\text{Ag}/^{109}\text{Ag}$ isotope ratio that was empirically optimised for each measurement session. To this end, the Ag-based normalization for interspersed analyses of the JMC Cd Münster standard was adjusted, such that this provided results that were essentially identical (typically to within less than 5 ppm) to those that were obtained by internal normalization of the Cd isotope ratios relative to $^{110}\text{Cd}/^{114}\text{Cd} = 0.438564$ (Table 4.3). This optimised normalization was then used for the mass bias correction of the data that had been acquired for the bracketed analyses of the Cd double spike. In essence, this means that the isotope ratios of the double spike were determined relative to the “normal” Cd isotope composition reported in Table 4.3, and in particular relative to the reference ratio of $^{110}\text{Cd}/^{114}\text{Cd} = 0.438564$ (Wombacher et al., 2004).

These analyses yielded a relatively large uncertainty for the isotope composition of the spike (Table 4.3), primarily due to the variable amounts of memory (with a nearly “normal” Cd isotope composition) that were present in the sample introduction system. The uncertainties that arise from such mixing processes, however, have no detrimental effect on the accuracy of the double spike based mass bias correction. Their main effect is to reduce, albeit only to a small extent, the accuracy of the Cd concentration data that can be obtained for spiked samples with the isotope dilution protocol.

The total Cd content of the double spike was precisely determined by reverse isotope dilution using a gravimetric solution of JMC Cd Zürich. Repeated analyses of two separate spike-standard mixtures yielded a Cd concentration of 149.899 ± 0.056 ng/g (2s.d.) for the double spike.

Table 4.3. Average Cd isotope ratios measured for the zero-epsilon Cd isotope standards and the Cd double spike.

Solution	n	$^{110}\text{Cd}/^{114}\text{Cd}$	$^{111}\text{Cd}/^{114}\text{Cd}$	$^{112}\text{Cd}/^{114}\text{Cd}$
JMC Cd Münster & Alfa Cd Zürich [§]	93	0.438564	0.448867 (50)	0.843269 (132)
^{110}Cd - ^{111}Cd Double Spike [§]	10	40.4982 (2824)	82.0864 (5698)	2.13564 (893)

The uncertainties given in the parentheses denote 2 standard deviations. n = number of measurements. § The isotopic data for the two zero-epsilon standards were obtained over a period of 1.5 years by internal normalization relative to $^{110}\text{Cd}/^{114}\text{Cd} = 0.438564$ with the exponential law. § The isotope data for the double spike were acquired over a period of 2 months by empirically optimized external normalizations to admixed Ag using fractionation factors that would yield accurate results (see above) for isotopically “normal” Cd.

4.2.4 Samples and Sample Handling

4.2.4.1 Seawater Samples

Three different seawater samples were utilized in this study: the international standard reference material NASS-5 (North Atlantic Surface Seawater) from the National Research Council of Canada and the in-house samples AHSW (Arctic Halocline Seawater) and PISW (Pacific Intermediate Seawater).

The NASS-5 sample was collected in the North Atlantic at a depth of 10 m, 35 km southeast of Halifax, Canada. The water was sampled with a peristaltic pump through cleaned polyethylene lined ethyl vinyl acetate tubing and 0.45 μm acrylic copolymer filters. It was then acidified to pH 1.6 with ultrapure nitric acid and transferred to 50 L acid leached polypropylene carboys. A large volume of this seawater was later homogenized in two linked 800 L polyethylene tanks and then transferred into cleaned 500 ml polyethylene bottles (see NASS-5 Certification Document for further details of the sample preparation procedure).

The AHSW seawater was collected at a depth of 50 m in the Canada Basin of the Arctic Ocean at 75°13' N, 149°57' E during the 2000 Arctic West Summer Expedition (AWS-2000; Trimble et al., 2004). Sample PISW constitutes intermediate water from 1200 m depth, that was collected in the western Pacific Ocean (at 24°15' N, 170°20' E) during the 2002 Intergovernmental Oceanographic Commission (IOC) Contaminant Baseline Survey Expedition (Measures et al., 2006). The sampling methods were very similar in both cases. Sample collection was carried out with a rosette that was fitted with Niskin bottles. Following retrieval, the seawater was immediately passed through 0.45 μm Millipore cellulose filters, transferred into precleaned polypropylene bottles and acidified to approximately pH 1-2 with concentrated HCl.

4.2.4.2 Sample Preparation

Approximately 200 to 1300 ml of seawater were weighed in to ensure that roughly 10 to 50 ng of natural Cd were available for analysis. For each sample, a suitable mass (~0.3-1.4 g) of the ^{110}Cd - ^{111}Cd double spike was then weighed into 15 ml Savillex beakers, to obtain a Cd spike-sample ratio (S/N) of about 4. The spike solution was evaporated to dryness, dissolved in ~10 ml 10 M HCl and admixed to the sample. Additional 10 M HCl was then added to the seawater to obtain a final HCl concentration of ~0.7 mol/l. The spiked samples were then left to equilibrate for at least 3 days prior to further processing.

4.2.4.3 Column Chemistry

A three stage column chemistry procedure, modified from the methods of Wombacher et al. (2003), was used to isolate clean fractions of Cd from the seawater samples (Table 4.4). The elution schemes that were utilized for the first and second stage of the separation protocol are identical and Biorad AG 1-X 8, 200-400 mesh anion-exchange resin was applied in both cases. Much larger columns were, however, employed for the first step and the eluent volumes were scaled approximately in proportion to size of the respective resin beds (Table 4.4).

Table 4.4. Column chemistry procedure for the separation of Cd from seawater samples prior to isotopic analysis.

First Stage Columns		Second Stage Columns
Biorad AG 1-X8 anion exchange resin, 200-400 mesh		
<i>1.5 ml resin in large qz-glass columns</i>		<i>100 µl resin in small Teflon columns</i>
11 ml 2 M HNO ₃	Resin cleaning	750 µl 2 M HNO ₃
0.5 ml H ₂ O		50 µl H ₂ O
16 ml 8 M HCl	Conversion to Cl ⁻ form	1000 µl 8 M HCl
11 ml 0.7 M HCl	Resin equilibration	800 µl 0.7 M HCl
Up to ~1.5 l seawater, 0.7 M in HCl	Sample loading	1400 µl sample solution in 0.7 M HCl
23 ml 0.7 M HCl	Matrix elution	1000 µl 0.7 M HCl
10 ml 1 M HCl	Matrix elution	650 µl 1 M HCl
10 ml 2 M HCl	Matrix elution	650 µl 2 M HCl
10 ml 8 M HCl	Elution of Ag	650 µl 8 M HCl
10 ml		650 µl
0.5 M HNO ₃ –0.1 M HBr	Elution of Zn	0.5 M HNO ₃ – 0.1 M HBr
2 ml 2 M HNO ₃		130 µl 2 M HNO ₃
10 ml 2 M HNO ₃	Collect Cd	700 µl 2 M HNO ₃
Third Stage Columns		
Eichrom TRU Spec resin		
<i>100 µl resin in small Teflon columns</i>		
10 ml 6 M HCl	Cleaning & equilibration	
200 µl sample solution in 8 M HCl	Sample loading & collect Cd	
200 µl 8 M HCl	Collect Cd	
1.4 ml 6 M HCl	Collect Cd	

Fresh resin beds were prepared for each sample and column immediately prior to use.

The first separation stage was performed in large quartz glass columns with 100 ml reservoirs and 1.5 ml resin beds (6 mm diameter) that are suitable for the loading of even large (1 to 1.5 l) seawater samples. Cadmium was eluted from the resin with 10 ml 2 M HNO_3 , and these fractions were evaporated to dryness, redissolved in 10 M HCl (to convert the residue into the chloride form), dried again, and finally taken up in ~ 1.4 ml 0.7 M HCl for loading of the second stage columns.

The second “cleanup” stage of the chemistry served to further isolate the Cd from any residual matrix elements and this was carried out in small columns made from shrink-fit Teflon with 100 μl resin beds. Following evaporation of the purified Cd fractions from the secondary columns, they were again converted into the chloride form by drying down with 10 M HCl , and then dissolved in 200 μl 8 M HCl , for loading of the columns of the third separation stage.

This last step of the separation procedure also utilized small Teflon columns, with 100 μl beds of Eichrom TRU Spec resin that served to separate Cd from residual Sn and traces of Nb, Zr, and Mo. The Cd fractions that were eluted from these columns were evaporated to dryness, dried again with a few drops of 14 M HNO_3 to remove any residual chloride, and redissolved in ~ 30 μl 14 M HNO_3 for storage. Just prior to use, the solutions were evaporated to near complete dryness and taken up in an appropriate volume of 0.1 M HNO_3 to obtain the desired Cd concentration for mass spectrometric analysis.

A detailed evaluation of the separation method demonstrated that high yields of $> 90\%$ were routinely achieved for Cd. All concentration data were corrected for the procedural blank, which averaged 52 ± 18 pg (1 s.d., $n = 8$) during the course of this study. At this level, the blank has a negligible effect on the measured isotope compositions, because it constitutes less than 0.25% of the indigenous Cd present in the seawater samples.

4.2.5 Mass Spectrometry

All isotopic measurements were carried out with a Nu Plasma MC-ICPMS instrument at the ETH Zürich. This is fitted with a large capacity (80 l/min) rotary pump for evacuation of the expansion chamber. The sample introduction system consisted of a CETAC Aridus desolvation unit, which was used with T1H nebulizers (CETAC) that were operated at flow rates of about 100 $\mu\text{l}/\text{min}$.

Each isotopic analysis consisted of a longer (~ 7.5 min) main measurement (“run”) and a subsequent shorter (~ 2.5 min) Pd interference run. In the main run, the ion currents of ^{110}Cd ,

^{111}Cd , ^{112}Cd , ^{114}Cd and ^{117}Sn were measured simultaneously with the Faraday cups (all equipped with $10^{11} \Omega$ resistors), whereas the Pd interference measurement served to determine the ion currents of ^{105}Pd and ^{110}Cd , ^{111}Cd (Table 4.2). The ion beams of ^{105}Pd and ^{117}Sn were monitored to correct for isobaric interferences from ^{110}Pd and ^{112}Sn , ^{114}Sn , respectively.

The data acquisition sequence of the main run comprised 60 integrations of 5 s each, in blocks of 20, whereas the interference run consisted of a single block of ten 5 s integrations. Prior to each block, the baseline signals were monitored for 15 s, whilst the ion beam was deflected in the electrostatic analyzer; these data were subsequently subtracted from the measured ion beam intensities. Each analysis was followed by a thorough (~10 min) washout, whereby the sample introduction system was flushed first with 1 M HNO_3 and then with 0.1 M HNO_3 .

A complete sample analysis with 60 plus 10 data acquisition cycles required about 10 min, during which ~1000 μl of sample solution were consumed. Most seawater samples were analyzed as solutions with total Cd concentrations of ~40 ng/ml (ppb). Typically, these samples were spiked to obtain a S/N ratio of ~4, such that each analysis consumed only about 8 ng of natural (seawater-derived) Cd. Cadmium solutions with concentrations of ~40 ppb generally yielded total ion beam intensities of 7 to 8×10^{-11} A for Cd, which is equivalent to a transmission efficiency of about 0.05 to 0.1%.

4.2.6 Data Reduction

The Cd isotope data that were collected during the mass spectrometric analyses were further processed, to calculate the “true” mass bias corrected isotope compositions of the *unspiked* samples. These results were then used to determine the respective $\epsilon^{114/110}\text{Cd}$ values. The same equations also yield the mass bias corrected $^{111}\text{Cd}/^{114}\text{Cd}$ isotope ratios of the spike-sample mixtures and these were used (in conjunction with the sample and spike weights) to determine the Cd concentrations of the seawater samples by isotope dilution.

The double spike data reduction that is required to obtain these values was performed offline, using a spreadsheet-based implementation of the iterative methods outlined by Siebert et al. (2001). This technique is similar to the “classical” methods that are utilized for the processing of double spike data from TIMS analyses, in that a geometric approach is used to solve the equations in 3-dimensional isotope space that is defined by isotope ratios with a common denominator (Hofmann, 1971). The numerical methods of Siebert et al. (2001),

however, are suitable for the accurate reduction of isotope ratio data collected by MC-ICPMS because they do not make the simplifying assumption that the instrumental mass bias is adequately described by a linear law (Galer, 1999). Such an assumption is valid for TIMS but not for MC-ICPMS because MC-ICPMS is associated with a significantly larger (factor of 10 or more) mass bias. Instead, the numerical methods of Siebert et al. (2001) apply an iterative procedure, which accounts for the curved trajectories that are obtained, when mass discrimination is described by an exponential, power, or equilibrium law relationship.

An important modification to the procedure of Siebert et al. (2001) is implemented in this study concerning the correction for isobaric interferences. Such corrections are generally most robust, if the ratios that are used to monitor interferences ($^{105}\text{Pd}/^{111}\text{Cd}$ and $^{117}\text{Sn}/^{111}\text{Cd}$ in this case) are corrected for instrumental mass fractionation (Wombacher et al., 2003). This was achieved with the following technique. The complete data reduction procedure was initially performed using Cd isotope ratios that were uncorrected for contributions from isobars. This yielded a sufficiently accurate result for the instrumental mass fractionation factor, which was then used for the mass bias correction of those isotope ratios that were applied as interference monitors. The interference corrections for the relevant Cd ion ratios were then carried out with these results and the complete data reduction scheme was repeated, albeit using the new Cd isotope data that had been corrected for isobaric interferences.

4.3 RESULTS AND DISCUSSION

4.3.1 Analyses of Standard Solutions

4.3.1.1 Results for “zero-epsilon” ($\epsilon^{114/110}\text{Cd} = 0$) Standards

At least 7 to 10 analyses of mixtures that were made up from the Cd double spike and a zero-epsilon standard (Table 4.1) to obtain a near-optimal S/N ratio of ~ 4 , were carried out on each measurement session. The results of Table 4.5 demonstrate that such analyses of spiked zero-epsilon standards typically displayed within-day reproducibilities of about ± 0.5 to ± 1.5 $\epsilon^{114/110}\text{Cd}$ (2s.d.) for solutions with total Cd concentrations of about 30 to 50 ppb. In this case, a single measurement consumed about 6 to 10 ng of sample-derived Cd. For regular (60 cycle) analyses of mixtures with Cd concentrations of 10 to 20 ppb, the precision of the data is somewhat lower at about ± 2 to ± 4 $\epsilon^{114/110}\text{Cd}$ (2s.d.), but such measurements consumed only about 2 to 4 ng of natural Cd (Table 4.5). Precise stable isotope data can be obtained for even smaller amounts of Cd but this is best done by reducing the analysis time rather than the Cd

concentration of the sample solutions. An extreme case are the short (10 cycle \approx 4 min) analyses that were conducted for solutions with 10 ppb total Cd. The available database for these analyses, which consumed less than 1 ng of sample Cd, indicate a typical within-day precision of about ± 4 to $\pm 8 \text{ } \epsilon^{114/110}\text{Cd}$ (2s.d.).

Table 4.5. Single-day reproducibility of Cd isotope data (reported as $\epsilon^{114/110}\text{Cd}$) obtained for multiple (~ 5 to 10) analyses of mixtures of the Cd double spike with the Alfa Cd Zürich standard at various concentration levels and using different data acquisition periods.

Total Cd Concentration (Spike + Std.)	n	cycles	Range of \pm 2s.d. reproducibility	Natural Cd consumed per analysis (ng)
50 ppb	3	60	~ 1.0	~ 10
40 ppb	10	60	$\sim 1.0 \pm 0.5$	~ 8
30 ppb	6	60	$\sim 1.4 \pm 0.7$	~ 6
20 ppb	5	60	$\sim 2.0 \pm 0.8$	~ 4
10 ppb	3	60	$\sim 3 \pm 1$	~ 2
10 ppb	3	10	$\sim 6 \pm 2$	~ 0.5

All data were acquired for mixtures with Cd spike-sample ratios (S/N) of ~ 4 . n = number of independent measurement sessions/days; cycles = number of 5 s integration cycles per run where a full 60-cycle analysis required about 10 min.

The observation that analyses of double spike-zero-epsilon standard mixtures often exhibited non-negligible deviations from $\epsilon^{114/110}\text{Cd} = 0$ when the exponential law was utilized for the correction of the instrumental mass bias, is important. These deviations were typically small at less than $\pm 1.5 \text{ } \epsilon^{114/110}\text{Cd}$ but larger deviations of up to $\pm 3 \text{ } \epsilon^{114/110}\text{Cd}$ were also observed on some occasions. The deviations were, furthermore, of random rather than systematic nature, because the combined data of several measurement sessions always yielded average Cd isotope compositions that were identical to the reference value to within less than $\pm 0.5 \text{ } \epsilon$ -units. These small but significant variations in the double spike results are thought to be related to changes in the mass bias of the MC-ICPMS instrument, such that the mass discrimination is not always adequately described by the exponential law (Vance and Thirlwall, 2002; Wombacher and Rehkämper, 2003).

Support for this interpretation is provided by (a) similar observations that were made by Bermin et al, (2006) in the application of a Zn double spike and (b) results that were obtained when the original data were reprocessed using the General Power Law (GPL) for mass fractionation correction:

$$R = r \times f^{(m_2^n - m_1^n)} \quad (4.2)$$

Here R and r denote the same isotope ratio, but r is fractionated relative to the “true” value R , f is the fractionation factor, and m_i denotes the mass of isotope i . The exponent n is a key parameter of the GPL because this can be varied to alter the mass dependence of the isotope fractionation. Previous work has shown that the GPL is equivalent to the equilibrium, exponential and power law for $n = -1$, $n \approx 0$, and $n = 1$, respectively (Maréchal et al., 1999; Wombacher and Rehkämper, 2003). The reprocessing of our results demonstrated that any offsets could be avoided if the GPL was employed in conjunction with small (generally less than ± 0.2) non-zero values for the parameter n . This is clearly indicative of an instrumental mass discrimination that deviates from “perfect” exponential law behaviour.

The precision of the Cd isotope data could not be improved by optimising the exponent n of the GPL, however. It was therefore decided that all further work would use a conventional exponential law technique for the instrumental mass bias correction. The application of the exponential law is also simpler and any offset was accounted for by referencing the sample data to the mean isotope composition that was obtained for repeated analyses (conducted on the same day) of a suitable mixture of the double spike with a zero-epsilon standard. In practice, this was simply carried out by adding or subtracting any offset for the $\epsilon^{114/110}\text{Cd} = 0$ standards from the ϵ -values determined for the samples. With this technique, the exponential law correction yielded results that were essentially identical (to within $\sim 0.1 \epsilon^{114/110}\text{Cd}$) to those produced with an optimised GPL, for both fractionated Cd isotope standards and seawater samples (see following sections).

A number of analyses were also performed to ascertain that the double spike technique could be used for the accurate determination of Cd isotope compositions over a reasonably wide range of Cd spike-sample (S/N) ratios. In these measurements the Cd isotope compositions of double spike-Alfa Cd Zürich mixtures with variable S/N were analyzed relative to a mixture characterized by an optimum value of $S/N \approx 4$ (Fig. 4.1). The results of these measurements demonstrate that the double spike methodology yields accurate results for S/N values ranging from about 1 to 10 (Fig. 4.1).

Even larger deviations from the optimum ratio may be possible but this has not been tested, because the Cd concentrations of unknown samples can generally be estimated to within about a factor of 10.

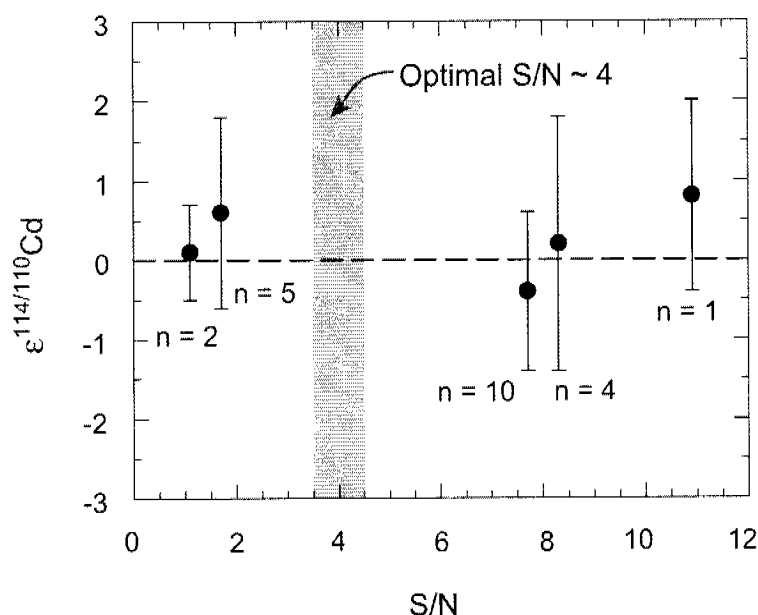


Fig. 4.1. Cadmium isotope data that were obtained for mixtures of the Cd double spike and the Alfa Cd Zürich standard, which exhibited spike-sample (S/N) ratios of between about 1 and 11. The ratio S/N is the molar ratio of Cd derived from the spike versus natural Cd from the sample. The analyses that are summarized in this figure were carried out relative to spike-standard mixtures that exhibited by an optimal S/N ≈ 4 (grey bar). n denotes the number of analyses. The error bars are based on either the internal precision of the analysis (n = 1), the range of observed results (n = 2), or the 2s.d. value determined for a dataset (n ≥ 4).

4.3.1.2 Results for Fractionated Cd Isotope Standards

The accuracy and reproducibility of the new Cd double spike methods were verified by repeated analyses of the three fractionated Cd isotope standards, for which isotopic reference data were available (Table 4.1). It is evident that the double spike results for BAM-I012 Cd, Münster Cd and JMC Cd Zürich all agree, within uncertainty, with the independent reference values that were obtained in various laboratories using different techniques (Table 4.1). The excellent agreement clearly demonstrates that the double spike method is able to provide accurate stable isotope data for Cd.

The great majority of the double spike results of Table 4.1 were acquired using solutions with total Cd concentrations of about 40 ppb in measurements that consumed ~ 8 ng of natural Cd. These data display reproducibilities of about ± 0.5 to ± 1.5 $\epsilon^{114/110}\text{Cd}$ (2s.d.) (Table 4.1),

and this is similar to the precision achieved for multiple analyses of zero-epsilon standards with similar concentrations on a single day (Table 4.5). Of particular interest are the double spike results for the BAM-I012 Cd reference material. During this study, this sample was analyzed 32 times on 25 separate measurement sessions over a period of 23 months and this yielded an excellent long-term reproducibility of $\pm 1.1 \text{ } \epsilon^{114/110}\text{Cd}$ (2.s.d.) (Table 4.1).

A detailed comparison of the measurement uncertainties that characterize the double spike data and the reference values shown in Table 4.1 is not possible, however. This is because the double spike results are averages, which are based on repeated analyses that consumed only small amounts of Cd, and that were carried out on several measurement sessions spread over a time period of weeks to months. In contrast, the reference results were generally acquired on a single measurement session (Wombacher and Rehkämper, 2004) and/or using techniques that consumed significantly larger quantities of Cd (Cloquet et al., 2005).

4.3.2 Analyses of Seawater Samples

This is the first study to publish Cd isotope data for seawater, such that there are no reference samples with well characterized Cd isotope compositions. Hence, it was necessary to validate the accuracy of the Cd double spike methods for seawater analyses using a variety of indirect methods. This was achieved by (a) a careful evaluation of systematic errors that arise from potential interferences from isobars and molecular ions, (b) carrying out a number of “matrix experiments” that are suitable for detecting the presence of both spectral interferences and matrix effects, and (c) repeated analyses of several seawater samples.

A published Cd concentration was, however, available for the seawater reference material NASS-5. A double spike analysis was carried out for this sample to verify the accuracy of our concentration data and to obtain a Cd isotope composition that may serve as a reference value for future studies.

4.3.2.1 Evaluation of Isobaric and Molecular Interferences

The procedure that was used for the correction of the isobaric interferences from ^{110}Pd and ^{117}Sn on Cd (Table 4.2) was evaluated using solutions of the Alfa Cd Zürich standard, which were doped with small amounts of Pd and Sn. Analyses of pure Cd standard solutions (Table 4.1) and the various seawater samples that were utilized in this study yielded $^{110}\text{Pd}/^{110}\text{Cd}$ and $^{114}\text{Sn}/^{114}\text{Cd}$ ratios of less than about 6×10^{-5} . Such small interferences are

readily corrected and measurements of Pd-Sn doped standards showed that the double spike technique yields accurate results for solutions with $^{110}\text{Pd}/^{110}\text{Cd}$ and $^{114}\text{Sn}/^{114}\text{Cd}$ interference ratios of up to about 6×10^{-4} . In contrast, doped standards with interference levels of $^{110}\text{Pd}/^{110}\text{Cd}$ and/or $^{114}\text{Sn}/^{114}\text{Cd}$ of between 1×10^{-3} and 5×10^{-3} yielded isotopic offsets of up to $\pm 7 \text{ } \epsilon^{114/110}\text{Cd}$.

Numerous elements are able to generate diatomic argide-, oxide-, or nitride-based molecular ions that can interfere with the present Cd isotope analyses (Table 4.2). A detailed study was therefore carried out to investigate whether such spectral interferences are indeed a problem for Cd isotope analyses of seawater. This involved (a) analyses that determined the formation rates of the various relevant diatomic argides, oxides and nitride ions and (b) repeated mass scans of various seawater sample solutions, which established the presence or absence of the respective metal ions (Table 4.2).

The formation rates of the various relevant diatomic ions (as measured at typical operating conditions using pure elemental solutions) were found to vary between about 2 to 4×10^{-3} for the refractory oxides YO^+ , ZrO^+ , less than 3×10^{-5} for all nitrides and other oxides, and less than 5×10^{-4} for argides. The mass scans, which were performed on aliquots of the final sample solutions of various seawater samples focused on the mass range between 60 and 120 amu. These analyses revealed the presence of traces of Cu, Zn, Ga, Ge, Se, Y, Zr, Mo, and Ru. In the following, the observed severity of the various molecular interferences is described by an interference ratio R_I , which is defined as:

$$R_I = \frac{I_x \times \alpha}{I_y} \quad (4.3)$$

where I_x refers to the ion beam intensity of an isotope that forms a molecular interference, α is the formation rate of the molecular ion, and I_y is the intensity of the corresponding Cd, Sn or Pd ion beam, which is affected by the interference. For all analyzed seawater samples, R_I was found to be less than 10^{-6} for $I_y = ^{110}\text{Cd}$, ^{111}Cd , ^{112}Cd , ^{114}Cd , less than 10^{-5} for $I_y = ^{117}\text{Sn}$ and less than 10^{-2} for $I_y = ^{105}\text{Pd}$. At this level, none of the interferences were observed to generate analytical artefacts that exceeded the measurement uncertainty. This indicates that the Cd sample solutions are pure enough following the column chemistry, such that data acquisition does not suffer from any spectral interferences.

4.3.2.2 Matrix Experiments

These experiments utilized a Cd-free seawater matrix, which was obtained by collecting the effluent from the first-stage ion exchange columns (Table 4.4) during loading of seawater samples. For this study, the Cd-free seawater matrices were prepared from 200 to 1500 ml aliquots of several Arctic and Pacific Ocean seawater samples (see caption of Fig. 4.2). Following collection of the effluent, this was doped with an appropriate amount (containing ~1 to 25 ng Cd) of either Alfa Cd Zürich or the BAM-I012 Cd (Fig. 4.2). After doping, the matrix samples displayed Cd concentrations from ~1 to less than 0.005 nmol/kg, and this covers almost the complete range of Cd contents found in seawater. These samples were then processed in a manner identical to ordinary seawater samples, in that a purified Cd fraction was isolated by column chemistry (Table 4.4), which was then analyzed by MC-ICPMS. The Cd isotope analyses of the matrix samples yielded results that were all identical, within the error, to the known isotope composition of the dopant (Fig. 4.2).

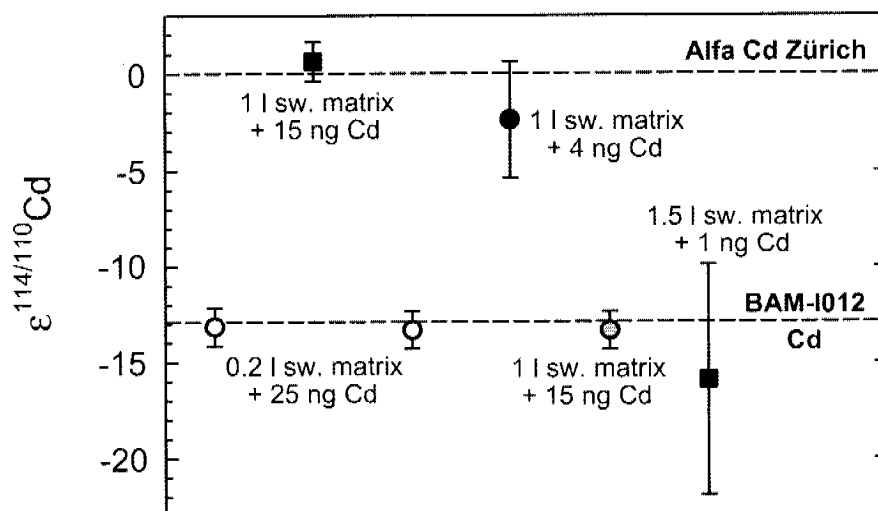


Fig. 4.2. Cadmium isotope data acquired for matrix experiments. In these experiments, the Cd-free seawater matrix of a seawater (sw.) sample was doped with small amounts of either Alfa Cd Zürich ($\epsilon^{114/110}\text{Cd} = 0$) or BAM-I012 Cd ($\epsilon^{114/110}\text{Cd} = -12.9$; Table 4.1). These mixtures were then treated and analyzed using the standard analytical protocol. The results show that all matrix experiments yielded the correct isotope composition for the dopant Cd (as denoted by the dashed lines). The error bars denote the typical within-day reproducibility achieved for standard solutions with similar concentrations (Table 4.4), as results for concentration-matched standards were typically not available for the same day. Different symbols denote the origin of the seawater samples: filled squares = Arctic seawater, 8 m depth; black circle = N. Pacific seawater, 10 m depth; grey circle = N. Pacific seawater, 100 m depth; white circles = N. Pacific seawater, 1200 m depth.

This is true for both samples that were doped with >10 ng Cd, such that they could be analyzed at high precision (about $\pm 1 \text{ } \epsilon^{114/110}\text{Cd}$) and the Cd-poor samples, for which the measurement uncertainties are larger at about ± 3 to $\pm 6 \text{ } \epsilon^{114/110}\text{Cd}$ (2s.d.). The interpretation of these results is straightforward, as they indicate that the Cd isotope data are not affected by analytical artefacts from spectral interferences or matrix effects and are accurate to within the given uncertainties.

4.3.2.3 Isotope Dilution Concentration Data

The Cd concentration data that were obtained for the three seawater samples is summarized in Table 4.6. Several separate aliquots were analyzed for PISW and AHSW, whereas only a single aliquot was available for NASS-5. The results of these analyses are superb as they display reproducibilities of only 0.05% (1s.d.) or better. The excellent quality of these data reflects two favourable circumstances. First, the measurements were carried out with relatively large quantities of Cd, because the concentration data are by-products of the double spike isotope composition analyses. Hence, the amount of Cd that was available exceeded the detection limit by several orders of magnitude.

Table 4.6. Cadmium concentration and isotope data for the three seawater samples analyzed in this study.

Seawater sample	Aliquot name	n	Concentration (nmol/kg)	$\epsilon^{114/110}\text{Cd}$
PISW	9/2 ($t_{\text{eq}} = 60$ d)	2	0.9946	3.0
	11/1 ($t_{\text{eq}} = 3$ d)	3	0.9941	3.7
	11/2 ($t_{\text{eq}} = 11$ d)	2	0.9943	3.1
	14/1 ($t_{\text{eq}} = 11$ d)	1	0.9935	2.9
	14/2 ($t_{\text{eq}} = 11$ d)	1	0.9934	3.0
	Average PISW	9	0.9941 ± 0.0009 (RSD = 0.05%)	3.2 ± 1.0
AHSW	7/2	1	0.3374	6.9
	19/5	4	0.3378	6.5
	Average AHSW	5	0.3378 ± 0.0004 (RSD = 0.05%)	6.6 ± 1.6
NASS-5	25/3	3	0.19784 ± 0.00003 (RSD = 0.007%)	6.4 ± 1.1

The average values were calculated as unweighted means of n independent measurements. The quoted uncertainties denote 2 standard deviations, except for NASS-5, where the error denotes the total range of the individual data. RSD = relative standard deviation. t_{eq} = duration of spike-sample equilibration prior to chemical processing of sample.

Second, the blank corrections are extremely small at about 0.0005 ± 0.0003 nmol/kg (2s.d.), such that they do not greatly enhance the overall uncertainty of the results.

The accuracy of the double spike concentration data is demonstrated by the excellent agreement of our result for the NASS-5 seawater of 0.19784 ± 0.00003 nmol/kg (2s.d.) with the Cd reference value of 0.199 ± 0.026 nmol/kg. The Cd concentrations determined for PISW and AHSW furthermore agree well with published Cd data for Pacific and Arctic Ocean seawater samples that were collected at similar depths (Boyle et al., 1976; Bruland, 1980; Moore, 1981; Bruland, 1983; Pai and Chen, 1994; Mackey et al., 2002)

4.3.2.4 Cd Isotope Data for Seawater Samples

The Cd isotope data that were acquired for the seawater samples are summarized in Table 4.6. A total of 9 analyses were carried out for the North Pacific seawater PISW over a time period of 4 months, and these used five independent sample aliquots that varied in volume between about 200 and 500 ml. It is important that the Cd, which is derived from double spike and the seawater are fully mixed and equilibrated prior to the column chemistry. To determine the minimum length of time that is required to achieve spike-sample equilibration, the various spiked aliquots of PISW were left to stand for 3, 11, and 60 days before carrying out the chemical separation procedure (Table 4.6). The nine analyses that were performed for this sample gave an average Cd isotope composition of $\epsilon^{114/110}\text{Cd} = +3.2 \pm 1.0$ (2s.d.). Data of similar quality were obtained for the Arctic seawater AHSW and the NASS-5 standard. For AHSW, two separate aliquots were analyzed a total of 5 times and this yielded a mean value of $\epsilon^{114/110}\text{Cd} = +6.6 \pm 1.6$ (2s.d.). A single aliquot of NASS-5 was analyzed three times on two measurement sessions and this gave an average result of $\epsilon^{114/110}\text{Cd} = +6.4 \pm 1.1$ (the uncertainty encompasses the total range of individual data). A number of important conclusions can be drawn from these data.

The Cd isotope compositions that were acquired for the 5 aliquots of PISW display no systematic differences despite variations in the spike-sample equilibration time (t_{eq}) of between 3 and 60 days (Table 4.6). This suggests that 3 days are likely to be sufficient to achieve full equilibration between the Cd derived from the double spike and from seawater. These results hence render it unlikely (but do not rule out) that spike-sample equilibration is significantly hindered by the presence of kinetically inert Cd complexes (e.g., with organic ligands; Bruland, 1992) that do not readily exchange with the main dissolved Cd species (which are likely to be readily exchangeable chloro-complexes of Cd; Bruland, 1992).

The results also demonstrate that the double spike procedure yields very precise Cd isotope data with uncertainties of about $\pm 1 \text{ } \epsilon^{114/110}\text{Cd}$ (2s.d.) not only for “clean” standard solutions but also for seawater samples with low Cd contents and unfavourable Cd to matrix ratios. Most of the isotope data of Table 4.6 was obtained in measurements that utilized sample solutions with total Cd concentrations of 40 to 60 ppb, such that the analyses consumed about 8 to 15 ng of natural Cd. In comparison, Wombacher et al. (2003) achieved a precision of ± 4 to $\pm 6 \text{ } \epsilon^{114/110}\text{Cd}$ (2s.d.) for analyses of geological samples (two silicate rocks and the Allende chondrite) that utilized external normalization to Ag and which consumed 10 to 30 ng of Cd. Cloquet et al. (2005) reported reproducibilities of about $\pm 1.2 \text{ } \epsilon^{114/110}\text{Cd}$ (2s.d.) for repeated analyses of various geological and anthropogenic samples by standard-sample bracketing. These measurements required about 200 ng of Cd, however, and this exceeds the amount used in the present study by more than an order of magnitude. A direct comparison of these reproducibilities is not useful in any case, due to the differences in the types of samples that were analyzed. Nonetheless, the results of this study offer sufficient evidence to state that the new double spike technique is clearly superior to previously published methods in terms of its ability to generate very precise Cd isotope data for samples of limited size.

The reproducibility of the Cd isotope data for seawater samples (Table 4.6) is similar to the within-day precision achieved for multiple measurements of zero-epsilon standards (Table 4.5) and the long term reproducibility obtained for repeated analyses of fractionated Cd standard solutions (Table 4.1). This provides further evidence that the double spike seawater data are unlikely to be inaccurate due to any significant systematic bias, because such a bias is unlikely to be highly reproducible.

The results of Table 4.6 also demonstrate that the Atlantic and Arctic Ocean samples (NASS-5, AHSW) display a small but well resolved offset in Cd isotope composition relative to the Pacific Ocean seawater PISW. This may be the most important result of this study because these data provide the first direct evidence for the fractionation of Cd isotopes in seawater. Given that the more Cd-depleted samples display heavier isotope compositions, it is most likely that the observed isotopic variation is caused by the uptake of dissolved seawater Cd by phytoplankton. Such biological processing is expected to generate kinetic isotope effects, whereby the light isotopes are enriched in the organic material. Additional evidence for this interpretation is provided by (a) the study of Lacan et al. (2005), who observed Cd isotope fractionation during biological uptake in laboratory experiments and (b) by the observation of Wombacher et al. (2003) who concluded that inorganic geological processes

(other than partial evaporation/condensation) are unable to generate significant Cd isotope effects.

The results of a recent investigation by Schmitt et al. (2006) suggest, however, that adsorption processes may also generate significant Cd isotope fractionations. These authors analyzed five ferromanganese (Fe-Mn) nodules from various locations and determined Cd isotope composition of between about -0.4 and +0.6 $\epsilon^{114/110}\text{Cd}$. It is presently unclear whether these results can be directly compared to our seawater data because the $\epsilon^{114/110}\text{Cd}$ values of Schmitt et al. (2006) are reported relative to an in-house Cd standard. If it is assumed that such a direct comparison is possible (which requires the zero-epsilon standards of both studies to have the same Cd isotope compositions) this would indicate that the adsorption of Cd from seawater onto Fe-Mn oxides produces a solid phase that is enriched in the light isotopes of Cd. It is hence at least conceivable that similar scavenging processes (by biological particles) may generate residual Cd depleted surface waters that feature an enrichment of the heavy isotopes. This demonstrates that further Cd isotope studies of marine samples are necessary to unequivocally demonstrate that the Cd isotope variations determined for seawater are dominated by biological fractionation effects rather than simple inorganic adsorption processes.

4.4 CONCLUSIONS

A new method, which utilizes a ^{110}Cd - ^{111}Cd double spike in conjunction with MC-ICPMS, has been developed for the determination of Cd stable isotope compositions at high precision. The technique was specifically set up to permit accurate and precise analyses of seawater samples that are characterized by low Cd contents and unfavourable Cd to matrix ratios. Multiple analyses of pure Cd standards and seawater samples that required only about 8 ng of natural Cd per measurement were found to display an external precision of about ± 1.0 to ± 1.6 $\epsilon^{114/110}\text{Cd}$ (2s.d.). Even analyses that utilized as little as 1 to 5 ng of natural Cd yielded reproducibilities of about ± 2 to ± 6 $\epsilon^{114/110}\text{Cd}$ (2s.d.). These results demonstrate that the new double spike method is clearly superior to previously published procedures for Cd stable isotope analysis.

The Cd isotope data that were acquired for three seawater samples provide the first evidence of Cd isotope fractionation in the marine environment. The most Cd-depleted water samples were found to be most enriched in the “heavy” isotopes, and this suggests that the fractionations are probably due to kinetic isotope effects that occurred during the uptake of

dissolved seawater Cd by phytoplankton. Further studies are required, however, to confirm this conclusion.

In summary, it is apparent that the present study has produced a number of important and promising results. In particular, it will be useful to apply the new analytical techniques to conduct Cd isotope analyses for a larger suite of seawater samples that characterize a variety of locations and depths. Such a study should aim to verify whether seawater indeed exhibits a global systematic relationship between Cd concentrations and isotope compositions. The identification of such a relationship would be an important result, because this would indicate that Cd isotopes could potentially be used to verify and supplement the Cd/Ca and $\delta^{13}\text{C}$ data that have been used in numerous paleoceanographic studies as proxies of nutrient utilization. Significant additional work would need to be carried out, however, to establish and validate such a Cd isotope proxy. In particular, this would require (a) a well-founded quantitative understanding of the processes that are responsible for the Cd isotope fractionation in seawater and (b) the identification of suitable sedimentary archives that reliably preserve the Cd isotope signatures of the past oceans.

Acknowledgements

We are grateful to Mark Baskaran, Martin Frank, Don Porcelli, and Bettina Zimmermann for kindly sharing their seawater samples and Frank Wombacher for making various Cd isotope reference materials available to us. H. Baur, U. Menet, D. Niederer, F. Oberli, C. Stirling, H. Williams and S. Woodland are thanked for their help in keeping the mass specs and clean labs running smoothly. Our thanks also go to the Captain and the Crew of the USCGC *Polar Star* and the R/V *Melville* for their help in obtaining samples during the AWS-2000 and the IOC 2002 cruises. Support for these cruises was provided by grant NSF-OPP-9996337 to Mark Baskaran (AWS-2000) as well as the Intergovernmental Oceanographic Commission and NSF grant OCE-0117917 to Chris Measures, Bill Landing, and Greg Cutter (IOC 2002). This project has profited from discussions with and the support of A. Halliday, J. McKenzic, R. Schiebel, D. Schmidt, D. Vance, and M. Schönbächler, as well as from the thoughtful reviews of three anonymous reviewers and constructive comments and editorial advice from K. Falkner. Financial aid for the study was provided by a grant from the Schweizerische Nationalfond (SNF).

CHAPTER 5

Cadmium Isotope Fractionation in Seawater - A Signature of Biological Activity

Accepted for publication in *Earth and Planetary Science Letters* as: Ripperger S., Rchkämper M., Porcelli D. and Halliday A. N. (2007) Cadmium isotope fractionation in seawater - a signature of biological activity.

Abstract

Investigations of cadmium isotope variations in the oceans may provide new insights into the factors that control the marine distribution and cycling of this element. Here we present the results of Cd isotope and concentration analyses for 22 seawater samples from the Atlantic, Southern, Pacific, and Arctic Oceans. The results reveal, for the first time, large and well resolved Cd isotope fractionations in the marine environment. The majority of the seawater samples display an inverse relationship between dissolved Cd contents and isotope compositions, which range from $\epsilon^{114/110}\text{Cd} \approx +3 \pm 0.5$ for Cd-rich waters (0.8-1.0 nmol/kg) to $\epsilon^{114/110}\text{Cd} \approx 38 \pm 6$ for surface water with a Cd concentration of only 0.003 nmol/kg (all $\epsilon^{114/110}\text{Cd}$ data are reported relative to the JMC Cd Münster standard). This suggests that the Cd isotope variations reflect kinetic isotope effects that are generated during closed system uptake of dissolved seawater Cd by phytoplankton. A few samples do not follow this trend, as they exhibit extremely low Cd contents (<0.008 nmol/kg) and nearly un-fractionated Cd isotope compositions. Such complexities, which are not revealed by concentration data alone, require that the Cd distribution at the respective sites was affected by additional processes, such as water mass mixing, atmospheric inputs of Cd and/or adsorption. Uniform isotope compositions of $\epsilon^{114/110}\text{Cd} = +3.3 \pm 0.5$ (1s.d.) were determined for seawater from ≥ 900 m depth, despite of Cd concentrations that display the expected increase along the global deep-water pathway from the Atlantic (~ 0.3 nmol/kg) to the Pacific Ocean (~ 0.9 nmol/kg). This indicates that the biomass, which is remineralized in the deeper ocean, is also characterized by a very constant Cd isotope composition. This observation is in accord with the interpretation that the Cd distribution in surface waters is primarily governed by Rayleigh fractionation during near-quantitative uptake of dissolved seawater Cd.

5.1 INTRODUCTION

The geochemistry of cadmium in the oceans has attracted significant scientific interest for more than 30 years. This interest is founded on the oceanic correlation of Cd concentrations with those of the macronutrient phosphorus (Boyle et al., 1976; Bruland, 1980), which plays a key role in marine biological productivity (Karl and Björkman, 2001). The cycling of phosphate is reasonably well understood, with a distribution that is dominated by phytoplankton uptake in surface waters and remineralization at depth (Ruttenberg, 2003). Cadmium, however is generally regarded as toxic for organisms at higher concentrations (Brand et al., 1986; Sunda, 1987; Lane and Morel, 2000) and the factors that regulate its uptake by phytoplankton and control the Cd versus phosphate relationship are not fully understood. Recent studies found that Cd can substitute for zinc in carbonic anhydrase when Zn-availability is limited, and this indicates that Cd may be a micronutrient with an important biological function (Price and Morel, 1990; Morel et al., 1994; Cullen et al., 1999; Sunda and Huntsman, 2000; Lane et al., 2005). Carbonic anhydrase is a Zn metalloenzyme that is ubiquitous in the bacteria, plant and animal kingdoms, and which catalyses the reversible conversion of CO_2 and water into carbonic acid and HCO_3^- ions (Lionetto et al., 2005). It plays a fundamental role in a number of physiological processes, such as respiration, ionic transport, acid-base regulation and calcification (Henry, 1996). The substitution of Zn by Cd was also suggested for other Zn metalloenzymes, such as alkaline phosphatase, which allows phytoplankton to acquire phosphate from organic compounds (Morel and Price, 2003). However, it has also been proposed that the nutrient-like distribution of Cd in the oceans could be caused by scavenging onto living or nonliving particulate material (Collier and Edmond, 1984; Yee and Fein, 2001; Dixon et al., 2006).

Recent analyses demonstrated that phytoplankton cells preferentially take up the light isotopes of Cd (Lacan et al., 2006) and this uptake is expected to leave a distinct isotopic fingerprint in the residual Cd-depleted seawater. Further insight into the processes that govern the marine distribution of Cd can hence be obtained from isotopic measurements of seawater. Similar analyses have previously provided a wealth of information on the marine cycling of nutrient elements, including nitrogen (Sigman et al., 1999) and silicon (De La Rocha et al., 1998; Reynolds et al., 2006).

At present, there exists only one published study of Cd isotope variations in seawater (Lacan et al., 2006), but this suffered from measurement uncertainties that were almost as

large as the observed isotopic variations. Here we present new high-precision Cd isotope data for seawater that were obtained with a recently developed method (Ripperger and Rehkämper, 2007b), which utilizes a Cd double spike technique in conjunction with MC-ICPMS (multiple collector inductively coupled plasma mass spectrometry). Our results for samples from four major ocean basins and depth profiles from the North Pacific and Arctic Ocean display large and clearly resolvable Cd isotope effects, which provide new constraints on the marine cycling of this element.

5.2 SAMPLES

Three water column profiles collected in the North Pacific and in the Arctic Ocean, and additional surface and deep-water samples from the North Atlantic, Southern and Arctic Oceans were analyzed in this study (Fig. 5.1, Table 5.1). The seawater samples represent different oceanic regimes and cover a wide range of Cd concentrations.

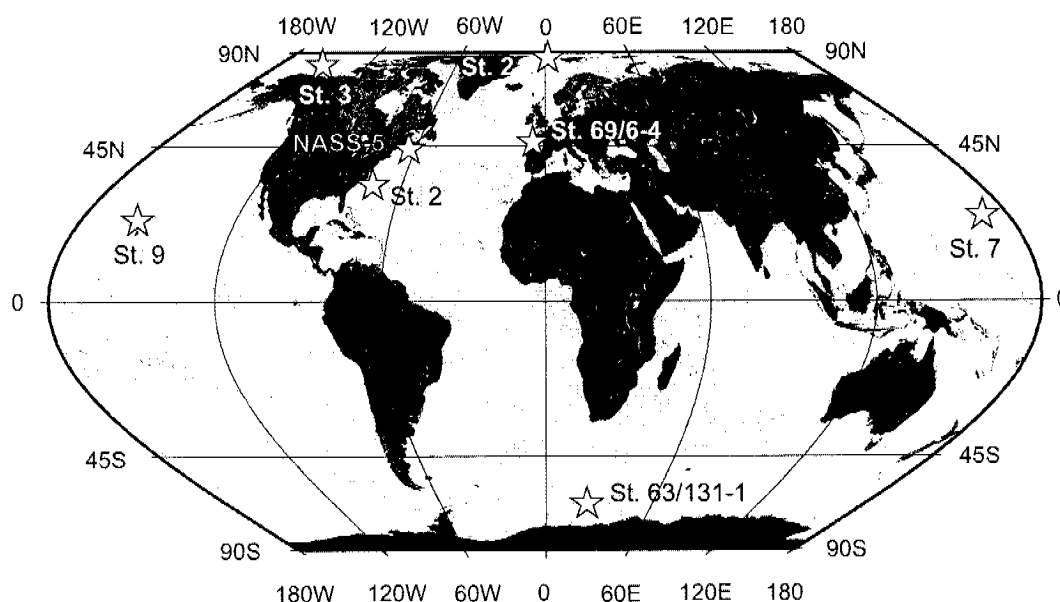


Fig. 5.1. Map showing the sampling locations (stars) and station numbers of the seawater samples analyzed in this study.

The North Pacific depth profiles were collected during the 2002 Intergovernmental Oceanographic Commission (IOC) Contaminant Baseline Survey Expedition (Measures et al., 2006). Three North Atlantic seawater samples were obtained in 2005 during the Antarctic expedition ANT XXIII/1 in the Bay of Biscay and the R/V Endeavor cruise 408. The international standard reference material NASS-5 (North Atlantic Surface Seawater), which

was collected 35 km southeast of Halifax (Canada), was purchased from the National Research Council of Canada. The Arctic seawater was sampled in 2000 and 2001 during the Arctic West Summer expedition (AWS 2000) in the Canada Basin (Trimble et al., 2004) and the Arctic Ocean Expedition (AO 2001) in the Amundsen Basin (Björk et al., 2002), respectively. The Southern Ocean was surveyed in 2002/03 as part of the Antarctic expedition ANT XX/2 (Hanfland et al., 2005).

The sampling methods for all seawater samples analyzed in this study (except NASS-5) were similar. Sample collection was carried out with a rosette that was fitted with Niskin bottles. Following retrieval, the seawater was immediately passed through 0.45 μm Millipore cellulose filters (0.22 μm for AO-2001), transferred into pre-cleaned polypropylene bottles and acidified to approximately pH 1-2 with concentrated, Teflon distilled HCl.

The NASS-5 reference material was sampled with a peristaltic pump through cleaned polyethylene lined ethyl vinyl acetate tubing and 0.45 μm acrylic copolymer filters. It was then acidified to pH 1.6 with ultrapure HNO_3 and transferred to 50 litre acid leached polypropylene carboys. A large volume of this seawater was later homogenized in two linked 800 litre polyethylene tanks and then transferred into cleaned 500 ml polyethylene bottles (see NASS-5 Certification Document for further details of the sample preparation procedure).

Table 5.1. Cadmium concentration and isotope composition data for seawater samples analyzed in this study.

Cruise name	Sampling site	Date	Station #	Latitude	Longitude	Water depth (m)	Cd (nM)	2 s.d.	$\epsilon^{114/110}\text{Cd}$	error	n-a
IOC 2002	North Pacific	22.05.02	7	24.3°N	170.3°E	10	0.0031	0.0002	38	6	1-1
IOC 2002	North Pacific	22.05.02	7	24.3°N	170.3°E	50	0.0153	0.0003	16.0	2.3	2-2
IOC 2002	North Pacific	22.05.02	7	24.3°N	170.3°E	100	0.0021	0.0001	-6	6	3-3
IOC 2002	North Pacific	22.05.02	7	24.3°N	170.3°E	600	0.6380	0.0008	4.3	1.0	2-1
IOC 2002	North Pacific	22.05.02	7	24.3°N	170.3°E	900	1.0062	0.0004	3.6	1.0	2-1
IOC 2002 ^s	North Pacific	22.05.02	7	24.3°N	170.3°E	1200	0.9941	0.0009	3.2	1.3*	9-5
IOC 2002	North Pacific	22.05.02	7	24.3°N	170.3°E	4000	0.8620	0.00004	3.0	1.0	2-1
IOC 2002	North Pacific	22.05.02	7	24.3°N	170.3°E	5700	0.8337	0.0018	3.2	1.6*	5-2
IOC 2002	North Pacific	30.05.02	9 (ALOHA)	22.8°N	158°W	10	0.0048	0.0004	6.2	2.7	2-2
IOC 2002	North Pacific	30.05.02	9 (ALOHA)	22.8°N	158°W	100	0.0076	0.0001	5.2	2.5	2-2
IOC 2002	North Pacific	30.05.02	9 (ALOHA)	22.8°N	158°W	1200	0.9876	0.00001	2.9	1.4	2-1
AWS 2000	Arctic, Canada Basin	24.08.00	3	75.2°N	149.9°W	5	0.2531	0.0002	5.8	1.0	3-2
AWS 2000 ^s	Arctic, Canada Basin	24.08.00	3	75.2°N	149.9°W	50	0.3378	0.0004	6.6	1.6*	5-2
AWS 2000	Arctic, Canada Basin	24.08.00	3	75.2°N	149.9°W	150	0.6962	0.0012	3.9	1.0	2-1
AWS 2000	Arctic, Canada Basin	24.08.00	3	75.2°N	149.9°W	400	0.2209	0.0005	4.2	1.0	3-2
AWS 2000	Arctic, Canada Basin	24.08.00	3	75.2°N	149.9°W	3000	0.2040	0.0003	4.4	1.0	3-2
AO 2001	Arctic, Amundsen Basin	19.08.01	2	88.9°N	2.2°E	8	0.0843	0.0002	7.0	1.4	4-4
NASS-5 ^s	North Atlantic	-	-	-	-	10	0.1978	0.00003	6.4	1.4	3-1
Endeavor 408	North Atlantic	12.07.05	2	33°N	72°W	2900	0.2812	0.00001	3.1	1.0	2-1
ANT XXIII/1	North Atlantic	20.10.05	69/6-4	45.8°N	5.5°W	10	0.0314	0.00007	8.4	1.2	1-1
ANT XXIII/1	North Atlantic	20.10.05	69/6-4	45.8°N	5.5°W	50	0.0284	0.00005	11.3	1.0	1-1
ANT XX/2	Antarctic	10.01.03	63/131-1	61°S	23°E	4000	0.8153	0.0006	2.9	1.0	2-1

The quoted uncertainties for the isotope and concentration data were derived as discussed in the main text (see section 5.3.3). The uncertainties of samples for which five or more individual analyses were available are marked with an asterisk *. n: total number of isotopic analyses. a: number of independent sample aliquots that were analyzed for their Cd isotope composition. ^s from Ripperger and Rehämper (2007b).

5.3 METHODS

A recent publication provides a detailed description of the analytical techniques that were used in this study (Ripperger and Rehkämper, 2007b). Only a brief summary of the methods is thus provided here, plus details of any modifications.

5.3.1 Chemical Separation

About 200 to 4500 ml of seawater were weighed to ensure that roughly 1 to 60 ng of natural (seawater-derived) Cd were available for analyses and a ^{110}Cd - ^{111}Cd double spike was added to achieve a Cd spike-sample ratio of about 4. Following equilibration of this mixture for at least 3 days, Cd was separated from the seawater matrix with a 3-stage column chemistry procedure. Up to 1500 ml seawater were loaded onto the first stage columns, and larger samples were split and loaded on several columns.

The chemical separation method routinely achieved yields of >90%. All Cd concentration data were corrected for the procedural blank of 52 ± 18 pg (1s.d., $n = 8$). At this level, the blank constitutes 1-5% of the indigenous Cd present in strongly depleted surface water samples with only 1 to 5 ng Cd. The majority of samples, however, contained about 10-60 ng of seawater-derived Cd and the blank contribution is thus about 0.1-0.5%. Importantly, the blank contamination has only a negligible effect on the measured isotope compositions in all cases and no correction was therefore applied.

5.3.2 Mass Spectrometry

The Cd isotope composition measurements were carried out with a Nu Plasma MC-ICPMS instrument at the ETH Zürich. For sample introduction, a CETAC Aridus desolvating nebulizer was used, which operated at flow rates of about 100 $\mu\text{l}/\text{min}$. Each isotopic analysis consisted of two measurement sequences ("runs"). In the "main run", the ion currents of ^{110}Cd , ^{111}Cd , ^{112}Cd , ^{114}Cd and ^{117}Sn were measured simultaneously with the Faraday cups, whereas the "Pd interference run" served to determine the ion currents of ^{105}Pd and ^{110}Cd , ^{111}Cd . The ion beams of ^{105}Pd and ^{117}Sn were monitored to correct for isobaric interferences from ^{110}Pd and ^{112}Sn , ^{114}Sn , respectively. The data acquisition sequence of the main run comprised 60 integrations of 5 s each, in blocks of 20, whereas the interference run consisted of a single block of ten 5 s integrations. However, for surface water samples with extremely low Cd concentrations (<0.02 nmol/kg) the acquisition sequence of the main run was reduced

to 10-40 integrations, to ensure that the solutions had Cd concentration of at least 7-30 ng/ml (ppb). Most seawater samples, however, were analyzed as solutions with total Cd concentrations of ~30 to 50 ppb, such that a single (10 min) analysis consumed about 6-10 ng of natural Cd.

5.3.3 Data Presentation

The Cd isotope data of samples are reported relative to results obtained for a standard with an ϵ -notation:

$$\epsilon^{114/110}\text{Cd} = \left(\frac{R_{\text{Sam}}}{R_{\text{Std}}} - 1 \right) \times 10,000 \quad (5.1)$$

where R_{Sam} and R_{Std} denote the $^{114}\text{Cd}/^{110}\text{Cd}$ isotope ratios of the sample and the standard, respectively. Two standards were used in this study: a JMC Cd Münster solution that defines $\epsilon^{114/110}\text{Cd} = 0$ and Alfa Cd Zürich, which has the same Cd isotope composition to within $\pm 0.5 \epsilon^{114/110}\text{Cd}$ (Ripperger and Rehkämper, 2007b). Lacan et al. (2006) also utilized JMC Cd Münster as “zero-epsilon” reference standard in their recent Cd isotope study but they reported their results with an ϵ per amu mass difference (ϵ/amu) notation, that was generally calculated from the measured $^{110}\text{Cd}/^{111}\text{Cd}$ ratios. These data can be rigorously converted into the $\epsilon^{114/110}\text{Cd}$ notation (Wombacher and Rehkämper, 2004) using:

$$\epsilon^{114/110}\text{Cd} = \left[\left(\frac{\epsilon^{110/111}\text{Cd}/\text{amu} \times (m_{111} - m_{110})}{10,000} + 1 \right)^{\beta} - 1 \right] \times 10,000 \quad (5.2)$$

where m_i denotes the atomic weight of the respective Cd isotope and the exponent is defined by $\beta = \ln(m_{114}/m_{110})/\ln(m_{111}/m_{110})$. The simple approximation

$$\epsilon^{114/110}\text{Cd} \approx \epsilon^{110/111}\text{Cd}/\text{amu} \times 4 \quad (5.3)$$

can be used for convenience, however, and the results are identical to the rigorous calculation to within ± 0.1 and $\pm 0.5 \epsilon^{114/110}\text{Cd}$, for $\epsilon^{114/110}\text{Cd}$ values of less +10 and +40, respectively.

The uncertainties of the Cd isotope data listed in Table 5.1 were obtained as follows. The majority of the results are based on two to four analyses but five or more individual measurements were performed for some samples. In the latter case, the uncertainty denotes

two standard deviations (2s.d.) of the dataset. These 2s.d. values are nearly identical to the single-day reproducibilities quoted by Ripperger and Rehkämper (2007b) for multiple analyses of mixtures of the Cd double spike with a Cd standard. Therefore, the uncertainty of samples analyzed less than five times was determined from the single-day reproducibility that was obtained for analyses of double spike-standard mixtures conducted with similar concentrations and data acquisition periods. The large uncertainties of the isotope data for the North Pacific shallow water samples from Station 7 (10 m and 100 m) reflect the extremely low Cd concentrations of the seawater (≤ 0.003 nmol/kg). Analyses of both samples consumed only about 1 ng of natural Cd, which is associated with a typical within-day precision of about ± 4 to ± 8 $\epsilon^{114/110}\text{Cd}$ (2s.d.) (Ripperger and Rehkämper, 2007b).

The quoted uncertainties for the Cd concentration data denote two standard deviations except for the ANT XXIII/1 samples, for which only one sample aliquot was analyzed. In this case, the uncertainty was derived from the internal precision (2s.d.) of the $^{111}\text{Cd}/^{114}\text{Cd}$ and $^{112}\text{Cd}/^{114}\text{Cd}$ ratios, which were used to determine the Cd concentrations.

5.4 RESULTS

5.4.1 General Depth Dependency of Cd Isotope Composition

The seawater samples from depths ≤ 150 m display large variations in Cd isotopic compositions, with $\epsilon^{114/110}\text{Cd}$ values that range from -6 ± 6 to $+38 \pm 6$ (Fig. 5.2). Most samples from the upper water column have low Cd concentrations of < 0.03 nmol/kg, with the exception of the shallow Arctic Ocean samples and the seawater reference material NASS-5 from the coast of Nova Scotia (Table 5.1).

In contrast, nearly identical Cd isotope compositions of $\epsilon^{114/110}\text{Cd} \approx +3$ were found for all seawater samples collected from depths ≥ 900 m (Fig. 5.2), including Arctic Deep Water (ADW), North Atlantic Deep Water (NADW), Antarctic Bottom Water (AABW) and North Pacific Intermediate (NPIW) and Deep Water (NPDW). The analyzed deep-water samples furthermore show the expected increase of Cd concentration along the global deep-water conveyor belt, from the North Atlantic ($[\text{Cd}] \approx 0.3$ nmol/kg), through the Southern Ocean ($[\text{Cd}] \approx 0.8$ nmol/kg) to the North Pacific ($[\text{Cd}] \approx 0.9$ nmol/kg).

There are only two samples from intermediate depths of 400 and 600 m and these have Cd isotope compositions slightly heavier than the deep-water average, with $\epsilon^{114/110}\text{Cd} \approx +4$.

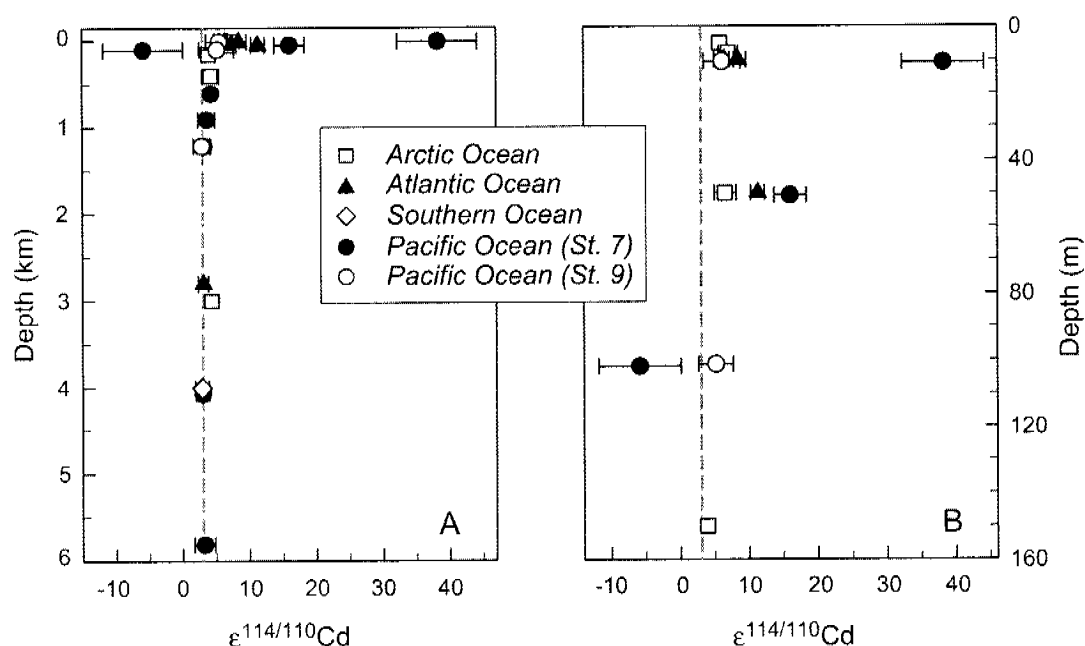


Fig. 5.2. Cd isotope data for the seawater samples plotted as a function of depth. Different ocean basins are denoted by distinct symbols. (a) Data for all seawater samples analyzed in this study. (b) Data for samples from the uppermost water column only (≤ 150 m depth).

5.4.2 North Pacific Water Column Profiles

Two water column profiles from the North Pacific subtropical gyre (NPSG) at Stations 7 and 9 were analyzed in this study (Fig. 5.1). Both stations display broadly similar depth profiles for Cd concentrations (Fig. 5.3a, b) as well as many other physical and chemical parameters, including temperature, oxygen and nutrient contents (Fig. 5.4). The samples analyzed at both stations also exhibit a close correlation between Cd and phosphate concentrations and the vertical Cd distribution is in agreement with published data for the North Pacific (Boyle et al., 1976; Bruland, 1980). However, small yet significant differences in salinities are observed for the two Stations at depths ≤ 500 m, in particular in the upper 50 m of the water column (Fig. 5.4a).

The largest Cd isotope fractionations are recorded at Station 7, where the three shallowest samples from 10 to 100 m depth have low Cd contents (of between 0.002 to 0.015 nmol/kg) and Cd isotope compositions that vary between $\epsilon^{114/110}\text{Cd} \approx +38 \pm 6$ and -6 ± 6 (Fig. 5.3a). It is notable that the lowest Cd concentration is found at 100 m depth, which coincides with a subsurface Chlorophyll-a maximum at ~ 125 m (Selph et al., 2005). The remaining samples of Station 7 from greater depths (600 to 5700 m) exhibit significantly higher Cd concentrations

of about 0.6-1.0 nmol/kg and a nearly constant $\epsilon^{114/110}\text{Cd} = +3.5 \pm 0.5$ (1s.d.). The highest Cd content of ~ 1 nmol/kg is observed near the oxygen minimum zone at 900 m (Figs. 5.3a, 5.4), and is likely to reflect biologically-mediated decomposition of soft tissue and remineralization of Cd.

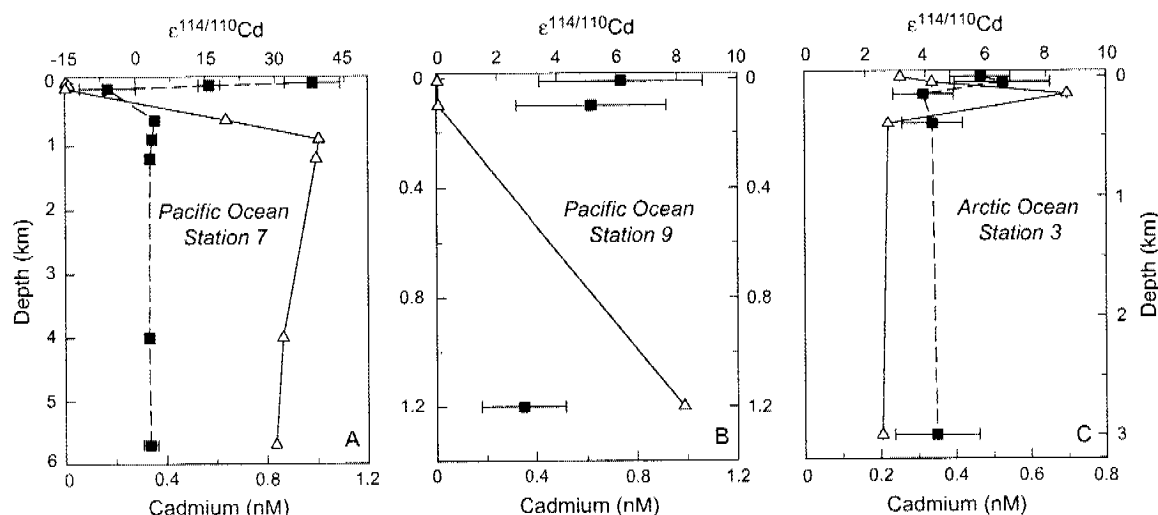


Fig. 5.3. Depth profiles of Cd concentration (open triangles) and Cd isotope composition (filled squares) for the Pacific Ocean Stations 7 and 9, as well as for the Arctic Ocean Station 3. The error bars for the Cd concentration data are within the size of the symbols.

For Station 9, which is situated in the vicinity of Hawaii about 32° east of Station 7 (Fig. 5.1), the Cd isotope data obtained for the uppermost water column differ significantly from the Station 7 results. Both the surface and subsurface samples (10 and 100 m depth) are isotopically fractionated relative to the 1200 m sample (which displays $\epsilon^{114/110}\text{Cd} = +2.9 \pm 1.4$), but the isotope fractionation is much less pronounced than at Station 7, with $\epsilon^{114/110}\text{Cd}$ values of $+6.2 \pm 2.7$ and $+5.2 \pm 2.5$ (Fig. 5.3b).

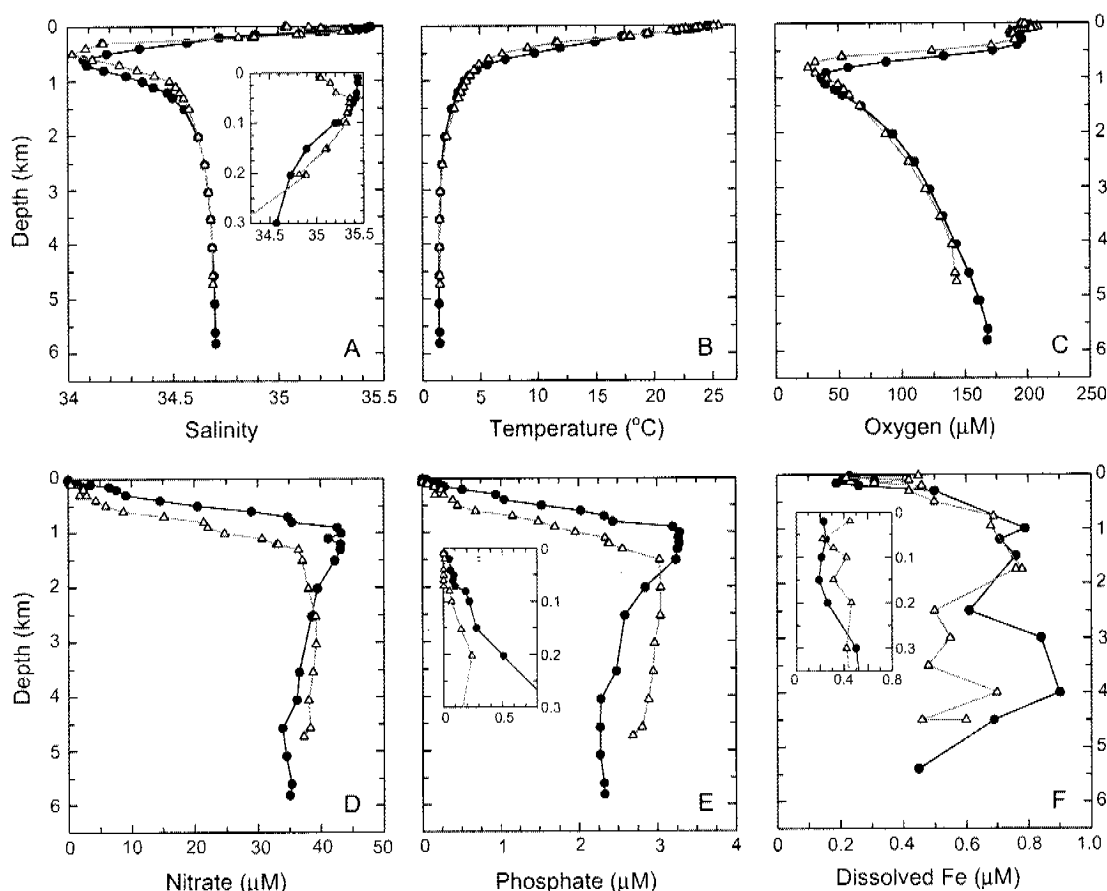


Fig. 5.4. Vertical distribution of various seawater parameters for the North Pacific Station 7 (filled circles) and Station 9 (open triangles). Depth profiles are shown for salinity (a), temperature (b), oxygen (c) and for the nutrients nitrate (d), phosphate (e), and dissolved iron (f). The data are taken from Measures (2002), Measures et al. (2006) and Brown et al. (2005).

5.4.3 Arctic Ocean Water Column Profile

The Station 3 profile from the Canada Basin of the Arctic Ocean (Fig. 5.1) displays a Cd maximum of ~ 0.7 nmol/kg in the halocline layer at ~ 150 m (Fig. 5.3c). Cadmium maxima at similar depths have been reported for various locations in the Arctic (Moore, 1981; Yeats and Westerlund, 1991) and they are generally thought to reflect the inflow of Pacific water that has been modified on the shelf by Cd addition (Jones et al., 1990). The shallow water samples from the surface mixed layer (5 m) and the upper halocline (50 m) have Cd isotope compositions of $\epsilon^{114/110}\text{Cd} \approx +6$ (Fig. 5.3c) and Cd contents of ~ 0.3 nmol/kg which greatly exceed the Cd levels of most surface waters from other ocean basins. The relatively high Cd

concentrations are in accord with previously published results and they are thought to reflect both lack of Cd removal due to the low overall primary productivity and Cd addition from external sources (Moore, 1981; Jones et al., 1990). These shallow Canada Basin samples have salinities of only about 26 (5 m depth) and 31 (50 m), and recent oxygen isotope data indicate that this reflects extensive mixing with river water rather than ice melt (Trimble et al., 2004; Andersen et al., 2007). The Cd concentrations of rivers draining into the Arctic Ocean are too low, however, to support the high Cd contents of the seawater (Dai and Martin, 1995; Guieu et al., 1996), and they are thus more likely to reflect Cd release from shelf sediments possibly by diagenetic or biogeochemical processes (Yeats and Westerlund, 1991). The Arctic sample from ~10 m depth in the Amundsen Basin is also characterized by a low salinity (~31) due to inputs from Siberian Rivers (Björk et al., 2002). Its low Cd content of ~0.08 nmol/kg (Table 5.1) cannot be due to these riverine inputs, however, but must be a consequence of recent Cd removal, most likely by biological uptake.

The Canada Basin samples from 400 m (Atlantic layer) and 3000 m (ADW) depth display nearly identical isotope compositions of $\epsilon^{114/110}\text{Cd} \approx +4$ and Cd contents (of ~0.2 nmol/kg) that are in accord with previous results obtained for Arctic Ocean samples of similar depths (Moore, 1981).

5.5 DISCUSSION

The following discussion focuses on three key features of the new Cd dataset (Fig. 5.5). (i) A clearly visible trend of increasing $\epsilon^{114/110}\text{Cd}$ with decreasing Cd concentration that is defined by the majority of samples. (ii) This trend displays significant scatter, however, and three shallow water samples from the North Pacific even combine un-fractionated or light Cd isotope compositions with very low Cd contents (<0.008 nmol/kg). (iii) Seawater samples from depths ≥ 900 m display nearly constant $\epsilon^{114/110}\text{Cd}$ values of about +3.

5.5.1 Biological Fractionation of Cd Isotopes

A large group of samples defines a trend of increasing $\epsilon^{114/110}\text{Cd}$ with decreasing dissolved Cd content (Fig. 5.5a). The Cd-rich end-member of this trend is given by intermediate and deep-water samples that display Cd concentrations of about 0.3-1.0 nmol/kg and $\epsilon^{114/110}\text{Cd} \approx +3$. From here, the trend extends to the Cd-depleted and high- $\epsilon^{114/110}\text{Cd}$ compositions that are exhibited by most seawater samples that were collected in the euphotic zone at depths of ≤ 50 m (Fig. 5.2). The most extreme composition is given by the 10 m sample from the NPSG

Station 7, which features $\epsilon^{114/110}\text{Cd} \approx +38 \pm 6$ and a Cd concentration of about 0.003 nmol/kg (Figs. 5.3a, 5.5a). A similar co-variation of Cd concentration and isotope composition for seawater was previously identified by Lacan et al. (2006), but their trend was significantly less well defined due to the larger (by a factor of ~ 3) measurement uncertainties and a much smaller spread of Cd concentrations.

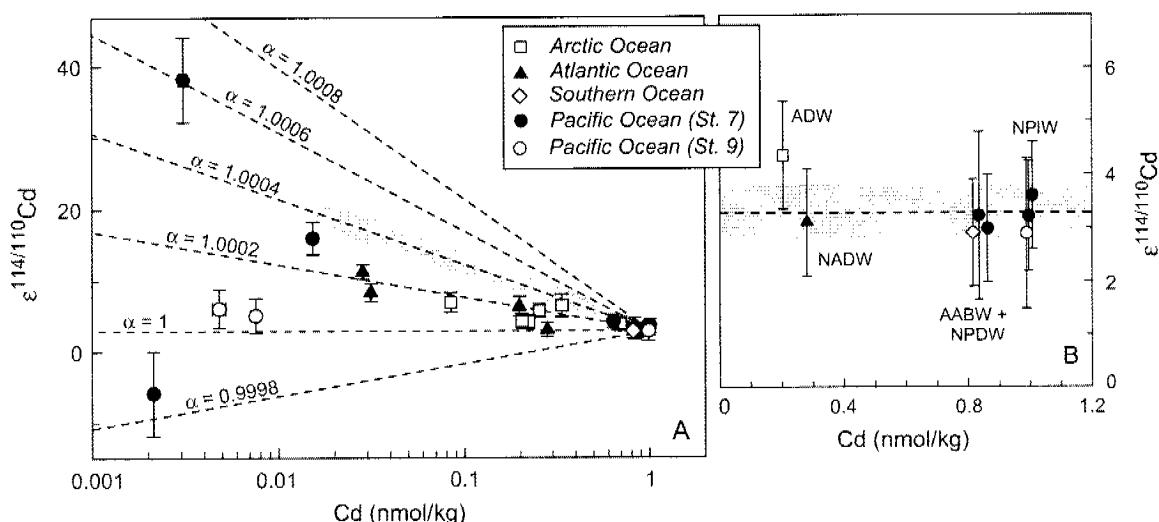


Fig. 5.5. Plot of Cd isotope composition versus Cd concentration. The various sampling locations are denoted by distinct symbols. The error bars for the Cd concentration data are within the size of the symbols. (a) Data for all seawater samples from this study. The grey arrow denotes the trend of increasing isotope fractionation with decreasing dissolved Cd content, which is defined by the majority of the samples. The dashed lines denote the calculated isotopic evolution of dissolved seawater Cd, assuming that biological uptake of Cd occurs by closed system Rayleigh fractionation with fractionation factors α of between 0.9998 and 1.0008 (see Appendix A5.2). (b) Data for intermediate and deep water samples from $\geq 900\text{m}$ depth only: Arctic Deep Water (ADW), North Atlantic Deep Water (NADW), Antarctic Bottom Water (AABW), North Pacific Intermediate Water (NPIW). These samples display a mean Cd isotope composition of $\epsilon^{114/110}\text{Cd} = +3.3 \pm 0.5$ (1s.d.; dashed line and shaded field).

The low Cd concentrations of (near-) surface water samples and the nutrient-like distribution of Cd in the oceans are generally thought to reflect uptake of Cd by phytoplankton (Bruland and Lohan, 2003). Evidence of true biological demand for the micronutrient Cd under Zn-limiting conditions was presented by a number of researchers (Price and Morel (1990), Lane and Morel (2000), Morel and Price (2003) and Lane et al. (2005)) and recent culture experiments (Lacan et al., 2006) furthermore demonstrated that phytoplankton preferentially take up isotopically light Cd with a fractionation factor of $\alpha = 1.0014 \pm 0.0006$ (2s.d.) for $^{114}\text{Cd}/^{110}\text{Cd}$. This, and the large Cd isotope variations observed for surface waters (Fig. 5.2), indicates that the trend of Fig. 5.5a reflects kinetic isotope fractionation from biological uptake of Cd.

If one accepts this interpretation, it is useful to consider two end-member models of nutrient utilization: (i) closed system Rayleigh fractionation and (ii) isotope fractionation in a steady state ocean system. (i) Rayleigh fractionation requires that a finite pool of Cd is available, as when a plankton bloom occurs in response to nutrient (and Cd) inputs to a stratified ocean system. In this case, more positive $\epsilon^{114/110}\text{Cd}$ values reflect increased utilization of Cd and nutrients. The Rayleigh fractionation lines shown in Fig. 5.5a are appropriate for such a scenario and they indicate that the data are in accord with fractionation factors of about 1.0002 to 1.0006 for $^{114}\text{Cd}/^{110}\text{Cd}$ (see Appendix equation (A5.2)). (ii) Ocean systems with temporally uniform nutrient and Cd concentrations are expected to be in steady state. In this case, the Cd isotope compositions of the input and output fluxes are identical, and variations in the isotope composition of the dissolved phase are primarily driven by changes in the fractionation factor associated with Cd uptake (see Appendix equation (A5.6)).

The observation that a large number of samples display a co-variation of Cd concentration with $\epsilon^{114/110}\text{Cd}$ (Fig. 5.5a) is most readily explained if the distribution of Cd in the upper water column is primarily governed by closed system Rayleigh fractionation. This interpretation is in accord with a previous empirical modelling study, which accounted for the global variability of Cd/P in seawater by assuming that the uptake of Cd and P from surface waters can be described by Rayleigh fractionation (Elderfield and Rickaby, 2000). Essentially identical Rayleigh models have also been used to describe isotope variations of the nutrient elements N and Si in surface waters (De La Rocha et al., 1998; Sigman et al., 2000; Reynolds et al., 2006). The similar isotopic distributions of Cd, Si, and N thus strengthens the interpretation that the cycling and isotope fractionation of Cd is primarily governed by biological uptake.

Further support for the general suitability of a closed system Rayleigh model to describe the behaviour of Cd in the euphotic zone, is provided by calculations, which show that biological utilization in a steady state scenario cannot generate Cd-depleted water samples with $\epsilon^{114/110}\text{Cd}$ values of greater than about +15 to +20 (as observed in this study), assuming (i) that the fractionation factor for uptake of dissolved seawater Cd is not larger than the value determined in the culture experiments (Lacan et al., 2006) and (ii) that the source and sink fluxes of marine Cd are characterized by $\epsilon^{114/110}\text{Cd} \approx +3$.

5.5.2 Variability of Cd Isotope Systematics

Inspection of Fig. 5.5a also reveals that the samples with high $\epsilon^{114/110}\text{Cd}$ do not define a single fractionation line but fall on a rather scattered trend. The dataset furthermore includes three samples that have low Cd contents and $\epsilon^{114/110}\text{Cd}$ values of between -6 and +6. It is possible that these deviations and outliers reflect contamination of originally fractionated samples (with high $\epsilon^{114/110}\text{Cd}$) with isotopically normal Cd ($\epsilon^{114/110}\text{Cd} \approx 0$; Wombacher et al. 2003) during sampling, ship-board handling, or storage. Contamination effects are deemed to be unlikely but they cannot be ruled out completely at present, given that the most unusual seawater samples have Cd contents of less than 0.008 nmol/kg. It is also conceivable that the deviations reflect filtration artefacts from the passage of biogenic particulates through the 0.45 or 0.22 μm filter disks. Mass balance calculations, which assume that unretained particulate matter (with $\epsilon^{114/110}\text{Cd} \approx 0$) provides up to 6% (Lacan et al., 2006) of the total Cd budget of filtered seawater, show that such particles can only shift the isotope composition of the filtrate by less than 2 and 0.5 $\epsilon^{114/110}\text{Cd}$ -units, if the (pure) dissolved Cd is characterized by $\epsilon^{114/110}\text{Cd} = +40$ and +10, respectively.

Taken together it is thus reasonable to assume that sample contamination and filtration artefacts were both negligible. The further discussion therefore focuses on two key natural mechanisms, which may be responsible for the variable Cd isotope systematics of seawater: (i) variations in the isotope fractionation factor of Cd and (ii) mixing processes which involve inputs of Cd from various sources. Of particular relevance to the discussion of these mechanisms are the samples from the euphotic zone of the NPSG Stations 7 (10m, 50m, 100m) and 9 (10m, 100m).

5.5.2.1 Variations in the Cd Fractionation Factor

It is possible that vital effects are (at least in part) responsible for the observation that the seawater data of Fig. 5.5a record lower net fractionation factors (1.0002-1.0006) than those determined for the freshwater phytoplankton (1.0014) by Lacan et al. (2006). Given the current absence of experimental data for marine phytoplankton, it is even conceivable that vital effects are responsible for the large differences in Cd isotope composition between the North Pacific surface water samples.

The incorporation of Cd into phytoplankton tissue is furthermore not only controlled by the phytoplankton assemblages. It can also depend on the concentrations of various trace

metals in seawater, for example on dissolved Zn contents (Sunda and Huntsman, 1996; Sunda and Huntsman, 2000). As Cd can substitute for Zn in various metalloenzymes, such as carbonic anhydrase and alkaline phosphatase (e.g., Morel and Price, 2003; Lane et al., 2005), it is possible that biological uptake and isotope fractionation of Cd may not play an important role in surface waters where Zn is not limited. Whether the enhanced availability of Zn at Station 9 compared to Station 7 in fact influenced Cd uptake by phytoplankton remains speculative because Zn data are presently not available for either Station.

Adsorption processes provide an alternative route for producing Cd-depleted seawater, and such seawater may exhibit nearly un-fractionated Cd isotope compositions. This conclusion is based on the data of Schmitt et al. (2006), who showed that Cd adsorbed onto Fe-Mn nodules has isotope compositions that are only slightly fractionated ($\epsilon^{114/110}\text{Cd} = -0.4$ to $+0.6$) relative to a putative deep-water source with $\epsilon^{114/110}\text{Cd} \approx +3$ (Fig. 5.5b). Laboratory culture experiments furthermore suggest that isotopically heavy Zn is preferentially adsorbed onto diatoms, but the observed isotope effects are also comparatively small compared to cellular uptake of Zn (Vance et al., 2006). Adsorption onto bacteria may play an important role in controlling marine trace metal budgets, as bacteria generally have extremely high specific surface areas (e.g., Dixon et al., 2006). This indicates that adsorption processes may be responsible for the scatter in the Rayleigh trend defined by the surface water samples (Fig. 5.5a), and the finding that the observed fractionation factors are much smaller than those determined in the culturing experiments (Lacan et al., 2006).

It is unlikely, however, that adsorption processes are responsible for the different Cd systematics of the samples from NPSG Stations 7 and 9. This explanation is implausible because it requires that the Cd distributions at Stations 7 and 9 are dominantly controlled by biological uptake (with significant isotope fractionation) and adsorption (with only minor isotope fractionation), respectively. Given the similarity in microbial communities (Selph et al., 2005) at both stations there is no supporting evidence for such a scenario

5.5.2.2 *Variations of External Inputs and Internal Mixing Processes*

Atmospheric inputs are an important source of Cd to the open ocean (e.g. Ucmatsu et al., 1983) and they may thus be responsible for the different Cd isotope compositions of seawater from Stations 7 and 9. This hypothesis can be rigorously evaluated because the main atmospheric Cd flux to the surface ocean is likely supplied by rain and the anomalously low salinity of Station 9 surface waters (Fig. 5.4) might be attributed to a particularly intense

rainstorm. Mass balance calculations (Table 5.2) demonstrate that $\sim 230 \text{ Lm}^{-2}$ of precipitation are necessary to account for the salinity anomaly observed at Station 9 surface waters relative to Station 7. Such an input of precipitation is not unrealistic because local storms can deposit up to 100 Lm^{-2} of rain per hour on Pacific islands (e.g., Lyman et al., 2005). Given that the precipitation rates are about a factor of 1.6 lower in the vicinity of Hawaii than on the Islands proper (Reed, 1980), the maximum open ocean rainfall rate is $\sim 60 \text{ Lm}^{-2}$ per hour. This indicates that 230 Lm^{-2} of rain can be deposited at Station 9 by one or several storms with a total duration of ~ 4 hours.

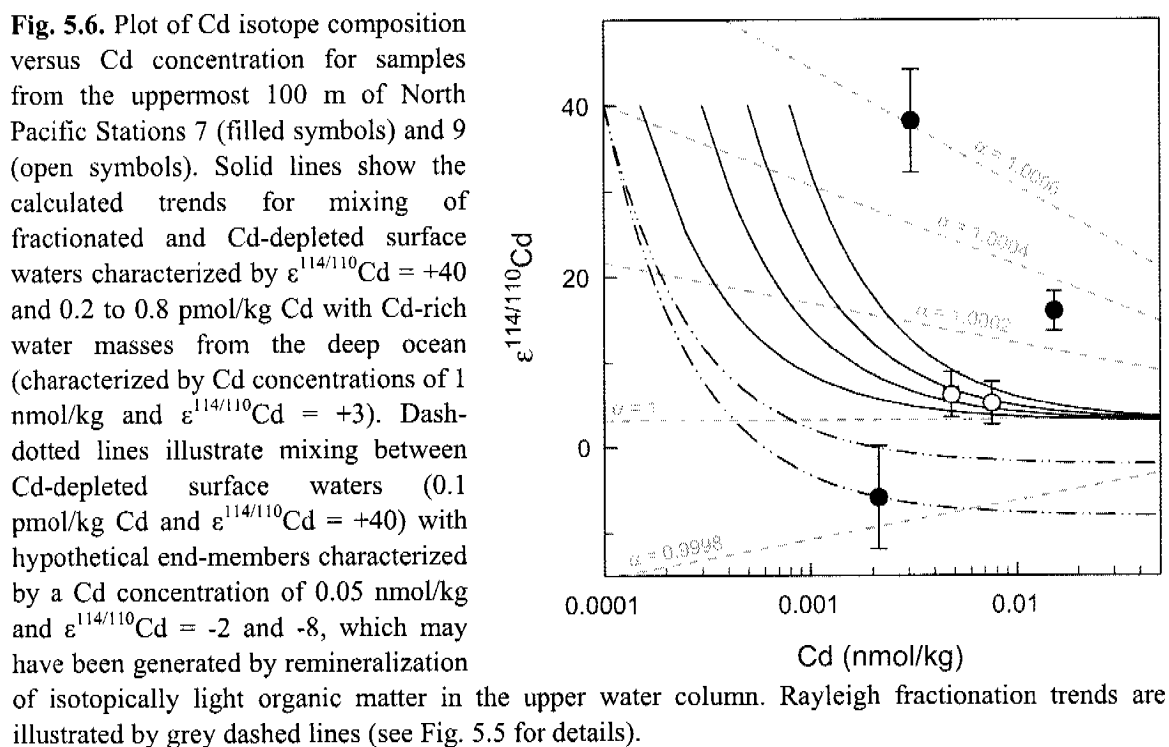
The present atmospheric Cd flux to the oceans is dominated by anthropogenic sources (Lantzy and Mackenzie, 1979; Duce et al., 1991; Patterson and Duce, 1991), which commonly emit either un-fractionated ($\epsilon^{114/110}\text{Cd} \approx 0$) or isotopically light Cd (Cloquet et al., 2005). Assuming that rainwater has a Cd concentration and isotope composition of $\sim 0.8 \text{ nmol/kg}$ and $\epsilon^{114/110}\text{Cd} = -6.4$, respectively (Table 5.2), a precipitation event of $\sim 230 \text{ Lm}^{-2}$ can generate the nearly un-fractionated isotope compositions observed for Station 9 surface waters ($\epsilon^{114/110}\text{Cd} \approx +6$; Table 5.1) from a source that originally resembled the upper water column of Station 7 (Tables 5.1, 5.2). This scenario produces surface water Cd contents that are about a factor of two higher (at $\sim 0.01 \text{ nmol/kg}$) than the measured Cd concentrations at 10 m depth of Station 9 (Table 5.1). This minor discrepancy can be readily resolved, however, as the concentration of dissolved seawater Cd can be reduced by adsorption, for example onto particles (such as Fe-rich colloids) that were formed by the precipitation event.

Table 5.2. Parameters of the mixing model that accounts for the nearly un-fractionated Cd isotope compositions of the Station 9 samples from 10 and 100 m by Cd addition through precipitation.

Depth of mixed layer (m)	Salinity at St. 9, 10 m	Salinity at St. 7, 10 m	Salinity of rain	Rainfall needed (L m^{-2})	Cd in rain (nmol/kg)	$\epsilon^{114/110}\text{Cd}$ of dust	Cd in mixture (nmol/kg)	$\epsilon^{114/110}\text{Cd}$ mixture
20 [#]	35.04 [*]	35.44 [*]	1	232	0.011-1.068 ^{&}	-6.4 ^{\$}	0.003-0.015	5.7-28.5

The modeling first determines the amount of rainfall that is required to account for the lower salinity of the mixed layer at Station (St.) 9 relative to Station 7. This value is then used to estimate the Cd concentration and isotope composition of the mixed layer, following addition of rainwater characterized by negative $\epsilon^{114/110}\text{Cd}$ values. The calculations assume (i) that the mixed layer was characterized by $[\text{Cd}] = 0.003 \text{ nmol/kg}$ and $\epsilon^{114/110}\text{Cd} = 30$ prior to the addition of rain and (ii) that 100% of the rain-derived Cd dissolved in the mixed layer (e.g., Duce et al., 1991; Patterson and Duce, 1991). [#] (Measures et al., 2006); ^{*} (Measures, 2002); [&] (Patterson and Duce, 1991); ^{\$} (Cloquet et al., 2005).

Internal mixing processes provide an alternative explanation for the nearly un-fractionated Cd isotope signatures of the 10 m and 100 m samples from Station 9. The modelled curves of Fig. 5.6 demonstrate that mixing of isotopically fractionated and Cd-depleted surface waters with deep- or intermediate water masses characterized by $[Cd] \approx 1$ nmol/kg and $\epsilon^{114/110}Cd \approx +3$ can account for the isotope systematics of the Station 9 samples (see Appendix equation A5.7)). This is also a reasonable explanation because aperiodic upwelling and mixing are typical features of oligotrophic gyres, such as the NPSG (Karl et al., 1996; Karl, 1999; McGillicuddy et al., 2007). To reconcile the Station 9 data with fractionation factors of 1.0002-1.0006, it is necessary to postulate, however, that the fractionated surface waters originally displayed very low Cd contents of about 0.0006 to 0.003 nmol/kg (Fig. 5.6).



A somewhat similar explanation can be developed for the low $\epsilon^{114/110}Cd$ value of -6 ± 6 observed at 100 m depth of Station 7. This scenario, which is analogous to that developed by Bermin et al. (2006) for seawater Zn isotope data, involves mixing between fractionated surface waters and water masses, which have Cd systematics that are dominated by the remineralization of phytoplankton biomass. Any biomass that is produced during the initial

stages of Cd uptake from a replenished surface water reservoir (originally characterized by $\epsilon^{114/110}\text{Cd} \approx +3$) will display $\epsilon^{114/110}\text{Cd}$ values of less than +3 (Fig. 5.7). Local production of such biomass and its remineralization could thus generate water masses characterized by $\epsilon^{114/110}\text{Cd} \leq +3$. Support for this recycling model is provided by a significant increase of the dissolved phosphate content at about 100 m at Station 7 (Fig. 5.4), which may reflect remineralization of organic matter.

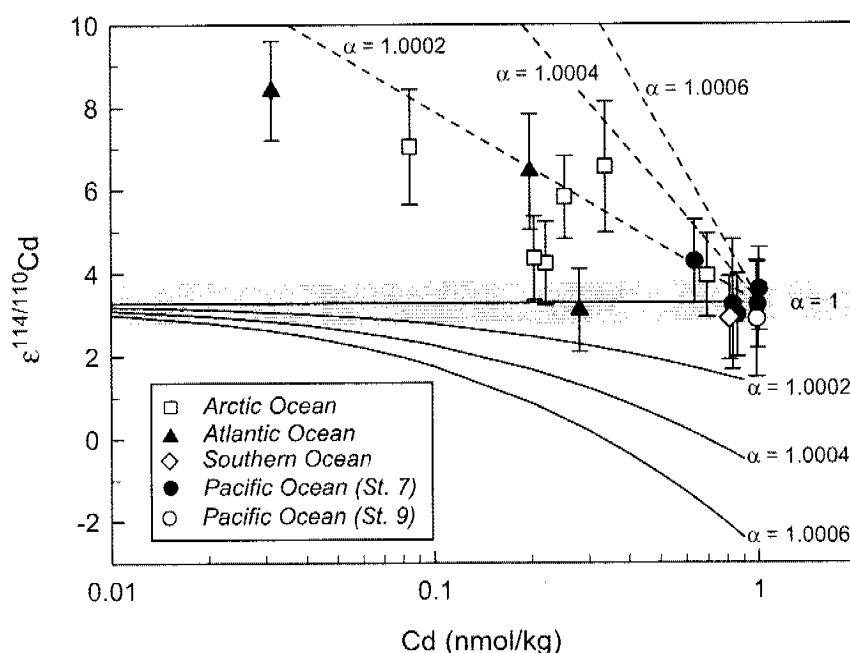


Fig. 5.7. Plot of Cd isotope composition versus Cd concentration that illustrates the Rayleigh fractionation curves for the average isotope composition of accumulated biomass (solid lines, see Appendix, equation (A5.4)), which preferentially takes up isotopically light Cd with fractionation factors of $\alpha = 1.0000$, 1.0002 , 1.0004 and 1.0006 . The dashed lines denote the contemporaneous isotopic evolution of the residual Cd-depleted seawater (see Fig. 5.5 for details). The calculated curves demonstrate that the accumulated biomass yields $\epsilon^{114/110}\text{Cd}$ values of about +3, if more than 90 to 98% of the initial Cd present in seawater are removed by biological utilization.

5.5.3 Constant Cd Isotope Composition of Deep Water

An important finding of this investigation is that 8 seawater samples collected at depth $\geq 900\text{m}$ in 4 ocean basins (Fig. 5.5b) display an almost constant isotope composition of $\epsilon^{114/110}\text{Cd} = +3.3 \pm 0.5$ (1s.d.). Lacan et al. (2006) also analyzed 11 seawater samples from depths $\geq 900\text{ m}$ but they are from only one station in the NW Pacific Ocean and the Mediterranean Sea. These latter samples yielded a mean isotope composition of $\epsilon^{114/110}\text{Cd} \approx$

$+0.8 \pm 1.2$ (1s.d) that is slightly lower than the deep water value of the present study. This offset is not considered to be significant, however, given that Lacan et al. (2006) quote a reproducibility of $\pm 3.2 \text{ } \epsilon^{114/110}\text{Cd}$ for their data.

Our results are therefore indicative of intermediate and deep water masses that have a nearly constant Cd isotope composition even though the Cd concentrations increase by about a factor of 3 to 4 along the global deep-water pathway, through the remineralization of sinking particulate matter (Bruland and Lohan, 2003). This suggests that the particulate matter, which increases the Cd content of deeper-water masses, is also characterized by a very constant Cd isotope composition of $\epsilon^{114/110}\text{Cd} \approx +3$.

The vertical mass flux of particulate matter is mainly composed of biominerals (e.g., CaCO_3 , opal) and organic matter (Honjo et al., 1982; De La Rocha, 2003). Although the majority (~90%) of the organic matter is recycled within the upper water column (Collier and Edmond, 1984; Fowler and Knauer, 1986; Martin et al., 1987), a substantial amount is also exported from the euphotic zone to deeper waters, as faecal pellets or large aggregates of "marine snow" (Fowler and Knauer, 1986; Turner, 2002; De La Rocha, 2003) and during mass sinking events following phytoplankton blooms (Karl et al., 1996; Turner, 2002). Organic matter furthermore has much higher Cd concentrations than biominerals (Collier and Edmond, 1984; Noriki et al., 1999) and this indicates that the total vertical Cd flux is probably dominated by organic particulate matter.

Given that the incorporation of Cd into organic tissue is associated with significant isotope fractionation (Lacan et al., 2006), the most plausible explanation for the constant Cd isotope composition of deep water is a near quantitative closed-system uptake of Cd from a shallow-water reservoir that is originally characterized by $\epsilon^{114/110}\text{Cd} \approx +3$ (Fig. 5.7). The modelled Rayleigh fractionation curves of Fig. 5.7 display the Cd isotope compositions of accumulated biological material, which removes Cd from the surface water reservoir with an isotope fractionation factor ($\alpha = 1.0002\text{--}1.0006$; see Appendix equation (A5.4)) that approximates the range seen in our seawater analyses (Fig. 5.5a). The fractionation curves for the biomass (Fig. 5.7) demonstrate that biological materials take on average Cd isotope compositions that are identical to the intermediate and deep water value (of $\epsilon^{114/110}\text{Cd} +3.3 \pm 0.5$), if more than 90–98% of the Cd that was originally present in dissolved form are removed by phytoplankton. This mass balance is in accord with the actual observations, as most water samples from the euphotic zone have Cd contents of less than 0.05 nmol/kg, whereas most deep-water masses contain >0.5 nmol/kg Cd (Fig. 5.5, Table 5.1).

5.6 CONCLUSIONS

Cadmium isotopic compositions were determined for seawater samples from different oceanic regimes with a ^{110}Cd - ^{111}Cd double spike and MC-ICPMS. The data provide the first evidence of large and well-resolved Cd isotope variations in the marine environment. The majority of the seawater samples exhibit a clear relationship of Cd isotope composition and concentration, whereby the most Cd-depleted samples show the most fractionated Cd isotope compositions (up to $\epsilon^{114/110}\text{Cd} \approx 38 \pm 6$). This suggests that the Cd isotope variations are due to kinetic isotope effects that are generated by the uptake of dissolved seawater Cd by phytoplankton. The fractionation follows closed system Rayleigh distillation curves and is in accord with fractionation factors of $\alpha \approx 1.0002$ to 1.0006 for $^{114}\text{Cd}/^{110}\text{Cd}$.

Cadmium-rich seawater samples collected at depths $\geq 900\text{m}$ display the expected increase of Cd concentration along the global flow path of deep water but exhibit nearly constant $\epsilon^{114/110}\text{Cd}$ values of about $+3.3 \pm 0.5$ (1s.d.). This indicates that organic matter, which increases the Cd content of deep-water masses by remineralization, is also characterized by very constant Cd isotope compositions of $\epsilon^{114/110}\text{Cd} \approx +3$. This constancy is in accord with a near-quantitative closed system uptake of Cd by phytoplankton from surface waters.

A few shallow water samples that have extremely low Cd contents (<0.008 nmol/kg) exhibit nearly un-fractionated Cd isotope compositions of between $\epsilon^{114/110}\text{Cd} = -6 \pm 6$ and $+6.2 \pm 2.7$. These signatures may have been produced by changes in the Cd fractionation factor that reflect, for example, vital effects or variations in the uptake mechanisms for Cd (e.g., adsorption vs. biological utilization). Alternatively, they may be due to atmospheric inputs of isotopically light Cd or mixing of fractionated surface waters with deeper water masses characterized by $\epsilon^{114/110}\text{Cd} \leq +3$.

The new dataset demonstrates that Cd isotope compositions reveal more complexity in the distribution and cycling of marine Cd, than can be discerned from Cd concentrations alone. Therefore, Cd isotopic compositions have the potential to provide new insights into the biogeochemical processes that govern the marine cycling of Cd. Further progress is expected once more isotopic datasets become available for seawater. Particularly desirable are studies, which simultaneously investigate (i) several trace metal and nutrient isotope systems (e.g., Si, Fe, Zn, Cu, and Cd) and (ii) the isotope systematics of Cd in both the dissolved and particulate phases of seawater at numerous localities. In addition, further studies are required to characterize the uptake mechanisms of Cd by marine microorganisms and its biological

function in phytoplankton and bacteria.. Overall, Cd isotope signatures may prove to be a selective tracer for biological activity, as inorganic geological processes (other than evaporation/condensation) do not generate isotope effects as large as those observed in the present study (Wombacher et al., 2003; Schmitt et al., 2006).

Appendix**Closed System Rayleigh Fractionation**

Seawater. To a first order, the Cd isotope variations determined for seawater can be accounted for by closed system Rayleigh fractionation (Mariotti et al., 1981):

$$R_{sw} = R_{sw,0} \cdot F^{\left(\frac{1}{\alpha} - 1\right)} \quad (A5.1)$$

where R_{sw} and $R_{sw,0}$ denote the $^{114}\text{Cd}/^{110}\text{Cd}$ isotope ratio of the remaining and initial seawater Cd, respectively. The fraction of remaining dissolved seawater Cd is given by $F = c / c_0$, where c and c_0 denote the residual and initial seawater Cd concentration, respectively. Our calculations assume a value of 1 nmol/kg for the latter. The fractionation factor α is defined as $\alpha = R_{sw} / R_{bio}$, where R_{sw} and R_{bio} denote the $^{114}\text{Cd}/^{110}\text{Cd}$ isotope ratios of seawater and biomass, respectively. Note that the fractionation factors reported by Lacan et al. (2006) are in units of ϵ_{Cd} per amu mass difference. Their (old) values can be translated into our (new) notation with the approximate relationship $\alpha_{\text{new}} = -10,000 \cdot (1/\alpha_{\text{old}} - 1)/4$.

Natural variations in the isotopic composition of seawater are expressed relative to a standard with an epsilon notation (see equation 5.1). A widely used approximation of the Rayleigh equation (A5.1), written in the epsilon notation, is given by (Mariotti et al., 1981):

$$\epsilon_{sw} = \epsilon_{sw,0} + 10,000 \cdot \left(\frac{1}{\alpha} - 1\right) \cdot \ln F \quad (A5.2)$$

where ϵ_{sw} and $\epsilon_{sw,0}$ denote the Cd isotope composition of the remaining and the initial seawater, respectively. Equation (A5.2) was used to model the fractionation curves for seawater shown in Figures 5.5a, 5.6 and 5.7, whereby $\epsilon_{sw,0}$ was assigned the average intermediate/deep-water value of $\epsilon^{114/110}\text{Cd} = +3.3$.

Biomass. In a closed system the isotopic mass balance requires that (Mariotti et al., 1981):

$$F \cdot R_{sw} + (1 - F) \cdot R_{bio,acc} = R_{sw,0} \quad (A5.3)$$

where $R_{\text{bio,acc}}$ is the $^{114}\text{Cd}/^{110}\text{Cd}$ isotope ratio of the accumulated biomass. In a common approximation (Mariotti et al., 1981), the isotope ratios R can be replaced by the corresponding epsilon values. By inserting ε_{sw} from equation (A5.2) one can obtain:

$$\varepsilon_{\text{bio,acc}} = \varepsilon_{\text{sw},0} - 10,000 \cdot \left(\frac{1}{\alpha} - 1 \right) \cdot \frac{F \cdot \ln F}{1 - F} \quad (\text{A5.4})$$

where $\varepsilon_{\text{bio,acc}}$ denotes the isotopic composition of the accumulated biomass. Equation (A5.4) was used to model the fractionation lines for the accumulated biomass of Fig. 5.7.

Open System at Steady State

In a steady state surface water reservoir, the Cd input from upwelling water masses (and other sources) must be balanced by the removal of Cd (mainly via biomass settling) and lateral outflow of water. The isotopic composition ε_{sw} of this reservoir can be expressed as:

$$\varepsilon_{\text{sw}} = \varepsilon_{\text{sw},0} - 10,000 \cdot \left(\frac{1}{\alpha} - 1 \right) \cdot (1 - f_{\text{lat}}) \quad (\text{A5.5})$$

where $\varepsilon_{\text{sw},0}$ denotes the isotopic compositions of the Cd input and f_{lat} describes the fraction of the Cd input that is lost through lateral outflow (Hayes, 2004). With the reasonable assumption that $f_{\text{lat}} \approx 0$ (because surface waters have very low Cd contents) equation (A5.5) simplifies to:

$$\varepsilon_{\text{sw}} = \varepsilon_{\text{sw},0} - 10,000 \cdot \left(\frac{1}{\alpha} - 1 \right) \quad (\text{A5.6})$$

Water Mass Mixing

According to Mariotti et al. (1988), the isotope composition of a mixture of two components A and B can be approximated with:

$$\varepsilon_{\text{M}} = \frac{c_{\text{A}} \cdot f \cdot \varepsilon_{\text{A}} + c_{\text{B}} \cdot (1 - f) \cdot \varepsilon_{\text{B}}}{c_{\text{M}}} \quad (\text{A5.7})$$

where c denotes concentrations and ε the isotope compositions of the components A and B. The mixing ratio f is given by $f = M_{\text{A}} / M_{\text{M}}$, with M_{A} and M_{M} denoting the masses of component A and the mixture, respectively. Equation (A5.7) was used to calculate the mixing curves of Fig. 5.6 and the following values were assumed for the Cd-depleted surface water (component A) and deep water (component B): $\varepsilon_{\text{A}} = +40$, $c_{\text{A}} = 0.15, 0.30, 0.50, 0.8$ pmol/kg,

and $\epsilon_B = +3$, $c_B = 1$ nmol/kg. For mixing between surface water (A) and an isotopically light water mass (B), we assumed $\epsilon_A = 40$, $c_A = 0.1$ pmol/kg, and $\epsilon_B = -2$ and -8 , $c_B = 0.05$ nmol/kg.

Acknowledgements

We would like to particularly thank P. S. Andersson, M. Baskaran, E. A. Boyle, M. Frank, W. Geibert, J. Rickli and B. Zimmermann for sampling of the seawater and sharing of samples. We are grateful to the Captain and the Crew of the USCGC *Polar Star*, the icebreaker *Oden*, the R/V *Endeavor* and R/V *Melville* for their help in obtaining the samples during the AWS 2000 (M. Baskaran), the AO 2001 (P.S. Andersson), the Endeavor 408 (E.A. Boyle) and the IOC 2002 (C. Measures, B. Landing, and G. Cutter) cruises, respectively. The ship time for the AWS 2000 Cruise was funded by a grant of the U.S. National Science Foundation to Mark Baskaran (NSF-OPP-9996337) at Wayne State University. We also thank the Captain and the Crew of the R/V *Polarstern* for their work during the ANT XXIII/1 and the ANT XX/2 cruises. This project was originally planned with the help of R. Schiebel and D. Schmidt. Its execution and the interpretation of the results have profited from discussions with and the support of J. McKenzie, G. Henderson, M. Lohan, and D. Vance. We thank M. Andersen for providing us with his unpublished manuscript and E. A. Boyle for constructive comments on a preliminary version of the paper. Financial support was provided by a grant from the Schweizerische Nationalfond (SNF).

CHAPTER 6

General Conclusions and Outlook

6.1 CONCLUSIONS

The behaviour of the trace element cadmium in the marine environment has been studied along two lines of investigation, which both involved the development of new analytical techniques. Two of the four studies in the main part of this thesis (Chapter 2 & 3) are concerned with Cd/Ca ratios in planktonic foraminiferal shells. The other two studies (Chapters 4 & 5) investigate variations in the isotopic composition of dissolved seawater Cd. In the following the main findings of these studies will be briefly summarized.

6.1.1 Cd/Ca Ratios of *in-situ* Collected Foraminiferal Tests

This thesis presents a novel method for the determination of Cd/Ca ratios in *in-situ* collected planktonic foraminiferal shells. Using an isotope dilution technique in conjunction with a MC-ICPMS instrument that is equipped with a multiple ion counting system, it was possible to obtain an improved precision for samples with low amounts of Cd. The results demonstrate that the new analytical techniques permit the determination of foraminiferal Cd/Ca ratios with an accuracy and reproducibility of about $\pm 1\%$, for samples with 3 to 12 pg of natural Cd. Even as little as 1 pg of foraminiferal derived Cd can be analysed. In this case, the accuracy and reproducibility is about $\pm 4\%$, mainly due to the uncertainty of the Cd blank correction.

A similar precision for such small amounts of Cd was not attained by previously published methods, which typically achieve a precision of about 2% for Cd/Ca when more than 15 to 20 pg of Cd are available for analysis (Lea and Martin, 1996; Rosenthal et al., 1999; Rickaby et al., 2000; Yu et al., 2005; Harding et al., 2006; Marchitto, 2006). However, some of these methods allow the simultaneous determination of several Element/Ca ratios. Such methods are therefore well suited for paleoceanographic studies, which utilize and interpret the Element/Ca ratios of sedimentary foraminiferal tests where sample material is generally not limited. In contrast, our method presented here is apt for resolving Cd/Ca variations of planktonic foraminifers in studies, where the amount of sample material available is limited.

Using this novel procedure, planktonic foraminiferal Cd/Ca ratios were determined for *G. ruber*, *G. sacculifer* and *G. bulloides* sampled *in-situ* from the water column and from surface sediments at approximately the same location. *In-situ* samples comprise specimens collected

from their habitat (live foraminifera) as well as settling tests sampled well below the live habitat (empty tests of dead foraminifera).

Live specimens of *G. ruber* collected in the Arabian Sea during different monsoon seasons exhibit different Cd/Ca ratios that generally correlate with seasonal changes in seawater phosphate concentration. No such correlation is observed for *G. sacculifer*, however. This indicates species-specific mechanisms of Cd incorporation into foraminiferal calcite and/or different ecological niches of the different species.

The results also revealed significantly lower Cd/Ca ratios for live collected specimens of *G. ruber*, *G. sacculifer* and *G. bulloides* than for tests from surface sediments. A significant post-depositional alteration of the foraminiferal tests is considered to be unlikely. This conclusion is based on the observation that fossil tests of *G. bulloides*, *G. truncatulinoides* and *O. universa* obtained from the same surface sediment show distinct differences in the Cd/Ca ratios that mirror specific ecological demands of these species. These differences would probably not be visible, if the Cd/Ca ratios of the shells had been significantly modified by secondary alteration. The differences in Cd/Ca of live collected and sedimentary tests can rather be explained by a combination of different mechanisms: (i) Both sets of samples may contain to a variable amount shells of foraminifers that underwent reproduction and therefore precipitated a GAM calcite crust that is enriched in Cd relative to the primary calcite. (ii) Tests of surface sediment samples represent an integrated signal spanning up to 2500 years (e.g., Manighetti et al., 1995) and may therefore reflect long-term changes in climate and monsoon strength. (iii) Most of the analyzed *in-situ* samples are not representative of the species-specific blooms, which, however, produce the majority of the foraminiferal tests that are deposited in surface sediments (Fowler and Knauer, 1986; Schiebel, 2002).

Moreover, settling tests of *G. ruber* reveal about a factor of 2-5 lower Cd/Ca ratios than their counterparts collected from the live habitat. This suggests that the tests are partially dissolved while they settle through the water column. The large offset in Cd/Ca evident for settling and sedimentary tests of *G. ruber* indicates that the latter tests are significantly less effected by dissolution processes. This can be most readily explained by different sinking velocities of the tests. The deposition of surface sediments is mainly dominated by mass sinking events that follow phytoplankton blooms. Such events are associated with high sinking velocities and dissolution effects should thus be less pronounced than for the slowly settling single shells that were collected from the water column (Schiebel, 2002).

The exact mechanisms that are responsible for the different Cd/Ca systematics of live specimens, settling shells and test of surface sediments remain speculative at present. Due to the limited number of samples, further studies will be needed to firmly establish the observed trends.

Given the small number of samples and the uncertainties in many of the seawater parameters it is difficult to draw general conclusions on the reliability of the Cd/Ca proxy from our results. However, a tentative interpretation is that the use of *G. ruber* might be preferable over *G. sacculifer* because it appears to record the surface seawater phosphate concentration more faithfully. Because secondary alteration in the sediment is regarded unlikely, no compelling reasons could be identified during the course of this study to question the use of Cd/Ca as a proxy of nutrient utilization in general.

6.1.2 Cadmium Isotope Variations in Seawater

This thesis presents the development and application of a Cd double spike technique in conjunction with MC-ICPMS for the accurate and precise determination of Cd isotope compositions of seawater. The method is suitable even for surface seawater samples that are characterized by low Cd contents and unfavourable Cd to matrix ratios. An external precision of about ± 1.0 to ± 1.6 $\epsilon^{114/110}\text{Cd}$ (2s.d.) was obtained for multiple analyses of pure Cd standards and seawater samples that required only about 8 ng of natural Cd. As little as 1 to 5 ng of natural Cd, however, are sufficient for the acquisition of accurate and precise Cd stable isotope data. Such analyses yielded reproducibilities of about ± 2 to ± 6 $\epsilon^{114/110}\text{Cd}$ (2s.d.). The superior precision compared to previously published MC-ICPMS procedures for Cd stable isotope analyses (e.g., Wombacher et al., 2003; Cloquet et al., 2005; Lacan et al., 2006) underlines the advantage of a double-spike technique over more common techniques like external normalization or standard-sample bracketing. It allows a precise separation of the natural fractionation of a sample from the instrumental mass bias as well as from laboratory-induced mass fractionation. In addition, it also provides precise Cd concentration data. These methodological improvements made it possible to clearly resolve Cd isotope fractionation in seawater and to provide the first systematic investigation of Cd isotope variations in seawater.

Cadmium isotopic compositions were determined for 22 seawater samples from four major ocean basins including three water column profiles collected in the North Pacific and in the Arctic Ocean. Moreover, the analyzed seawater samples cover a wide range of Cd concentrations. The great majority of seawater samples exhibit a clear relationship of Cd isotope composition and concentration, whereby the most Cd-depleted samples show the most fractionated Cd isotope compositions (up to $\epsilon^{114/110}\text{Cd} \approx 38 \pm 6$). This suggests that Cd fractionation is due to kinetic isotope effects that occurred during biological uptake of dissolved seawater Cd. The fractionation follows a Rayleigh distillation curve for a closed system and is in accord with fractionation factors of $\alpha \approx 1.0002$ to 1.0006 for $^{114}\text{Cd}/^{110}\text{Cd}$.

Cadmium-rich water samples collected from a depth ≥ 900 m show nearly constant $\epsilon^{114/110}\text{Cd}$ values of $+3.3 \pm 0.5$ (1s.d.), although their Cd concentration increases along the global flow path of deep water from the Atlantic Ocean (with $[\text{Cd}] \approx 0.3$ nmol/kg) to the Pacific Ocean (with $[\text{Cd}] \approx 0.9$ nmol/kg). This observation indicates that organic matter, which increases the Cd content of deeper water upon remineralization, is also characterized by a constant Cd isotope composition of $\epsilon^{114/110}\text{Cd} \approx +3$. The latter can be explained by a near-quantitative closed system uptake of Cd by phytoplankton from surface waters, which is in accord with the finding that most water samples from the euphotic zone have Cd contents of less than 0.05 nmol/kg.

In addition, a few shallow water samples that are characterized by extremely low Cd contents (<0.008 nmol/kg) exhibit nearly un-fractionated Cd isotope compositions (between $\epsilon^{114/110}\text{Cd} = -6 \pm 6$ and $+6.2 \pm 2.7$). Such Cd signatures may be attributed to changes in the Cd fractionation factor, for example due to vital effects or variations in the uptake mechanisms for Cd (e.g., adsorption vs. biological utilization). Alternatively, they could reflect atmospheric input of isotopically light Cd or mixing processes of highly fractionated surface waters with deeper water masses that exhibit $\epsilon^{114/110}\text{Cd} \approx +3$. Such mixing processes may also explain the formation of isotopically light water masses, if the remineralized organic matter is characterized by a non-quantitative Cd uptake.

At present, the exact mechanisms responsible for the different Cd isotope systematics of the analyzed surface water samples cannot be determined conclusively. The new dataset implies, however, that combined Cd isotope and concentration data reveals more complexity in the marine distribution and cycling of Cd than Cd concentration data alone.

6.2 OUTLOOK

6.2.1 Cd/Ca Ratios of Foraminiferal Tests

In the last few years several new techniques for the determination of Cd/Ca ratios in tests of foraminifers have been published (e.g., Lea and Martin, 1996; Rosenthal et al., 1999; Rickaby et al., 2000; Yu et al., 2005; Harding et al., 2006; Marchitto, 2006). However, most of these groups have verified the reproducibility of their methods only by analyses of standard solutions while thorough testing of foraminiferal sample material, particularly with regard to the accuracy of the analyses, has yet to be carried out. This demonstrates that there is a need to establish well-characterized and widely available reference materials that can be used to validate the accuracy and precision of Element/Ca ratio measurements for natural carbonates and to improve the interlaboratory compatibility.

Moreover, an interlaboratory comparison study as performed for Mg/Ca and Sr/Ca analyses of foraminiferal tests (Rosenthal et al., 2004) should also be carried out for the Cd/Ca proxy. Such an investigation is expected to unravel to which extent the Cd/Ca proxy is reproducible among different laboratories that use different foraminiferal cleaning protocols, analytical procedures and measurement techniques.

Although the application of our new technique generally allows analyses of *in-situ* collected foraminifers with low Cd contents, replicate picks were only possible in some cases due to the generally limited sample material. However, replicate picks are an important means to characterize the uncertainty of the data for a foraminiferal sample, because the inter-specimen variability of a foraminiferal sample is generally larger than the within-day analytical precision (Boyle, 1995). For limited sample material it is therefore desirable to minimize sample loss during foraminiferal cleaning in order to decrease the initial sample size. The two major causes of sample loss during foraminiferal cleaning are loss of small shell fragments during solution transfers and dissolution of the tests during the reductive cleaning step and the weak acid leach. Improvements could include the development of pipette tip inserts that are permeable for a distinct size fraction only and a reduction of the total amount or concentration of acidified cleaning solutions as well as a shortening of the ultrasonic treatment. However, every modification of the cleaning procedure needs to be verified against established cleaning methods.

In addition to the analytical improvements outlined above, several conceptual suggestions for further research are discussed in the following. Analyses of *in-situ* collected planktonic

foraminifers are, besides laboratory culturing experiments, an important tool to characterize the Cd partition coefficient and to detect species-specific variations. However, this study showed that water column parameters such as temperature, salinity, nutrient levels (particularly phosphate concentration) and seawater Cd concentration recorded during foraminiferal sampling are an essential prerequisite for definite conclusions. Further *in-situ* studies should moreover be supplemented by analyses of additional Elemental/Ca ratios such as Mg/Ca, a proxy for seawater temperature.

To gain a better understanding of the processes causing differences between *in-situ* and surface sediment samples it is important to (i) increase the sampling density of *in-situ* samples during the species-specific blooms (ii) better constrain the sedimentation rates of the sampling areas and (iii) clarify the impact of calcite crusts and its chemical composition. Distinct chamber and chamber-wall layer Cd contents may be resolved with laser-ablation ICP-MS or ion probe analyses of individual shells, as shown for other foraminiferal trace elements (Eggins et al., 2003; Hathorne et al., 2003). If such studies would detect differences in Cd/Ca of different parts of the shell (e.g., outer and inner calcite layers; primary calcite and gametogenic calcite crusts), different Cd/Ca ratios could be attributed to effects of shell formation and dissolution.

6.2.2 Cadmium Isotope Variations in Seawater

Cadmium isotopic compositions have the potential to provide new insights into the biogeochemical processes that govern the marine cycling of Cd. To evaluate if Cd isotopes have the potential to become a useful proxy of past nutrient utilization, that could supplement existing nutrient proxies, we have to gain a better understanding of the processes causing Cd isotope fractionation in the marine environment.

Further progress is expected once larger isotopic datasets become available. Particularly desirable are studies, which simultaneously investigate (i) several trace metal and nutrient isotope systems (e.g., N, Si, Fe, Zn, Cu, and Cd) and (ii) Cd isotope systematics of the dissolved and particulate phase of seawater at numerous sites.

In addition, further studies are required to characterize the uptake mechanisms of Cd by marine microorganisms and its biological function in phytoplankton and bacteria. Laboratory culturing experiments of marine phytoplankton may help to better understand Cd fractionation associated with biological uptake and adsorption processes. Such analyses are

also desirable to better constrain the fractionation factor relating the Cd isotope composition of biomass and seawater.

Moreover, Cd isotopic analyses of phytoplankton biomass may be able to validate the assumption that in the case of a near quantitative uptake of Cd the accumulated phytoplankton biomass is characterized by an approximately constant Cd isotope composition similar to the one determined for deep water. This will be difficult to prove in culturing experiments but might be revealed through analyses of bulk biomass samples collected from the water column.

In addition, further studies are needed to better characterize the Cd isotope composition of the main input and output sources. Of great interest are Cd analyses of dust and rainwater, as this study suggests, that these fluxes might influence the Cd isotopic composition of strongly depleted surface waters. Finally, Cd isotope signatures may be an excellent selective tracer for biological activity in general, as inorganic geological processes (other than evaporation/condensation) do not generate Cd isotope effects as large as those observed in the present study (Wombacher et al., 2003; Schmitt et al., 2006).

References

- Almogi-Labin A. (1984) Population-dynamics of planktic foraminifera and pteropoda Gulf of Aqaba, Red-Sea. *Proceedings of the Koninklijke Nederlandse Akademie Van Wetenschappen Series B-Palaeontology Geology Physics Chemistry Anthropology* **87** (4), 481-511.
- Anand P., Elderfield H., and Conte M. H. (2003) Calibration of Mg/Ca thermometry in planktonic foraminifera from a sediment trap time series. *Paleoceanography* **18**, 1050, doi: 10.1029/2002PA000846.
- Andersen M. B., Stirling C. H., Porcelli D., Halliday A. N., Andersson P. S., and Baskaran M. (2007) The tracing of riverine U in Arctic seawater with very precise $^{234}\text{U}/^{238}\text{U}$ measurements. *Earth and Planetary Science Letters* **259** (1-2), 171-185.
- Barker S., Broecker W., Clark E., and Hajdas I. (2007) Radiocarbon age offsets of foraminifera resulting from differential dissolution and fragmentation within the sedimentary bioturbated zone. *Paleoceanography* **22**, PA2205, doi:10.1029/2006PA001354.
- Barker S., Greaves M., and Elderfield H. (2003) A study of cleaning procedures used for foraminiferal Mg/Ca paleothermometry. *Geochemistry Geophysics Geosystems* **4**, 8407, doi:10.1029/2003GC000559.
- Bauer S., Hitchcock G. L., and Olson D. B. (1991) Influence of monsoonally-forced Ekman dynamics upon surface layer depth and plankton biomass distribution in the Arabian Sea. *Deep-Sea Research* **18** (5), 531-553.
- Bé A. W. H. (1977) An ecological, zoogeographic and taxonomic review of recent planktonic foraminifera. In *oceanic Micropaleontology* (ed. A. T. S. Ramsay), pp. 1-100. Academic Press, London.
- Bé A. W. H. (1980) Gametogenic calcification in a spinose planktonic foraminifer, *Globigerinoides sacculifer* (brady). *Marine Micropaleontology* **5**, 283-310.
- Bender M. L. and Gagner C. L. (1976) Dissolved copper, nickel, and cadmium in the Sargasso Sea. *Journal of Marine Research* **34**, 327-339.
- Bermin J., Vance D., Archer C., and Statham P. J. (2006) The determination of the isotopic composition of Cu and Zn in seawater. *Chemical Geology* **226**, 280-297.
- Bertram C. J., Elderfield H., Shackleton N. J., and MacDonald J. A. (1995) Cadmium/calcium and carbon isotope reconstructions of the glacial northeast Atlantic Ocean. *Paleoceanography* **10**, 563-578.
- Bewers J. M. and Yeats P. A. (1977) Oceanic residence times of trace-metals. *Nature* **268** (5621), 595-598.
- Bijma J., Erez J., and Hemleben C. (1990) Lunar and semi-lunar reproductive cycles in some spinose planktonic foraminifers. *Journal of Foraminiferal Research* **20** (2), 117-127.
- Bijma J. and Hemleben C. (1994) Population dynamics of the planktic foraminifer *Globigerinoides sacculifer* (Brady) from the central Red Sea. *Deep-Sea Research I* **41** (3), 485-510.
- Björk G., Söderkvist J., Winsor P., Nikolopoulos A., and Steele M. (2002) Return of the cold halocline layer to the Amundsen Basin of the Arctic Ocean: Implications for the sea ice mass balance. *Geophysical Research Letters* **29** (11), doi: 10.1029/2001GL014157.

- Boyle E. and Rosenthal Y. (1996) Chemical hydrography of the South Atlantic during the last glacial maximum: Cd vs. $\delta^{13}\text{C}$. In *The South Atlantic: Present and Past Circulation* (ed. G. Wefer, W. H. Berger, G. Siedler, and D. J. Webb), pp. 423-443. Springer.
- Boyle E. A. (1981) Cadmium, zinc, copper, and barium in foraminifera tests. *Earth and Planetary Science Letters* **53**, 11-35.
- Boyle E. A. (1983) Manganese carbonate overgrowths on foraminifera tests. *Geochimica Et Cosmochimica Acta* **47**, 1815-1819.
- Boyle E. A. (1988) Cadmium: chemical tracer of deepwater paleoceanography. *Paleoceanography* **3**, 471-489.
- Boyle E. A. (1992) Cadmium and $\delta^{13}\text{C}$ paleochemical ocean distributions during the Stage 2 glacial maximum. *Annu. Rev. Earth Planet. Sci.* **20**, 245-287.
- Boyle E. A. (1995) Limits on benthic foraminiferal chemical-analyses as precise measures of environmental properties. *Journal of Foraminiferal Research* **25** (1), 4-13.
- Boyle E. A. and Keigwin L. (1987) North Atlantic thermohaline circulation during the past 20,000 years linked to high-latitude surface temperature. *Nature* **330**, 35-40.
- Boyle E. A. and Keigwin L. D. (1982) Deep circulation of the North Atlantic over the last 200,000 years: geochemical evidence. *Science* **218**, 784-787.
- Boyle E. A. and Keigwin L. D. (1985/86) Comparison of Atlantic and Pacific paleochemical records for the last 215,000 years: changes in deep ocean circulation and chemical inventories. *Earth and Planetary Science Letters* **76**, 135-150.
- Boyle E. A., Sclater F., and Edmond J. M. (1976) On the marine geochemistry of cadmium. *Nature* **263**, 42-44.
- Brand L. E., Sunda W. G., and Guillard R. L. (1986) Reduction of marine phytoplankton reproduction rates by copper and cadmium. *J. Exp. Mar. Biol. Ecol.* **96**, 225-250.
- Broecker W. S. (1997) Thermohaline circulation, the Achilles heel of our climate system: will man-made CO_2 upset the current balance? *Science* **278**, 1582-1588.
- Brown M. T., Landing W. M., and Measures C. I. (2005) Dissolved and particulate Fe in the western and central North Pacific: Results from the 2002 IOC cruise. *Geochemistry Geophysics Geosystems* **6** (10), Q10001, doi:10.1029/2004GC000893.
- Bruland K. W. (1980) Oceanographic distributions of cadmium, zinc, nickel, and copper in the North Pacific. *Earth and Planetary Science Letters* **47** (2), 176-198.
- Bruland K. W. (1983) Trace elements in sea-water. In *Chemical Oceanography*, Vol. 8 (ed. J. P. Ripley and R. Chester), pp. 157-220. Academic Press.
- Bruland K. W. (1992) Complexation of cadmium by natural organic-ligands in the central North Pacific. *Limnology and Oceanography* **37** (5), 1008-1017.
- Bruland K. W. and Lohan M. C. (2003) Controls of trace metals in seawater. In *The Oceans and Marine Geochemistry: in Treatise on Geochemistry*, Vol. 6 (ed. H. Elderfield), pp. 23-47. Elsevier, Oxford.

- Burns S. J., Fleitmann D., Mudelsee M., Neff U., Matter A., and Mangini A. (2002) A 780-year annually resolved record of Indian Ocean monsoon precipitation from a speleothem from south Oman. *Journal of Geophysical Research-Atmospheres* **107** (D20), doi:10.1029/2001JD001281.
- Cloquet C., Rouxel O., Carignan J., and Libourel G. (2005) Natural cadmium isotopic variations in eight geological reference materials (NIST SRM 2711, BCR 176, GSS-1, GXR-1, GXR-2, GSD-12, Nod-P-1, Nod-A-1) and anthropogenic samples, measured by MC-ICP-MS. *Geostandards and Geoanalytical Research* **29** (1), 95-106.
- Colby B. N., Rosecrance A. E., and Colby M. E. (1981) Measurement parameter selection for quantitative isotope-dilution gas chromatography-mass spectrometry. *Analytical Chemistry* **53** (12), 1907-1911.
- Collier R. and Edmond J. M. (1984) The trace element geochemistry of marine biogenic particulate matter. *Progress in Oceanography* **13**, 113-199.
- Cullen J. T., Lane T. W., Morel F. M. M., and Sherrell R. M. (1999) Modulation of cadmium uptake in phytoplankton by seawater CO₂ concentration. *Nature* **402**, 165-167.
- Dai M.-H. and Martin J.-M. (1995) First data on trace metal level and behaviour in two major Arctic river-estuarine systems (Ob and Yenisey) and in the adjacent Kara Sea, Russia. *Earth and Planetary Science Letters* **131**, 127-141.
- De La Rocha C. L. (2003) The biological pump. In *The Oceans and Marine Geochemistry: in Treatise on Geochemistry*, Vol. 6 (ed. H. Elderfield), pp. 83-111. Elsevier, Oxford.
- De La Rocha C. L., Brzezinski M. A., DeNiro M. J., and Shemesh A. (1998) Silicon-isotope composition of diatoms as an indicator of past oceanic change. *Nature* **395**, 680-683.
- Delaney M. L. (1989) Uptake of cadmium into calcite shells by planktonic foraminifera. *Chemical Geology* **78** (2), 159-165.
- Dixon J. L., Statham P. J., Widdicombe C. E., Jones R. M., Barquero-Molina S., Dickie B., Nimmo M., and Turley C. M. (2006) Cadmium uptake by marine micro-organisms in the English Channel and Celtic Sea *Aquatic Microbial Ecology* **44** (1), 31-43.
- Duce R. A., Liss P. S., Merrill J. T., Atlas E. L., Buat-Menard P., Hicks B. B., Miller J. M., Prospero J. M., Arimoto R., Church T. M., Ellis W., Galloway J. N., Hansen L., Jickells T. D., Knap A. H., Reinhardt K. H., Schneider B., Soudine A., Tokos J. J., Tsunogai S., Wollast R., and Zhou M. (1991) The atmospheric input of trace species to the world ocean. *Global Biogeochem. Cycles* **5**, 193-259.
- Duplessy J. C., Be A. W. H., and Blanc P. L. (1981) Oxygen and carbon isotopic composition and biogeographic distribution of planktonic foraminifera in the Indian Ocean. *Palaeogeography Palaeoclimatology Palaeoecology* **33**, 9-46.
- Eggins S., De Deckker P., and Marshall J. (2003) Mg/Ca variation in planktonic foraminifera tests: implications for reconstructing palaeo-seawater temperature and habitat migration. *Earth and Planetary Science Letters* **212** (3-4), 291-306.
- Eggins S. M., Sadekov A., and De Deckker P. (2004) Modulation and daily banding of Mg/Ca in *Orbulina universa* tests by symbiont photosynthesis and respiration: a complication for seawater thermometry? *Earth and Planetary Science Letters* **225** (3-4), 411-419.

- Elderfield H., Bertram C. J., and Erez J. (1996) A biomineralization model for the incorporation of trace elements into foraminiferal calcium carbonate. *Earth Planet. Sci. Lett.* **142**, 409-423.
- Elderfield H. and Rickaby R. E. M. (2000) Oceanic Cd/P ratio and nutrient utilization in the glacial Southern Ocean. *Nature* **405**, 305-310.
- Erez J., Almogi-Labin A., and Avraham S. (1991) On the live history of planktonic foraminifera: Lunar reproduction cycle in *Globigerinoides sacculifer* (Brady). *Paleoceanography* **6** (3), 295-306.
- Fowler S. W. and Knauer G. A. (1986) Role of large particles in the transport of elements and organic-compounds through the oceanic water column. *Progress in Oceanography* **16** (3), 147-194.
- Galer S. J. G. (1999) Optimal double and triple spiking for high precision lead isotopic measurements. *Chemical Geology* **157**, 255-274.
- Garcia H. E., Locarnini R. A., Boyer T. P., and Antonov J. I. (2006) *World Ocean Atlas 2005, Volume 4: Nutrients (phosphate, nitrate, and silicate)*. S. Levitus, Ed. NOAA Atlas NESDIS 64, U.S. Government Printing Office.
- Guieu C., Huang W. W., Martin J.-M., and Yong Y. Y. (1996) Outflow of trace metals into the Laptev Sea by the Lena River. *Marine Chemistry* **53**, 255-267.
- Halicz L., Galy A., Belshaw N. S., and O'Nions R. K. (1999) High-precision measurement of calcium isotopes in carbonates and related materials by multiple collector inductively coupled plasma mass spectrometry (MC-ICP-MS). *Journal of Analytical Atomic Spectrometry* **14**, 1835-1838.
- Halliday A. N., Christensen J. N., Lee D.-C., Rehkämper M., Hall C. M., and Luo X. (2000) Multiple-collector inductively coupled plasma mass spectrometry. In *Inorganic Mass Spectrometry* (ed. C. M. Barslik, D. C. Duckworth, and D. H. Smith), pp. 291-328. Dekker.
- Hamelin B., Manhès G., Albarede F., and Allègre C. J. (1985) Precise lead isotope measurements by the double spike technique: A reconsideration. *Geochimica Et Cosmochimica Acta* **49**, 173-182.
- Hanfland C., Geibert W., Vöge I., and Boebel O. (2005) Naturally occurring radionuclides as tracers for water mass characterisation. In *Reports on Polar and Marine Research, The Expedition ANTARKTIS-XX of RV Polarstern in 2002/2003 Reports of Legs 1 and 2*, Vol. 495 (ed. D. K. Fütterer and G. Kattner). AWI Bremerhaven.
- Harding D. J., Arden J. W., and Rickaby R. E. M. (2006) A method for precise analysis of trace element/calcium ratios in carbonate samples using quadrupole inductively coupled plasma mass spectrometry. *Geochemistry Geophysics Geosystems* **7** (6), Q06003, doi:10.1029/2005GC001093.
- Hathorne E. C., Alard O., James R. H., and Rogers N. W. (2003) Determination of intratest variability of trace elements in foraminifera by laser ablation inductively coupled plasma-mass spectrometry. *Geochemistry Geophysics Geosystems* **4** (12), 8408, doi:10.1029/2003GC000539.
- Hayes A. (2004) An introduction to isotopic calculations. http://www.nosams.whoi.edu/research/staff_hayes.html.
- Hemleben C., Spindler M., and Anderson O. R. (1989) *Modern planktonic foraminifera*. Springer.

- Henry R. P. (1996) Multiple roles of carbonic anhydrase in cellular transport and metabolism. *Annual Review of Physiology* **58**, 523-538.
- Hiller B. (1996) Planktic Foraminifera. In *Meteor-Berichte 96-4, Östliches Mittelmeer, Rotes Meer, Arabisches Meer, Cruise No. 31, 30 December 1994 - 22 March 1995* (ed. C. Hemleben, W. Roether, and P. Stoffers), pp. 165-169.
- Hofmann A. (1971) Fractionation correction for mixed-isotope spikes of Sr, K, and Pb. *Earth and Planetary Science Letters* **10**, 397-402.
- Honjo S., Manganini S. J., and Cole J. J. (1982) Sedimentation of biogenic matter in the deep ocean. *Deep-Sea Research* **29**, 609-625.
- Ivanova E., Schiebel R., Singh A. D., Schmiedl G., Niebler H. S., and Hemleben C. (2003) Primary production in the Arabian Sea during the last 135000 years. *Palaeogeography Palaeoclimatology Palaeoecology* **197** (1-2), 61-82.
- Jones E. P., Nelson D. M., and Treguer P. (1990) Chemical Oceanography. In *Polar Oceanography, Part B: Chemistry, Biology, and Geology* (ed. W. O. Smith), pp. 407-469. Academic Press.
- Karl D. M. (1999) A sea of change: Biogeochemical variability in the North Pacific subtropical gyre. *Ecosystems* **2**, 181-214.
- Karl D. M. and Björkman K. M. (2001) Phosphorus cycle in seawater: Dissolved and particulate pool inventories and selected phosphorus fluxes. *Methods in Microbiology* **30**, 239-270.
- Karl D. M., Christian J. R., Dore J. E., Hebel D. V., Letelier R. M., Tupas L. M., and D. W. C. (1996) Seasonal and interannual variability in primary production and particle flux at Station ALOHA. *Deep-Sea Research, Part II* **43**, 539-568.
- Knauer G. A. and Martin J. H. (1981) Phosphorus and cadmium cycling in northeast Pacific waters. *Journal of Marine Research* **39**, 65-76.
- Kurbjeweit F. (2000) Abundance, composition, diversity and biomass of deep sea benthic foraminifera. In *Ostatlantik 1998, Cruise No. 42, Meteor-Berichte 00-1* (ed. O. Pfannkuche, T. J. Mueller, W. Nellen, and G. Wefer), pp. 79-82.
- Lacan F., Francois R., Ji Y., and Sherrell R. (2005) Does oceanic productivity production lead to a cadmium isotope fractionation? Field vs. culture data. *Geophys. Res. Abstr.* **7**, 07657.
- Lacan F., Francois R., Ji Y. C., and Sherrell R. M. (2006) Cadmium isotopic composition in the ocean. *Geochimica Et Cosmochimica Acta* **70** (20), 5104-5118.
- Lane T. W. and Morel F. M. M. (2000) A biological function for cadmium in marine diatoms. *Proc. Natl. Acad. of Sci. USA* **97** (9), 4627-4631.
- Lane T. W., Saito M. A., George G. N., Pickering I. J., Prince R. C., and Morel F. M. M. (2005) A cadmium enzyme from a marine diatom. *Nature* **435**, 42-42.
- Lantzy R. J. and Mackenzie F. T. (1979) Atmospheric trace metals: global cycles and assessment of man's impact. *Geochimica Et Cosmochimica Acta* **43**, 511-525.
- Lea D. W. (1999) Trace elements in foraminiferal calcite. In *Modern Foraminifera* (ed. B. K. Sen Gupta), pp. 259-277. Kluwer.

- Lea D. W. and Martin P. A. (1996) A rapid mass spectrometric method for the simultaneous analysis of barium, cadmium and strontium in foraminiferal shells. *Geochimica Et Cosmochimica Acta* **60**, 3143-3149.
- Lionetto M. G., Caricato R., Erroi E., Giordano M. E., and Schettino T. (2005) Carbonic anhydrase-based environmental bioassay. *International Journal of Environmental Analytical Chemistry* **85** (12-13), 895-903.
- Locarnini R. A., Mishonov A. V., Antonov J. I., Boyer T. P., and Garcia H. E. (2006) *World Ocean Atlas 2005, Volume 1: Temperature*. S. Levitus, Ed. NOAA Atlas NESDIS 61, U.S. Gov. Printing Office.
- Lohmann G. P. (1995) A model for variation in the chemistry of planktonic foraminifera due to secondary calcification and selective dissolution. *Paleoceanography* **10** (3), 445-457.
- Lyman R. E., Schroeder T. A., and Barnes G. M. (2005) The heavy rain event of 29 October 2000 in Hana, Maui. *Weather and Forecasting* **20** (4), 397-414.
- Lynch-Stieglitz J. and Fairbanks R. G. (1994) A conservative tracer for glacial ocean circulation from carbon isotope and palaeo-nutrient measurements in benthic foraminifera. *Nature* **369**, 308-310.
- Lynch-Stieglitz J., van Geen A., and Fairbanks R. G. (1996) Inter-ocean exchange of glacial North Atlantic intermediate water: evidence from subantarctic Cd/Ca and carbon isotope measurements. *Paleoceanography* **11**, 191-201.
- Mackey D. J., O'Sullivan J. E., Watson R. J., and Dal Pont G. (2002) Trace metals in the Western Pacific: temporal and spatial variability in the concentrations of Cd, Cu, Mn and Ni. *Deep-Sea Research I* **49**, 2241-2259.
- Manighetti B., McCave I. N., Maslin M., and Shackleton N. J. (1995) Chronology for climate change: Developing age models for the Biogeochemical Ocean Flux Study cores. *Paleoceanography* **10** (3), 513-525.
- Marchitto T. M. (2006) Precise multielemental ratios in small foraminiferal samples determined by sector field ICP-MS. *Geochemistry Geophysics Geosystems* **7** (5), Q05P13, doi:10.1029/2005GC001018.
- Maréchal C. N., Télouk P., and Albarède F. (1999) Precise analysis of copper and zinc isotopic compositions by plasma-source mass spectrometry. *Chemical Geology* **156**, 251-273.
- Mariotti A., Germon J. C., Hubert P., Kaiser P., Letolle R., Tardieux A., and Tardieux P. (1981) Experimental-determination of nitrogen kinetic isotope fractionation - some principles - illustration for the denitrification and nitrification processes. *Plant and Soil* **62** (3), 413-430.
- Mariotti A., Landreau A., and Simon B. (1988) ¹⁵N isotope biogeochemistry and natural denitrification process in groundwater - application to the chalk aquifer of northern France. *Geochimica Et Cosmochimica Acta* **52** (7), 1869-1878.
- Martin J. H., Knauer G. A., Karl D. M., and Broenkow W. W. (1987) Vertex: carbon cycling in the northeast Pacific. *Deep-Sea Research Part a-Oceanographic Research Papers* **34** (2), 267-285.

- Martin J. M. and Whitfield M. (1983) The significance of the river input of chemical elements to the ocean. In *Trace Metals in Sea Water* (ed. C. S. Wong, E. Boyle, K. W. Bruland, J. D. Burton, and E. D. Goldberg), pp. 265-296. New York: Plenum.
- Martin P. A. and Lea D. W. (1998) Comparison of water mass changes in the deep tropical Atlantic derived from Cd/Ca and carbon isotope records: Implications for changing Ba composition of deep Atlantic water masses. *Paleoceanography* **13** (6), 572-585.
- Martin P. A. and Lea D. W. (2002) A simple evaluation of cleaning procedures on fossil benthic foraminiferal Mg/Ca. *Geochemistry Geophysics Geosystems* **3** (10), 8401, doi: 10.1029/2001GC000280.
- Mashiotto T. A., Lea D. W., and Spero H. J. (1997) Experimental determination of cadmium uptake in shells of the planktonic foraminifera *Orbulina universa* and *Globigerina bulloides*: Implications for surface water paleoreconstructions. *Geochimica Et Cosmochimica Acta* **61** (19), 4053-4065.
- Mayewski P. A., Rohling E. E., Stager J. C., Karlen W., Maasch K. A., Meeker L. D., Meyerson E. A., Gasse F., van Krevelend S., Holmgren K., Lee-Thorp J., Rosqvist G., Rack F., Staubwasser M., Schneider R. R., and Steig E. J. (2004) Holocene climate variability. *Quaternary Research* **62** (3), 243-255.
- McCorkle D. C., Martin P. A., Lea D. W., and Klinkhammer G. P. (1995) Evidence of a dissolution effect on benthic foraminiferal shell chemistry $\delta^{13}\text{C}$, Cd/Ca, Ba/Ca and Sr/Ca: Results from the Ontong Java plateau. *Paleoceanography* **10**, 699-714.
- McGillicuddy D. J., Anderson L. A., Bates N. R., Bibby T., Buesseler K. O., Carlson C. A., Davis C. S., Ewart C., Falkowski P. G., Goldthwait S. A., Hansell D. A., Jenkins W. J., Johnson R., Kosnyrev V. K., Ledwell J. R., Li Q. P., Siegel D. A., and Steinberg D. K. (2007) Eddy/wind interactions stimulate extraordinary mid-ocean plankton blooms. *Science* **316** (5827), 1021-1026.
- Measures C. I. (2002) IOC NW Pacific cruise 2002 web-page. <http://www.soest.hawaii.edu/oceanography/chris/IOPacific/IOPacific2002.html>.
- Measures C. I., Cutter G. A., Landing W. M., and Powell R. T. (2006) Hydrographic observations during the 2002 IOC Contaminant Baseline Survey in the western Pacific Ocean. *Geochemistry Geophysics Geosystems* **7** (3), doi:10.1029/2004GC000855.
- Mitchell J. W., Harris T. D., and Blitzer L. D. (1980) Safe handling and purification of aqueous hydrazine. *Analytical Chemistry* **52** (4), 774-776.
- Moore R. M. (1981) Oceanographic distributions of zinc, cadmium, copper and aluminum in waters of the Central Arctic. *Geochimica Et Cosmochimica Acta* **45** (12), 2475-2482.
- Morel F. M. M. and Price N. M. (2003) The biogeochemical cycles of trace metals in the oceans. *Science* **300**, 944-947.
- Morel F. M. M., Reinfelder J. R., Roberts S. B., Chamberlain C. P., Lee J. G., and Yee D. (1994) Zinc and carbon co-limitation of marine phytoplankton. *Nature* **369** (6483), 740-742.
- Noriki S., Hamahara K., and Harada K. (1999) Particulate flux and Cd/P ratio of particulate material in the Pacific Ocean. *J. Oceanography* **55**, 693-703.

- Nürnberg D., Bijma J., and Hemleben C. (1996) Assessing the reliability of magnesium in foraminiferal calcite as a proxy for water mass temperatures. *Geochimica Et Cosmochimica Acta* **60**, 803-814.
- Oasim S. Z. (1982) Oceanography of the northern Arabian Sea. *Deep-Sea Research, Part A* **29** (9), 1041-1068.
- Oppo D. W. and Horowitz M. (2000) Glacial deep water geometry: South Atlantic benthic foraminiferal Cd/Ca and $\delta^{13}\text{C}$ evidence. *Paleoceanography* **15**, 147-160.
- Orr W. N. (1967) Secondary Calcification in Foraminiferal Genus Globorotalia. *Science* **157** (3796), 1554-1555.
- Pai S. C. and Chen H. Y. (1994) Vertical distribution of cadmium in marginal seas of the western Pacific Ocean. *Marine Chemistry* **47** (1), 81-91.
- Patterson T. L. and Duce R. A. (1991) The cycle of atmospheric cadmium over the North Pacific Ocean. *Tellus Series B-Chemical and Physical Meteorology* **43** (1), 12-29.
- Pomies C., Davies G. R., and Conan S. M. H. (2002) Neodymium in modern foraminifera from the Indian Ocean: implications for the use of foraminiferal Nd isotope compositions in paleo-oceanography. *Earth and Planetary Science Letters* **203** (3-4), 1031-1045.
- Price N. M. and Morel F. M. M. (1990) Cadmium and cobalt substitution for zinc in marine diatom. *Nature* **344**, 658-660.
- Rehkämper M. and Halliday A. N. (1999) The precise measurement of Tl isotopic compositions by MC-ICPMS: Application to the analysis of geological materials and meteorites. *Geochimica Et Cosmochimica Acta* **63**, 935-944.
- Rehkämper M., Schönbachler M., and Stirling C. H. (2001) Multiple collector ICP-MS: Introduction to instrumentation, measurement techniques and analytical capabilities. *Geostandards Newsletter* **25**, 23-40.
- Rehkämper M., Wombacher F., and Aggarwal J. K. (2004) Stable isotope analysis by multiple collector ICP-MS. In *Handbook of Stable Isotope Analytical Techniques* (ed. P. de Groot). Elsevier.
- Reynolds B. C., Frank M., and Halliday A. N. (2006) Silicon isotope fractionation during nutrient utilization in the North Pacific. *Earth and Planetary Science Letters* **244**, 431-443.
- Rickaby R. E. M. and Elderfield H. (1999) Planktonic foraminiferal Cd/Ca: paleonutrients or paleotemperature? *Paleoceanography* **14**, 293-303.
- Rickaby R. E. M., Greaves M. J., and Elderfield H. (2000) Cd in planktonic and benthic foraminiferal shells determined by thermal ionization mass spectrometry. *Geochimica Et Cosmochimica Acta* **64**, 1229-1236.
- Riepe W. and Kaiser H. (1966) Massenspektrometrische Spurenanalyse von Calcium, Strontium und Barium in Natriumazid durch Isotopenverdünnungstechnik. *Zeitschrift für Analytische Chemie Fresenius* **223** (5), 321-335.
- Ripperger S. and Rehkämper M. (2007a) A highly sensitive MC-ICPMS method for Cd/Ca analysis of foraminiferal tests. *Journal of Analytical Atomic Spectrometry*, DOI:10.1039/b704267a.

- Ripperger S. and Rehkämper M. (2007b) Precise determination of cadmium isotope fractionation in seawater by double spike MC-ICPMS. *Geochimica Et Cosmochimica Acta* **71** (3), 631-642.
- Ripperger S., Rehkämper M., Porcelli D., and Halliday A. N. (2007) Cadmium isotope fractionation in seawater - a signature of biological activity. *Earth and Planetary Science Letters*, in press.
- Rohling E. J., Sprovieri M., Cane T., Casford J. S. L., Cooke S., Bouloubassi I., Emeis K. C., Schiebel R., Hayes A., Jorissen F. J., and Kroon D. (2004) Ecological controls on planktonic foraminiferal shell chemistry: stable isotope records of eleven major species through a Mediterranean anoxic event. *Marine Micropaleontology* **50**, 89-123.
- Rosenthal Y. and Boyle E. A. (1993) Factors controlling the fluoride content of planktonic foraminifera: An evaluation of its paleoceanographic applicability. *Geochimica Et Cosmochimica Acta* **57**, 335-346.
- Rosenthal Y., Field M. P., and Sherrell R. M. (1999) Precise determination of element/calcium ratios in calcareous samples using sector field inductively coupled plasma mass spectrometry. *Analytical Chemistry* **71**, 3248-3253.
- Rosenthal Y., Lam P., Boyle E. A., and Thomson J. (1995) Authigenic cadmium enrichments in suboxic sediments - precipitation and postdepositional mobility. *Earth and Planetary Science Letters* **132** (1-4), 99-111.
- Rosenthal Y., Perron-Cashman S., Lear C. H., Bard E., Barker S., Billups K., Bryan M., Delaney M. L., deMenocal P. B., Dwyer G. S., Elderfield H., German C. R., Greaves M., Lea D. W., Marchitto T. M., Pak D. K., Paradis G. L., Russell A. D., Schneider R. R., Scheiderich K., Stott L., Tachikawa K., Tappa E., Thunell R., Wara M., Weldeab S., and Wilson P. A. (2004) Interlaboratory comparison study of Mg/Ca and Sr/Ca measurements in planktonic foraminifera for paleoceanographic research. *Geochemistry Geophysics Geosystems* **5** (4), Q04D09, doi:10.1029/2003GC000650.
- Rosman K. J. R. and De Laeter J. R. (1976) Isotopic fractionation in meteoritic cadmium. *Nature* **261**, 216-218.
- Rosman K. J. R. and De Laeter J. R. (1988) Cadmium mass fractionation in unequilibrated ordinary chondrites. *Earth and Planetary Science Letters* **89**, 163-169.
- Russell W. A., Papanastassiou D. A., and Tombrello T. A. (1978) Ca isotope fractionation on the Earth and other Solar System materials. *Geochimica Et Cosmochimica Acta* **42**, 1075-1090.
- Ruttenberg K. C. (2003) The global phosphorus cycle. In *Biogeochemistry: in Treatise on Geochemistry*, Vol. 8 (ed. H. W. Schlesinger), pp. 585-643. Elsevier, Oxford.
- Saager P. M., Debaar H. J. W., and Howland R. J. (1992) Cd, Zn, Ni and Cu in the Indian-Ocean. *Deep-Sea Research Part a-Oceanographic Research Papers* **39** (1A), 9-35.
- Schiebel R. (2002) Planktic foraminiferal sedimentation and the marine calcite budget. *Global Biogeochemical Cycles* **16** (4), 1065, doi:10.1029/2001GB001459.
- Schiebel R., Barker S., Lendt R., Thomas H., and Bollmann J. (2007) Planktic foraminiferal dissolution in the twilight zone. *Deep-Sea Research, II* **54**, 676-686.
- Schiebel R. and Bayer M. (1996) Particle flux in the benthic boundary layer, benthic foraminiferal habitats, and early diagenetic processes in deep sea environments. In *Meteor-Berichte 96-5, Biogeochemical fluxes in the deep-sea and investigations of geological structures in the*

Indian Ocean, Cruise No. 33, 22 September - 30 December 1995 (ed. K. Lochte, P. Halbach, and B. Flemming), pp. 78-80.

- Schiebel R., Bijma J., and Hemleben C. (1997) Population dynamics of the planktic foraminifer *Globigerina bulloides* from the eastern North Atlantic. *Deep-Sea Research I* **44** (9-10), 1701-1713.
- Schiebel R. and Hemleben C. (2000) Interannual variability of planktic foraminiferal populations and test flux in the eastern North Atlantic Ocean (JGOFS). *Deep-Sea Research Part II-Topical Studies in Oceanography* **47** (9-11), 1809-1852.
- Schiebel R. and Hemleben C. (2001) Protozoa, planktonic foraminifera. In *Encyclopedia of Ocean Sciences* (ed. J. Speele, S. Thorpe, and K. Turekian). Academic Press.
- Schiebel R. and Hemleben C. (2005) Modern planktic foraminifera. *Paläontologische Zeitschrift* **79** (1), 135-148.
- Schiebel R., Hiller B., and Hemleben C. (1995) Impacts of storms on recent planktic foraminiferal test production and CaCO₃ flux in the North Atlantic at 47 degrees N, 20 degrees W (JGOFS). *Marine Micropaleontology* **26** (1-4), 115-129.
- Schiebel R., Struck U., Grimm G., Hübner H., and Themann S. (2000) Calcareous plankton and paleoceanography of the Azores Front-Current System. In *North Atlantic 1999, Cruise No. 45. Meteor-Berichte 00-4* (ed. F. Schott, G. Meinecke, S. Neuer, and E. Zenk), pp. 104-108.
- Schiebel R., Waniek J., Bork M., and Hemleben C. (2001) Planktic foraminiferal production stimulated by chlorophyll redistribution and entrainment of nutrients. *Deep-Sea Research Part I-Oceanographic Research Papers* **48** (3), 721-740.
- Schiebel R., Waniek J., Zeltner A., and Alves M. (2002) Impact of the Azores Front on the distribution of planktic foraminifers, shelled gastropods, and coccolithophorids. *Deep-Sea Research Part II-Topical Studies in Oceanography* **49** (19), 4035-4050.
- Schiebel R., Zeltner A., Treppke U. F., Waniek J. J., Bollmann J., Rixen T., and Hemleben C. (2004) Distribution of diatoms, coccolithophores and planktic foraminifers along atrophic gradient during SW monsoon in the Arabian Sea. *Marine Micropaleontology* **51** (3-4), 345-371.
- Schmitt A. D., Galer S. J. G., and Abouchami W. (2006) High-precision cadmium isotope fractionation determined by double spike thermal ionisation mass spectrometry. *Geophysical Research Abstracts* **8** (EGU06-A-07567).
- Sellmer C., Fehner U., Nachtigall K., Reineke C., Fritsche P., Lisok K., Obermüller B., and Adam D. (1998) Planktological studies. In *Meteor-Berichte 98-2, Nordatlantik 1996* (ed. J. Mienert, Graf, G., Hemleben, C., Kremling, K., Pfannkuche, O., Schulz-Bull, D), pp. 197-200.
- Selph K. E., Shacat J., and Landry M. R. (2005) Microbial community composition and growth rates in the NW Pacific during spring 2002. *Geochemistry Geophysics Geosystems* **6** (12), doi:10.1029/2005GC000983.
- Siebert C., Nägler T. F., and Kramers J. D. (2001) Determination of molybdenum isotope fractionation by double-spike multicollector inductively coupled plasma mass spectrometry. *Geochemistry Geophysics Geosystems* **2**, Paper number 2000GC000124.

- Sigman D. M., Altabet M. A., McCorkle D. C., Francois R., and Fischer G. (1999) The $\delta^{15}\text{N}$ of nitrate in the Southern Ocean: Consumption of nitrate in surface waters. *Global Biogeochemical Cycles* **13** (4), 1149-1166.
- Sigman D. M., Altabet M. A., McCorkle D. C., Francois R., and Fischer G. (2000) The $\delta^{15}\text{N}$ of nitrate in the Southern Ocean: Nitrogen cycling and circulation in the ocean interior. *Journal of Geophysical Research-Oceans* **105** (C8), 19599-19614.
- Spero H. J. and Lea D. W. (1993) Intraspecific stable-isotope variability in the planktic foraminifera *Globigerinoides sacculifer* - results from laboratory experiments. *Marine Micropaleontology* **22** (3), 221-234.
- Stramma L. (2001) Current systems in the Atlantic Ocean. In *Encyclopedia of Ocean Sciences* (ed. J. Speele, S. Thorpe, and K. Turekian), pp. 589-598. Academic Press.
- Sunda W. G. (1987) Neritic-oceanic trends in trace-metal toxicity to phytoplankton communities. In *Oceanic processes in marine pollution* (ed. J. M. Capuzzo and D. R. Kester). Krieger.
- Sunda W. G. and Huntsman S. A. (1996) Antagonisms between cadmium and zinc toxicity and manganese limitation in a coastal diatom. *Limnology and Oceanography* **41** (3), 373-387.
- Sunda W. G. and Huntsman S. A. (2000) Effect of Zn, Mn, and Fe on Cd accumulation in phytoplankton: Implications for oceanic Cd cycling. *Limnology and Oceanography* **45** (7), 1501-1516.
- Tachikawa K. and Elderfield H. (2002) Microhabitat effects on Cd/Ca and $\delta^{13}\text{C}$ of benthic foraminifera. *Earth and Planetary Science Letters* **202** (3-4), 607-624.
- Trimble S., Baskaran M., and Porcelli D. (2004) Scavenging of thorium isotopes in the Canada Basin of the Arctic Ocean. *Earth and Planetary Science Letters* **222**, 915-932.
- Turner J. T. (2002) Zooplankton fecal pellets, marine snow and sinking phytoplankton blooms. *Aquatic Microbial Ecology* **27** (1), 57-102.
- Uematsu M., Duce R. A., Prospero J. M., Chen L., Merrill J. I., and McDonald R. L. (1983) Transport of mineral aerosol from Asia over the North Pacific Ocean. *Journal of Geophysical Research* **88** (C9), 5343-5352.
- Vance D., Archer C., Bermin J., Kennaway G., Cox E. J., Statham P. J., Lohan M. C., and Ellwood M. J. (2006) Zn isotopes as a new tracer of metal micronutrient usage in the oceans. *Geochimica Et Cosmochimica Acta* **70** (18), A666.
- Vance D. and Thirlwall M. (2002) An assessment of mass discrimination in MC-ICPMS using Nd isotopes. *Chemical Geology* **185** (3-4), 227-240.
- Webster P. J., Magana V. O., Palmer T. N., Shukla J., Tomas R. A., Yanai M., and Yasunari T. (1998) Monsoons: Processes, predictability, and the prospects for prediction. *Journal of Geophysical Research* **103** (14), 451-510.
- Weldeab S., Schneider R. R., and Kölling M. (2006) Comparison of foraminiferal cleaning procedures for Mg/Ca paleothermometry on core material deposited under varying terrigenous-input and bottom water conditions. *Geochemistry Geophysics Geosystems* **7** (4), Q04P12, doi:10.1029/2005GC000990.
- White W. M. (1998) The oceans as a chemical system. In *Geochemistry*. online textbook.

- Wichtlhuber S., Rehkämper M., Schiebel R., and Halliday A. N. (2004) A new MC-ICPMS method for the determination of Cd/Ca ratios in foraminiferal tests. *Geochimica Et Cosmochimica Acta* **68** (11), A486.
- Wombacher F. and Rehkämper M. (2003) Investigation of the mass discrimination of multiple collector ICP-MS using neodymium isotopes and the generalised power law. *Journal of Analytical Atomic Spectrometry* **18** (11), 1371-1375.
- Wombacher F. and Rehkämper M. (2004) Problems and suggestions concerning the notation of cadmium stable isotope compositions and the use of reference materials. *Geostandards and Geoanalytical Research* **28** (1), 173-178.
- Wombacher F., Rehkämper M., Mezger K., Bischoff A., and Münker C. (2007) Cadmium stable isotope cosmochemistry. *Geochimica Et Cosmochimica Acta*, under review.
- Wombacher F., Rehkämper M., Mezger K., and Münker C. (2003) Stable isotope compositions of cadmium in geological materials and meteorites determined by multiple collector-ICPMS. *Geochimica Et Cosmochimica Acta* **67** (23), 4639-4654.
- Wombacher F., Rehkämper M., Mezger K., and Münker C. (2004) Determination of the mass-dependence of cadmium isotope fractionation during evaporation. *Geochimica Et Cosmochimica Acta* **68**, 2349-2357.
- Yeats P. A. and Westerlund S. (1991) Trace metal distributions at an Arctic Ocean ice island. *Marine Chemistry* **33**, 261-277.
- Yee N. and Fein J. (2001) Cd adsorption onto bacterial surfaces: A universal adsorption edge? *Geochimica Et Cosmochimica Acta* **65** (13), 2037-2042.
- Yu J. M., Day J., Greaves M., and Elderfield H. (2005) Determination of multiple element/calcium ratios in foraminiferal calcite by quadrupole ICP-MS. *Geochemistry Geophysics Geosystems* **6** (8), Q08P01, doi:10.1029/2005GC000964.
- Zahn R. and Stüber A. (2002) Suborbital intermediate water variability inferred from paired benthic foraminiferal Cd/Ca and $\delta^{13}\text{C}$ in the tropical West Atlantic and linking with North Atlantic climate. *Earth and Planetary Science Letters* **200**, 191-205.
- Zeitzschel T. P., Waniek J., Bülow K., and Schröder P. (1998) Hydrographical studies. In *Meteor-Berichte 98-2, Nordatlantik 1996* (ed. J. Mienert, Graf, G., Hemleben, C., Kremling, K., Pfannkuche, O., Schulz-Bull, D), pp. 181-185.
- Zhu X. K., Guo Y., Williams R. J. P., O'Nions R. K., Matthews A., Belshaw N. S., Canters G. W., de Waal E. C., Weser U., Burgess B. K., and Salvato B. (2002) Mass fractionation processes of transition metal isotopes. *Earth and Planetary Science Letters* **200** (1-2), 47-62.

Acknowledgements

First of all, I would like to thank Mark Rehkämper. Thanks Mark for your great advice in the lab and on the mass specs, for an almost 24 hours phone hotline, for all the animated discussions we had during the last years, for your enthusiasm and optimism, for many night shifts you spent reading my manuscripts and for your constructive criticism. Going hiking with you and your family was also always good fun.

I am grateful to Alex Halliday for all the scientific discussions and for sharing with me his incredible enthusiasm and motivation for science. Being part of your geochemistry group was a great experience. Although the group was huge during the first years of my PhD the atmosphere was very relaxed and the social and scientific working environment was perfect.

Furthermore, I would like to thank Ralf Schiebel for his expert assistance in picking foraminifers and the scientific discussions about foraminifer ecology.

Special thanks to Judy McKenzie for becoming my official supervisor after Alex left. I would also like to thank Gideon Henderson for agreeing to be my external examiner and for his constructive suggestions on my Cd seawater manuscript. Although he was not directly involved in my PhD project, I am grateful to Bernard Bourdon for his support since he has become head of the ETH geochemistry group.

Furthermore, I would like to say thank you to all my colleagues from ETH:

Thanks to Sarah Aciego, Heiri Baur, Thorsten Kleine, Urs Menet, Donat Niederer, Felix Oberli, Mark Rehkämper, Ben Reynolds, Claudine Stirling, Andreas Stracke, Andreas Süssli, Helen Williams and Sarah Woodland for their help in keeping the mass specs and clean labs running smoothly. Thanks Sarah W. for sharing with me the secrets of lens cleaning and thank you Marie-Theres for all your help in the lab. Heiri Baur and Bruno Rütscle are thanked for their excellent computer support. Special thanks to Britt Meyer for all the administrative work she did for me during the last years and for all the nice conversations we had. Thanks for administrative work also goes to Valentina Müller-Weckerle.

A big thank you goes to Agnès Markowski, Veronika & Leo Klemm, and Bettina Zimmermann. During the last years I grew very fond of you. Thanks for all the great conversations and discussions we had, for all the nice lunch breaks, coffees, hiking tours, and all the evenings we spent together. And thanks Agnès for having shared the lab with me during the last two years, I could not have wished for a better lab-mate.

Last but not least, thanks to all the other people from our group with whom I had many coffees, lunch breaks and beers during the last years: Sarah Aciego, Morten Andersen, Sarah Bureau, Manuela Fehr, Caroline Fitoussi, Tina van de Flierdt, Martin Frank, Bastian Georg, Ansgar Grimberg, Marcus Gutjahr, Caroline Harris, Darrell Harrison, Veronika Heber, Philipp Heck, Mirjam Kiczka, Thomas Magna, Sune Nielsen, Emma-Kate Potter, Claudia Pudack, Ghylaine Quitte-Levasseur, Ben Reynolds, Jörg Rickli, Claudine Stirling, Nadya Teutsch, Mathieu Touboul, Jan Wiederhold, Helen Williams, and Sarah Woodland.

Since work is not everything, a special thank to all the members of the geochemistry knitting group for all the funny evenings and for being lenient with me being a lazy knitter during the last weeks. I promise to do better in the future....

Many thanks also to Christa & Ralf, Tanja & Harald, and Ämi & Felix for always being great hosts during numerous visits in Munich.

Finally, my biggest thank goes to my husband Johannes for the good time here in Zurich. All the weekends in the Swiss Alps together with you were just great and reminded me that there is something else in life beside geochemistry. Thanks also for the survival kits (coffee, pizza, etc.) you brought me, when I was almost starving in front of the mass spec late in the night. Thanks for joining me on regular late night walks to the lab when I had to refill my columns. Thanks for never getting tired discussing with me about Cd geochemistry. I cannot believe that I still could not convince you that it is much more fun than geophysics.

Curriculum Vitae

Sonja Ripperger

Date of birth: November 29, 1970
Place of birth: Munich, Germany
Birth name: Wichtlhuber
Citizenship: German

- 2003 - 2007 Doctoral studies at the Institute for Isotope Geochemistry and Mineral Resources, ETH Zürich, Switzerland

Ph.D. thesis: "Cadmium in the Oceans - Studies of Cd Isotope Variations in Seawater and Cd/Ca in in-situ Sampled Planktonic Foraminifera"
- 2002 - 2003 Geotechnical engineering company GHB-Consult, Starnberg, Germany
- 1996 - 2002 Undergraduate studies in Geology/Palaeontology at the Ludwig-Maximilians-University Munich, Germany

Diploma thesis: "Geologische Kartierung in den Hohenschwangauer Alpen unter besonderer Berücksichtigung der Aptychenschichten"
- 1991 - 1995 Acquirement of the general qualification of university entrance (Allgemeine Hochschulreife) at the Münchenkolleg in Munich, Germany